70262

NASA CONTRACTOR REPORT
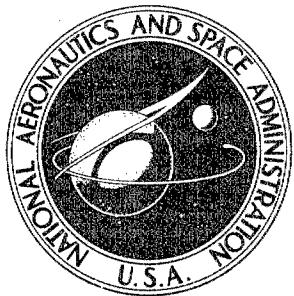
NASA CR-901

NASA CR-901

20000229 100

CRACK PROPAGATION THEORIES

by Fazil Erdogan

Prepared by
LEHIGH UNIVERSITY
Bethlehem, Pa.
for

AMPTIAC

NATIONAL AERONAUTICS AND SPACE ADMINISTRATION • WASHINGTON, D. C. • OCTOBER 1967

CRACK PROPAGATION THEORIES

By Fazil Erdogan

ABSTRACT

This article consists of two parts. In the first part, the crack propagation theories for brittle and quasi-brittle solids fracturing under a single application of the external loads are considered. The emphasis has been on the dynamic aspects of the fracture phenomenon and the related quantitative theories. Thus, the problem is discussed only from the viewpoint of continuum mechanics and classical thermodynamics. Two theoretical approaches are presented in detail. These are the dynamic crack propagation theory based on the concept of modulus of cohesion proposed by Barenblatt and various forms of the energy balance theory based essentially on the ideas proposed by Griffith. A detailed analysis of the energy balance around the periphery of the crack is given and it is shown that the energy available at the crack periphery to create new fracture surfaces is equivalent to the crack closure energy, which is different from the released strain energy if the inertia effects are not negligible. The results are applied to plane extensional and anti-plane shear problems. The techniques used in and the results obtained from the available experimental studies are then discussed.

In the second part, the theories dealing with the fatigue crack propagation in plates are considered. After a brief review of the existing models, a simple model based on the plastic deformations around the crack tip is discussed in detail. The model is intended to be largely a comparative tool in studying the fatigue crack propagation in structures with the same material but different geometries and loading conditions. The ⟶

results are used to analyze the experimental results obtained
from the plates under cyclic tension with variable mean loads
and plates under cylindrical bending.

TABLE OF CONTENTS

CRACK PROPAGATION THEORIES

Introduction

The fracture of solids may be considered as the formation of new surfaces in the medium in a thermodynamically irreversible manner. The essential feature of the phenomenon is the rupture of cohesive bonds in the material. In simplified terms, then the fracture is a process of nucleation and growth and/or coalescence of voids or cracks. Even though the details of this process may vary with the material, the type of external loading and the environmental conditions, generally speaking from the macroscopic standpoint, one may classify the fracture of solids in two broad categories, namely brittle and ductile. The ductile fracture is usually associated with large deformations, very high rates of energy dissipation and slow fracture velocities. Brittle fracture is a low energy failure and, for unstable loading conditions, takes place in a catastrophic manner, meaning that the fracture velocities are usually high.

The study of the fracture process for a given solid requires the simultaneous consideration of such widely diverse factors as the macroscopic effects, (e.g., the environmental and loading conditions, particularly stress states around macroscopic imperfections where the fracture is likely to initiate and their effect on the material behavior through yielding or constraining), the nature and the composition of the material, and the

1

microscopic phenomenon taking place at the locations where the fracture nucleates or grows. In the lowest end of the scale is then the process of rupturing some cohesive bonds within the material. In this range, one is interested in the phenomena taking place in the material within distances of order 10^{-7} cm and the tools available to study the problem are those of quantum mechanics. In the other end of the scale involving material behavior at distances 10^{-2} cm and up, the material may usually be considered as a homogeneous continuum and the tools of continuum mechanics and classical thermodynamics may be used to study the phenomenon. The phenomena taking place within the material between these two extreme scales, such as dislocation movements, formation of subgrain precipitates, the slip bands and the grain inclusions and voids, are very heavily dependent on the micro-structure of the material and may require a different approach*. Thus, due to the highly complex nature of the phenomenon and, as a result, the lack of its full physical understanding as well as the lack of sufficiently powerful mathematical tools, at the present time, there is no consistent single theory dealing with all the relevant aspects of fracture, and, generally speaking, the existing theories tend to treat the subject from only one of the three points of view mentioned above.

The fracture theories based on the approach of statistical

---

*For a discussion and a schematic representation of various scales of fracture, see [1].

mechanics simplify and idealize the material with respect to the kinetics of its atomic structure on one hand and ignore its local geometry and mechanics with respect to microstructures and stress state on the other. Hence, they provide some phenomenological insight but not a satisfactory quantitative theory. At this level, the approach is quite general and is applicable to all solids.

Since the fracture initiation means formation of cracks or voids, it is essential that in studying fracture, the microstructure of the material and the loading conditions should be considered. This means that the mechanism may be basically different for crystalline and amorphous solids. The current state of various theories dealing with the crack initiation and its growth to a certain size has been discussed in [2 to 8] for crystalline materials and in [9 to 13] for amorphous polymers. The main emphasis in all these microstructural theories is on the understanding of the mechanism of fracture initiation and they tend to be largely qualitative.

The macroscopic theories of fracture on the other hand assume the existence of cracks, voids or other imperfections which may readily act as fracture nucleus. The size of these imperfections are assumed to be sufficiently large compared to the characteristic dimensions of the microstructure to justify the use of the tools of continuum mechanics. These theories consider the material to be a homogeneous continuum with certain, usually idealized, properties and approach the

problem from an entirely field point of view using the tools of continuum mechanics and classical thermodynamics.

In the macroscopic approach to the problem, it becomes necessary to devise a "model" for the actual phenomenon and postulate a "criterion" for fracture. Among such criteria, one may mention a maximum strain criterion proposed by McClintock [14] and Krafft [15], the critical stress intensity factor criterion of Barenblatt [16], which may be considered as a maximum stress or an energy criterion depending on the interpretation of the stress intensity factor [17] and the energy balance criteria. In general terms, all the energy balance criteria are based on a simple thermodynamic notion that the fracture will ensue or continue to propagate if for a unit increase in fracture surface, the increase of externally added or internally released energy is greater than the amount of stored and dissipated energies. Partly due to the generality and physical soundness of the underlying principle and partly due to its flexibility, these criteria form the basis of by far the most widely used theories of fracture.

The first energy balance theory was formulated by Griffith [18,19] for the fracture of ideally brittle materials in which surface free-energy is the only source of energy dissipation. The subsequent theories have dealt largely with the modification and generalization of Griffith's work. Among the notable generalizations, we may mention the work by Rivlin and Thomas [20], who studied the tearing of a rubber vulcanizate and

introduced the concept of characteristic tear energy to re-
place the surface free-energy in Griffith theory. Rivlin-
Thomas theory has been very useful in studying the high
energy-type fracture and has successfully been applied to the
fracture of polymers [21 - 24]. The modifications offered
by Orowan [25] and Irwin [26] deal with the introduction of
plastic work as an additional source for energy dissipation,
extending the usefulness of the theory to the fracture of
metallic materials. Another significant extension of Griffith
theory was made by Mott [27] who included the kinetic energy
in the energy balance in studying the dynamics of fracture.
In these theories, the rate of change of dissipative energy
with respect to fracture area called surface free-energy, tear
energy, fracture energy or fracture toughness plays an impor-
tant role, is considered to be an intrinsic property of the
material and is dependent on the environmental conditions and
the type of loading as well as the nature and the composition
of the material.

In discussing the fracture of solids under a single appli-
cation of the load, one may differentiate three types of ma-
terial response. One would be the so-called crystalline
shatter of a perfect crystal with an ideally uniform geometry
and under ideally uniform external loads. In this case, the
fracture may be a complete shatter of the material or the
instantaneous rupture along a plane. Another ideal situation
may arise if the geometry and loading conditions are such that
the fracture nucleation and growth, that is, the formation

5

and the propagation of microcracks, take place uniformly and
simultaneously along a certain plane. In such a case, each
microcrack may experience similar velocities while propagating.
Even though these crack velocities may be somewhat limited,
due to the multiplicity of fracture nuclei, the final phase
of the fracture, i.e., the phase of rapid fracture propagation
may be of very short duration. A carefully grooved homogeneous
thin sheet under uniform tension may come close to satisfying
these conditions. A more realistic and common material re-
sponse is the propagation of a dominant flaw in the material.
In this case too, for some materials, one may observe the
coalescense of cracks or voids; however, the cracks or voids
in question here form ahead of main propagating crack and due
to the stress concentration caused by the main crack. The
term fracture or crack propagation in current literature on
the subject is used only for the type of fracture which con-
sists of the growth of a dominant crack and hence, this will
be the only type of phenomenon which will be discussed in
this chapter.

The terminology of crack propagation is also used in con-
nection with the growth of fatigue cracks which take place
in materials subjected to repeated loading. There is no sig-
nificant change in the atomistic theories of fracture with
regard to fatigue. However, the microstructural and macro-
scopic or continuum theories of fatigue differ considerably
from those dealing with fracture under a single application
of the load. The microstructural theories are based on the

slip movements taking place in the slip bands and resulting in the formation of intrusions and extrusions [28 - 33]. The main objective of these theories is to explain the mechanism of formation of the fatigue cracks rather than to provide a quantitative working tool. Again, the quantitative theories of fatigue also are based on the continuum models and are mostly semi-empirical in the sense that they contain constants which have to be determined experimentally, which are not in a rational way related to the known simple material constants and into which most of the indefiniteness and perhaps some of the inaccuracies in the line of reasoning are lumped [34 - 42].

In this article, we will consider only the quantitative aspects of the fracture or crack propagation theories; hence, in most part, the discussion will be restricted to the continuum-based models. In the first part, after a brief review of various fracture propagation theories, the more acceptable energy balance theory will be discussed in detail. The fatigue crack propagation will be considered in the second part of the article.

1. Dynamic Crack Propagation Theories

A given solid with a certain geometric singularity, usually a crack, a sharp notch or an inclusion, may fracture catastrophically at load levels exceeding a critical limit. There is ample experimental evidence that in such low energy-type failures, the fracture velocities in some cases may be of the order of magnitude of elastic wave velocities in the solid. Hence, in studying the problem, it becomes necessary to take into account the dynamic nature of the phenomenon. Basically, the problem is the following:

A given solid is subjected to a system of time-dependent external loads, generally consisting of surface tractions, T_i, surface displacements, u_i, and body forces F_i, and contains an initial imperfection which serves as a fracture nucleus (Figure 1). Let A be the portion of the surface of the solid created as a result of fracture. If the external loads are increased beyond a critical level, the fracture propagation will ensue. The question is then the determination of the size and the shape of the fracture area A as a function of time — knowing the material characteristics and the environmental conditions. At this generality, even the formulation of the problem does not seem to be so simple. However, if we restrict ourselves to a narrow class of problems in which fracture takes place along a plane and the fracture area A is characterized by a single length parameter $a(t)$, then the dynamic problem reduces to the determination of four func-

tions, namely the displacements $u_i(x_j,t)$, $(i,j = 1,2,3)$ and the characteristic fracture length, $a(t)$. The equations of motion in the deformable solid provide three equations. The fourth equation necessary to complete the formulation of the problem will have to be provided by some kind of a failure theory or a fracture criterion which is discussed in the following sections.

1.1 Theories Based On Statistical Mechanics

There have been some attempts to explain the phenomenon of delayed fracture in brittle solids by considerations based on statistical mechanics [43 - 45]. These theories are assumed to apply to the crack initiation as well as the rapid crack propagation phases of fracture. For crack propagation, they lead to an expression of the form

$$V_0 = A\, e^{-f(\sigma,T,E,Q)} \tag{1}$$

where V_0 is the crack velocity, A is a constant, usually the shear wave velocity c_2, σ is the "external stress", T is the absolute temperature, E is the modulus of elasticity and Q is the energy of binding. Depending on the author, the function f takes various forms. In most of these theories, the arguments leading to (1) are essentially based on the proposition that the velocity ratio V_0/c_2 is the same as the percentage of atomic bonds which have reached the energy level corresponding to the unstable equilibrium [43,44] and the reason given being that all the bonds behind the crack front

9

must necessarily be ruptured. In others, it is assumed that the crack growth is caused by thermal fluctuations and a limiting velocity of crack propagation may be obtained from the condition that the bond fluctuation breakage probability is unity [45,46]. In still others [47,48], to obtain an equation in the form of (1), the statistical theory of chemical reaction rates developed by Eyring and others [49 - 52] has been used. It is assumed that the propagation of fracture may be considered to be a unit process proceeding by jumps as individual pairs of atoms are separated. Starting then with the Eyring equation, giving the probability of passage of a system over an energy barrier per unit time and assuming this to represent the probability of breaking a bond at the crack tip, a relation for the crack propagation rate may be obtained.

Originally, these theories have been developed as alternatives to the critical-flaw concept of Griffith to explain the fracture of solids — the main difference being that according to this approach, there is no flaw in the solid until it is created by the applied stress and after its creation, the limiting velocity, which is estimated to be approximately $0.5 \ c_2$, is reached very quickly. Whatever the merit of the existing statistical rate-process theories in providing a mechanism for crack initiation may be, as pointed out by Hall [53], they are almost certainly incorrect as crack propagation theories. Without a detailed discussion of any of these theories, the main objections commonly applicable to all may be that they are based on notions developed for systems in

equilibrium which a material undergoing fracture with near-sonic velocities is not and the superficial manner in which "the external stress" is brought into the rupture phenomenon at the crack tip.

1.2 Barenblatt's Theory

Barenblatt's theory of the so-called equilibrium cracks is essentially a critical flaw approach to fracture similar to that of Griffith leading to identical results and differing only in its interpretation of the stress and deformation states at the crack tip [16]. Both approaches deal with the problem from continuum standpoint and use the tools of linear elasticity. Griffith theory is based on the energy balance at the crack tip. Barenblatt, objecting to the notion of infinite stress at the crack tip, and to overcome the shortcomings of the continuum elasticity within the range of intermolecular distances encountered in studying the phenomenon around the crack tip, has introduced the effect of cohesive forces acting across the faces of the crack close to its tips. Starting with the hypotheses that a) the end region in which the cohesive forces are active is "very small" compared to crack length, b) the stresses at the crack tip are finite, and c) the crack surfaces close smoothly, i.e., the crack tip has a cusp shape rather than being parabolic as predicted by the elastic theory, he points out that a non-singular stress state obtained by the superposition of stresses due to the external loads and those due to cohesive forces would satisfy these

conditions. He thus obtains a fracture criterion by writing the combined stress intensity factor equal to zero. The result is the comparison of the stress intensity factor calculated from the external loads with a material parameter called the modulus of cohesion. He further indicates the relationship between the surface tension and the modulus of cohesion and arrives at the Griffith criterion. His further attempts to extend the same line of reasoning to quasi-brittle materials involving plastic deformations is rather unrealistic[*].

Using the hypotheses mentioned above, Barenblatt and others have extended the concept of the modulus of cohesion to propagating cracks [56 - 58]. In [56], a stationary (plane

---

[*]In the case of equilibrium cracks, the plastic zone is not a thin layer surrounding the crack as assumed in [16]. The shape is rather complex and is difficult to determine. The problem which would result from its removal and subsequent replacement by appropriate surface tractions seems to be quite difficult to handle and has not even been attempted yet.

It should be noted that by using the only available mathematical tool, that is the method of linear elasticity, Barenblatt may partly be open to the same criticism as he addressed to Griffith, namely that for small cracks in which Griffith was interested in, the size of the end region in which the cohesive forces may be active is possibly small enough to render a linear continuum approach meaningless. Aside from this, in real materials, the nonlinear and inelastic behavior would have sufficient blunting effect on the crack tip to make any cohesion on the crack surfaces inconsequential. It is also interesting to note that Orowan has used an alternative approach for crack extension by stating that over an area of atomic dimensions, the stress at the crack tip must be the same as the theoretical bond strength and has shown that, within the approximations of calculations involved, his results agree with that of Griffith [54,55].

strain) wedging of an ideally brittle solid is considered. The problem is that of a semi-infinite slender wedge with a given nose profile moving through an infinite medium at a constant velocity V_0. Again, two separate stress states are considered: $\sigma_{ij}^{(1)}$, due to cohesion forces,

$$\sigma_y^{(1)} = G(\xi), \quad \tau_{\xi y}^{(1)} = 0 \ , \ 0 \le \xi \le d, \ \xi = x + V_0 t$$

active in the end region of the crack (Figure 2) and $\sigma_{ij}^{(2)}$ due to the external loads. From the solution of the wave equations, it is shown that in the neighborhood of the crack tip for $y = 0$

$$\sigma_y^{(1)} = - \frac{1}{\pi \sqrt{r}} \int_0^d \frac{G(t) dt}{\sqrt{t}} = - \frac{K}{\sqrt{r}} \tag{2}$$

where r is a small distance from the crack tip. In deriving (2), it is assumed that $G(\xi)$ and d are independent of V_0 and depend only on the material properties; hence, K is a constant and is assumed to have the same value as the modulus of cohesion defined for equilibrium cracks. This velocity-independence of G and d may not be justified and will be remarked upon later. Thus in any stationary problem where a semi-infinite crack propagates with a velocity V_0, if the cleavage stress in the vicinity of the crack tip resulting from the external loads is given by

$$\sigma_y^{(2)} = \frac{N(V_0)}{\sqrt{r}} \tag{3}$$

13

the finiteness condition of the stresses gives the fracture criterion or the equation determining the propagation velocity V_0 as

$$N(V_0) = K \qquad (4)$$

Since N is the dynamic stress intensity factor for σ_y and K is a material constant, in this form Barenblatt criterion is similar to that of Irwin [59,60], N^2 and K^2 corresponding to crack driving force and fracture toughness, respectively, with the difference that the dynamic fracture toughness as used by Irwin and others is assumed to be dependent on the crack velocity.

The nonstationary plane crack propagation problem is considered in [58] where it is assumed that at t = 0, a cut of length $2a_0$ is introduced to a plane subjected to a uniaxial tension at infinity. The cut is perpendicular to the direction of loading and is assumed to be greater than the critical length, so that the crack immediately starts to grow. The crack propagation is assumed to consist of three stages: an initial non-uniform stage associated with the effect of the perturbation waves originating from the crack; a uniform growth with constant velocity V_0; the final accelerated growth which may result in the branching of the crack (isotropic brittle materials) or attaining the Rayleigh wave velocity (highly anisotropic crystals and elastic half planes bonded with a weak non-dissipative glue). The duration of

the initial stage is assumed to be very small and its effect
to be negligible. Thus for the uniform propagation stage,
the problem may be approximated with that considered by
Broberg [61], who gives the dynamic solution for a uniaxially
stressed plane in which a crack starts from zero length and
propagates at a constant velocity.

In [58], it is assumed that the size of the end
regions of the crack in which the cohesive forces are active
(Figure 2) is $d = V_1 t$ with the constant V_1 small compared to
and independent of V_0 and that the cohesive force, g, aside
from the material constants, is a function of s/d only.
Approximating the stress field induced by the cohesive forces
by a stationary field discussed earlier, it is found that

$$\sigma_y^{(1)} = - \frac{1}{\pi\sqrt{r}} \int_0^d \frac{g(s/d)ds}{\sqrt{s}} = - \frac{\sqrt{V_1 t}}{\pi\sqrt{r}} \int_0^1 \frac{g(u)du}{\sqrt{u}} \qquad (5)$$

or defining a "material constant"

$$R = \frac{\sqrt{V_1}}{\pi} \int_0^1 \frac{g(u)du}{\sqrt{u}} \qquad (6)$$

the cleavage stress is obtained as

$$\sigma_y^{(1)} = - R \sqrt{\frac{t}{r}} \qquad (7)$$

On the other hand at y = 0 and a small distance r
ahead of the running crack, the dynamic solution gives the

cleavage stress due to the external loads as [61]

$$\sigma_y^{(2)} = p \sqrt{\frac{c_2 t}{2r}} \, F(v)$$

$$F(v) = \sqrt{v(1-k^2 v^2)} \, [4\sqrt{(1-k^2 v^2)(1-v^2)}$$

$$- (v^2-2)^2]/\{v^2 \, [4k^2 + v^2(1-4k^2)] \, K(\sqrt{1-k^2 v^2})$$

$$- 4v^2(1-k^2 v^2) \, K(\sqrt{1-v^2}) - [v^4 - 4(1+k^2)v^2 + 8] \, E(\sqrt{1-k^2 v^2})$$

$$+ 8(1-k^2 v^2) \, E(\sqrt{1-v^2})\}, \quad k = c_2/c_1; \quad v = V_0/c_2 \qquad (8)$$

where p is the uniaxial stress at infinity, c_2 is the shear
wave velocity, c_1 is the dilatational wave velocity, K and E
are the complete elliptic integrals of first and second kind,
respectively. The condition of finiteness of σ_y at the crack
tip then gives

$$p \sqrt{\frac{c_2}{2}} \, F(v) = R \qquad (9)$$

Since R is a constant, (9) determines the uniform crack propa-
gation velocity for a given load p. The function F(v), which
is essentially a measure of dynamic stress intensity factor for
σ_y is plotted in Figure 3 for $\nu = 1/4$. Writing (9) as
$F(v) = \sqrt{2/c_2} \, R/p$, it is seen that for p less than a certain
value p* (9) has no real solution. For p > p*, there are two
solutions. Since at the smaller velocity v_1, an increase in
p results in a decrease in v, it is not acceptable on thermo-

16

dynamic grounds; hence, v_2 is the only possible solution. From t = 0, then the crack will propagate at a constant velocity v_2 until its resistance reaches the value corresponding to the stationary propagation. Comparing (2) and (7), it is seen that the uniform crack propagation phase will end at

$$t_2 = K^2/R^2 \tag{10}$$

In the last phase of crack propagation, $t > t_2$, the stress intensity factor will be greater than the modulus of cohesion, i.e.,

$$p\sqrt{\frac{c_2 t}{2}} \, F(v) > K = p\sqrt{\frac{c_2 t_2}{2}} \, F(v)$$

and as a result the crack velocity will grow either to the branching velocity (isotropic materials) or to the Rayleigh wave velocity (highly anisotropic materials with weak cleavage planes).

It should be pointed out that the hypothesis of finiteness of crack tip stresses, which is so strongly emphasized in this particular approach to fracture, is only partially satisfied by the model outlined above. The reason for this is that in combining the crack tip stresses $\sigma_{ij}^{(1)}$ due to cohesion and $\sigma_{ij}^{(2)}$ due to the external loads, only the cleavage stress, σ_y is rendered finite. Since for $\sigma_{ij}^{(1)}$ a stationary solution, (that is, a solution for semi-infinite crack growing at a constant velocity), is used and since for a stationary solution and that for a uniformly growing crack

17

the stresses around the crack tip have different θ as well as different V_0-dependence[*], the combined stresses on planes other than $\theta = 0$ would still have a singularity at the crack tip.

1.3 Discussion And Some Modifications Of Barenblatt's Theory

If the plane has an initial flaw of length $2a_0$ and if the modulus of cohesion of the material is K, the solution for the equilibrium crack indicates that at an external load

$$p = \sqrt{\frac{2}{a_0}}\ K \qquad\qquad (11)$$

the crack starts to propagate. Hence, for this value of the load from (9), (10) and (11), the duration t_2 of uniform crack growth may be obtained as

$$t_2 = \frac{a_0}{c_2}\ \frac{1}{(F(v))^2}$$

which is very small for practical ranges of F(v). Thus, in most cases, t_2 may be ignored and the stationary crack growth criterion (4), may be applied from the instant crack starts to propagate. In this case, the stress intensity factor $N(V_0)$ should be obtained from a dynamic solution with accelerated crack growth. Since such a solution is analytically not fea-

_____

[*]This can be seen by comparing the results of [61] and [62]. In [62], constant surface tractions moving with the semi-infinite crack are applied on a finite portion of the crack surface.

18

sible, for qualitative description of the phenomenon, one may assume the solution with uniform velocities to be valid at successive intervals. Also, in order to apply Broberg's solution, we may associate the half-crack-length a_0 with a time t_0 such that $a_0 = V_0 t_0$. Recalling that $v = V_0/c_2$, from (2), (8) and (11), we obtain

$$p \sqrt{\frac{c_2 t}{2}} \, F(v) = K$$

or

$$F(v) = \sqrt{v \, \frac{t_0}{t}} \qquad (12)$$

Equation (12) provides a descriptive relation between crack velocity and time and is obtained from the condition that at any given time, the stress intensity factor is equal to the modulus of cohesion.

According to this simplified version of Barenblatt's theory, for $t = t_0$, $v = 0$ is the only possible velocity. However, in propagating cracks, p is usually slightly greater than the equilibrium value; hence, the crack growth will take place, and at a certain time, t_0, one may assume a nonzero crack velocity. As t increases, the stress intensity factor will increase while resistance to crack growth remains constant. For a few values of t, the solution of (12) is shown in Figure 3 which shows that if the branching does not occur and the external load p is held constant, the crack velocity would asymptotically approach the Rayleigh wave velocity.

If we assume with Barenblatt that the resistance to the crack propagation in brittle fracture comes solely from the cohesive forces at the crack tip, it may be argued that the resulting "material constant" characterizing the resistance will have to be a function of crack velocity. One of the weaknesses of the Barenblatt theory is that this point is handled in an arbitrary fashion with no physical foundation. For example, one may easily argue that, in the initial stage of the crack propagation, the velocity V_1, of development of the cohesion zone size d is not constant, but is dependent on crack velocity V_0. For simplicity, if we assume this relationship to be linear[*], i.e., $V_1 = \beta V_0$, where β now is a material property, from (5) we obtain

$$\sigma_y^{(1)} = - \frac{\sqrt{V_0 t}}{\sqrt{r}} Q, \quad Q = \frac{\sqrt{\beta}}{\pi} \int_0^1 \frac{g(u)du}{\sqrt{u}} \tag{13}$$

For the finiteness condition, $\sigma_y^{(1)} + \sigma_y^{(2)} = 0$, from (8) and (13), we find

$$\frac{P \, F(v)}{\sqrt{2v}} = Q, \quad v = V_0/c_2 \tag{14}$$

---

[*]For a heuristic justification, see Appendix A, where it is shown that in an anti-plane problem, a Dugdale type of model gives the velocity of the development of plastic zone size approximately proportional to crack velocity.

Now Q is a constant and (13) and (14) are valid for all possible crack velocities during the initial phase of the crack propagation. On the other hand, for very small crack velocities, $\sigma_y^{(1)}$ is approximately the same as the stress in equilibrium cracks. Thus, letting $V_0 t = a_0$, the initial crack length corresponding to the fracture initiating load p, and comparing (2) and (13), the constant Q is seen to be

$$Q = \alpha_1 K / \sqrt{a_0}, \quad \alpha_1 \leq 1 \tag{15}$$

where K is modulus of cohesion of the material and the constant α_1 is introduced to take into account the possible change in resistance to crack growth resulting from the change in crack velocity. $\alpha_1 = 1$ for $V_0 = 0$; for $V_0 \geq 0$, the effect of dissipation at the crack tip due to plastic deformation or viscous flow decreases and α_1 becomes less than unity [63]. For crack propagation, again using the condition (see (11))

$$p = \alpha_2 \sqrt{\frac{2}{a_0}} \, K, \quad \alpha_2 \geq 1 \tag{16}$$

From (14), (15) and (16), we obtain the equation giving the crack propagation velocity as

$$F(v) = \sqrt{v} \, \frac{\alpha_1}{\alpha_2} \tag{17}$$

It should be noted that, unlike (12), the solution of (17) is independent of time; that is, for a given value of α_2/α_1, the solution of (17), shown in Figure 3 as the intersection of F(v) and the parabolas, is the expected uniform

crack velocity in an infinite plane. According to this interpretation of Barenblatt's theory, the transition from the equilibrium crack to the crack propagating at a limiting velocity is explained by the variation in α_1 which depends on the fracture properties of the material and α_2 which may now be assumed to be the ratio of the external load at a given time to the load associated with the equilibrium crack. This means that during the crack propagation, a decrease in external load, i.e., α_2, would result in a decrease in crack velocity, if the decrease in α_2 is high enough to reduce α_2/α_1, to unity, theoretically, the crack would stop. Also, one may note that if the solution of (17) is above the branching velocity, the crack would branch before the limiting velocity is reached.

Practically all the available experimental results indicate that the limiting crack velocity in brittle fracture is approximately constant and that a reduction in the external loads causes a decrease in crack velocity. This implies that the foregoing model conforms to the main features of the brittle crack propagation. It should again be emphasized that, since it lacks a firm physical foundation, the model described above is not a theory which can be used to explain the phenomenon of fracture propagation, it is simply a convenient continuum model.

1.4 Theories Based On The Energy Balance

Consider a solid subjected to certain external loads and containing an internal or an external "dominant" crack. The external loads may be any one or combination of surface tractions, surface displacements and body forces. In the most general case, thermodynamic equilibrium of the body requires that

$$\frac{dU}{dt} = \frac{dV}{dt} + \frac{dT}{dt} + \frac{dD}{dt} \tag{18}$$

where t is the time, U is the work done by the external loads, V is the recoverable (elastic) component of the stored energy, T is the kinetic energy and D is the sum of all the irreversible energies such as the surface free-energy or fracture energy, plastic work and viscous dissipation. If T_i^n are the components of stress vector, u_i are components of the displacement vector at a point on the surface S with the outward normal $\vec{n}$, F_i are the body forces and ρ is the mass density, we have

$$\frac{dU}{dt} = \int_S \int \sum_1^3 T_i^n \dot{u_i} \, dS + \int_R \int \int \sum_1^3 F_i \dot{u_i} \, dR \tag{19}$$

$$\frac{dT}{dt} = \int \int_R \int \rho \sum_1^3 \dot{u_i} \dot{u_i}{}^{\cdot} \, dR \tag{20}$$

where R is the total volume and dot indicates differentiation with respect to time.

Equations (18) to (20) are valid for all solids which

may or may not be undergoing fracture at the time under consideration. If we consider a special case of a linearly elastic solid in which the only energy dissipation takes place on the advancing periphery of the crack, the remaining two energy rates may be written as

$$\frac{dV}{dt} = \int\int_R\int \sum_1^3 \sum_1^3 \sigma_{ij}\dot{\epsilon}_{ij} \, dR \tag{21}$$

$$\frac{dD}{dt} = \frac{dD}{dS}\frac{dS}{dt} = \frac{dD}{dA}\frac{dA}{dt} = \gamma_f \frac{dA}{dt} \, , \quad S = S_o + A \tag{22}$$

where S_o is the surface of the solid excluding the crack, A is the total crack surface, γ_f is the amount of energy required to create a unit amount of fracture surface, which will henceforth be called the specific fracture energy or simply the fracture energy of the solid and $\frac{dA}{dt}$ is the measure of fracture velocity.

Formally, the formulation of the problem may be completed by introducing the equations of motion for the elastic solid:

$$(\lambda+\mu) \frac{\partial e}{\partial x_i} + \mu\nabla^2 u_i + F_i = \rho \frac{\partial^2 u_i}{\partial t^2} \, , \quad (i = 1,2,3) \tag{23}$$

where λ and μ are the Lame's constants and $e = \sum_1^3 (\partial u_i/\partial x_i)$ is the dilatation. Equations (18) and (23) provides a system of four equations to determine the unknown functions $u_i(x_j,t)$ and $a(x_j,t)$, where, assuming that fracture takes place along a known plane, the function a describes the plane curve representing the crack front and replaces the function A(t) as the

24

unknown. Because of (18), the system is highly nonlinear
with the additional difficulty arising from the time-depend-
ence of the surface S due to the propagating crack.

In the absence of body forces and for solids in which
the points of application of the external loads are so far re-
moved from the fracture zone that the main part of the fracture
process is completed before the first elastic waves generated
by the fracture initiation reach the loaded boundaries, the
term $\frac{dU}{dt}$ in (18) will be zero and the released elastic energy
will provide the necessary source for kinetic energy and dis-
sipation. Such is the case in long bars loaded at the ends
and fracturing in the mid-section and very large solids with
a dominant internal crack. $\frac{dU}{dt}$ vanishes also in cases where
the external loads are applied through ideally fixed grips,
i.e., if $u_i = 0$ on part and $T_i^n = 0$ on the remainder of S
during fracture.

If the problem has symmetry in geometry as well as
the loading conditions, the function $a(x_j,t)$ and the governing
equations (18) and (23) may be considerably simplified. For
example, in plane problems with internal dominant crack (gen-
eralized plane stress, plane strain and longitudinal shear or
anti-plane strain) a is simply the half-crack-length and is
function of time only and in axially symmetric problems, a is
the radius of the (penny-shaped) crack and again depends on
time only. Furthermore, in the plane strain, plane stress
and axially symmetric problems two components, in longitudinal

shear problems only one component of the displacement vector will be unknown. In these problems, the rate of dissipation energy may be written as

$$\frac{dD}{dt} = 4 \gamma_f a \cdot h \quad \text{(plane problems)}$$

$$(24)$$

$$\frac{dD}{dt} = 2\pi\gamma_f a \, a \cdot \quad \text{(axially symmetric case)}$$

where h is the thickness and γ_f is usually a function of the crack velocity. Even with γ_f = constant, the solution of the problem as formulated above does not seem to be possible. In what follows, we will review the quasi-static approximation proposed by Mott [27] and offer some modifications of the general theory outlined above.

1.4.1 Mott's Theory

The problem considered by Mott [27] was the propagation of a centrally located through crack in an infinitely large plate subjected to a time-independent uniaxial tension perpendicular to the plane of the crack. Mott's main contribution was his recognition that the kinetic energy must be included in the energy balance, and the key assumption in his analysis to estimate the effect of kinetic energy was that the stress and displacement fields for the dynamic problem are the same as those for the elastostatic problem with the same crack length. Thus, if u, v are the components of the displacement, a(t) is the half-crack length and if $\frac{da}{dt}$ is small compared to the shear wave velocity in the material, the com-

ponents of the velocity at a given point in the plate may be
written as

$$\dot{u} = \dot{a} \frac{\partial u}{\partial a} \, , \, \dot{v} = \dot{a} \frac{\partial v}{\partial a}$$

Then kinetic energy becomes,

$$T = \frac{1}{2} \rho \dot{a}^2 \int_R \int [(\frac{\partial u}{\partial a})^2 + (\frac{\partial v}{\partial a})^2] \, dx \, dy \qquad (25)$$

where ρ is the mass per unit area of the plate. Mott argued
that since u, v are proportional to ap/E, $\partial u/\partial a$ and $\partial v/\partial a$
would be proportional to p/E. Also, since a is the only
characteristic dimension in the material, tacitly assuming
that the domain R covers the entire plate, the area integral
in (25) would be proportional to a^2. Hence, (25) may be
written as

$$T = \frac{1}{2} k \rho a^2 \dot{a}^2 \frac{p^2}{E^2} \qquad (26)$$

where k is now a constant and may depend only on the Poisson's
ratio, ν. Mott considered the energy balance equation (18) in
integrated form, i.e.,

$$T + D + V - U = E_0 \qquad (27)$$

where E_0 is a constant. From the elastic solution of the
plate under either fixed grip or constant stress at infinity
for the change in the quantity U-V due to the existence of a
crack of length 2a, we may write

$$U - V = \frac{\pi p^2 a^2}{E} \qquad (28)$$

Thus, with the dissipative energy $D = 4\gamma_f a$ (γ_f now being the fracture energy for plate thickness h rather than unit area), (27) becomes

$$\frac{k\rho a^2 \dot{a}^2 p^2}{2E^2} - \frac{\pi p^2 a^2}{E} + 4\gamma_f a = E_0 \tag{29}$$

To eliminate the constant E_0, Mott and Roberts and Wells [64] differentiated (29) with respect to a and assumed that $\frac{\partial \dot{a}}{\partial a} = 0$, that is, the crack is travelling at a constant (terminal) velocity. Also using the following Griffith condition for fracture initiation at t = 0 with crack length a_0 and load p

$$\gamma_f = \frac{p^2 \pi a_0}{2E} \tag{30}$$

From (29), they obtained

$$\dot{a} = \left(\frac{2\pi E}{k\rho}\right)^{1/2} \left(1 - \frac{a_0}{a}\right)^{1/2} \tag{31}$$

As pointed out by Berry [65] and Dulaney and Brace [66], (31) is in error because of the assumption $\partial a / \partial a = 0$. Following largely Berry's line of reasoning and assuming that the applied load p is somewhat greater than the critical load p_c obtained from Griffith condition, (30), in order to avoid the condition of zero crack acceleration at t = 0, (29) may be written as

$$\frac{k\rho a^2 \dot{a}^2 p^2}{2E^2} - \frac{\pi p^2 a^2}{E} + \frac{2\pi a_0 a p_c^2}{E} = E_0 \tag{32}$$

28

At $t = 0$, $\dot{a} = 0$, $a = a_0$ and (32) becomes

$$- \frac{\pi p^2 a_0^2}{E} + \frac{2\pi a_0^2 p_c^2}{E} = E_0 \tag{33}$$

Letting

$$p_c = n\,p, \quad (n \leq 1) \tag{34}$$

From (32) and (33), we obtain

$$\dot{a}^2 = \frac{2\pi E}{k\rho} \left(1 - \frac{a_0}{a}\right)\left[1 - (2n^2-1)\frac{a_0}{a}\right] \tag{35}$$

which can be integrated to give the relationship between the crack length and time as

$$\left(\frac{a}{a_0} - 1\right)^{1/2} \left[\frac{a}{a_0} - (2n^2-1)\right]^{1/2} + 2n^2 \log\left\{\left(\frac{a}{a_0} - 1\right)^{1/2}\right.$$

$$\left. + \left[\frac{a}{a_0} - (2n^2-1)\right]^{1/2}\right\} - n^2 \log(2-2n^2)$$

$$= \left(\frac{2\pi E}{k\rho}\right)^{1/2} \frac{t}{a_0} \tag{36}$$

From (35), we observe that for $a \gg a_0$, the crack velocity will approach a terminal velocity V_T given by

$$V_T = \left(\frac{2\pi}{k}\right)^{1/2} c_\ell \; , \; c_\ell^2 = E/\rho \tag{37}$$

where c_ℓ is the velocity of the longitudinal waves for the material.

Thus, the problem reduces to the evaluation of the constant k and then going back and investigating the valid-

ity of the key assumptions on which the solution is based, namely, the quasi-static assumption for stress and displacement fields and the velocity independence of fracture energy. To find k, Roberts and Wells evaluated the integral given in (25) numerically and plotted the quantitity $(2\pi/k)^{1/2}$ as a function of r/a, r being the radius of the domain R. This was done partly because of convergence difficulties as $r \to \infty$ and partly because of the fact that outside the circle $r = c_1 t$, the material is undistrubed and the kinetic energy density is zero, where $c_1 = (E/\rho(1-\nu^2))^{1/2}$ is the dilatational wave velocity in plane stress. In order to find the proper value of k, it was further assumed that

$$\frac{r}{a} = \sqrt{\frac{k}{2\pi}} \tag{38}$$

implying that a) longitudinal and dilatational wave velocities are the same and, b) at time t, the crack length is $a = V_T t$, V_T being the terminal velocity defined by (37). For numerical calculations, a Poisson's ratio of 1/4 was used, hence, the effect of assumption a) on the result would be insignificant. Strictly speaking, b) is valid only for $t \to \infty$, however, for reasonably large values of t and considering all the other approximations involved, its effect may also be neglected. Thus, for $\nu = 1/4$, it is found that $\sqrt{\frac{2\pi}{k}} = 0.38$.

If in principle, the existence of terminal velocity, V_T, is accepted and if the size of the medium is sufficiently large to permit the fracture velocity to reach V_T

30

then the assumption of γ_f = constant may always be justified. Even though γ_f is in some cases very highly velocity and temperature-dependent, within the confines of Mott's theory, the fracture propagating at a terminal velocity is a steady-state phenomenon and hence, this variation in γ_f would be expected to affect only the acceleration stage of the crack growth. The definitive work relating the fracture energy to velocity and temperature is lacking and will be remarked upon later in this chapter; however, it is generally agreed that in metal compounds as well as polymers, the value of γ_f to initiate the fracture growth from an existing crack is higher than the value corresponding to the propagating crack, γ_f first decreases with the velocity and then increases with increasing crack velocities. The high values of γ_f are due to the plastic work or viscous dissipation at lower velocities and to the high energy dissipation caused by the surface roughening at very high velocities. It is also worth to note that the terminal velocity is independent of the constant, $n = p_c/p$ and the load p as long as the condition for fracture initiation, $p > p_c$, is satisfied.

Main defect of the Mott's theory lies primarily in its quasi-static assumption for the stress and displacement fields. The only quantitative argument in support of this assumption has been the photoelastic studies made by Wells and Post [67] on Columbia Resin in which the isochromatic fringe pattern around a running crack was photographed. However, a gross similarity observed between the dynamic and

31

and static fringe patterns may not necessarily mean that the singular behavior of the two stress states at the crack tip will be the same. Since the strength of this singularity is the primary load factor in fracture (as a stress intensity factor in cleavage or through strain energy release rate or rate of external work flowing into the crack tip), one may not be justified in approximating the dynamic case with the static solution without a quantitative comparison of the corresponding stress singularities.

Since the dynamic solution for a plate with a central crack propagating at a constant velocity is available [61,68], such a comparison can easily be made. For this, we refer to Figures 3 and 4. In Figure 3, the stress intensity factor for the cleavage stress σ_y is given for the dynamic case as a function of the velocity ratio $v = (V_T/c_2)$ and for the corresponding static case. Figure 4 shows the variation of σ_θ with the polar angle θ for values of V_T/c_2 ranging from 0.2 to 0.96. In these figures, a Poisson's ratio of $\nu = 0.25$ has been used which is the same as that used in [64] to evaluate the kinetic energy constant k. For $\nu = 0.25$, $c_2 = 0.634 \, c_\ell$, and from $V_T = 0.38 \, c_\ell$, we have $V_T = 0.6 \, c_2$. It is apparent from the figures that for a velocity ratio which is in the range of 0.3 to 0.6, there is a considerable difference between static and dynamic stress intensity factors and hence, the quasi-static approximation for the dynamic fields does not seem to be justifiable. Particularly since the energy exchange takes place in the immediate vicinity of the crack tip

any misrepresentation of the stress and displacement fields in this region is likely to alter the results even if the gross fields away from the crack tips were approximately the same*.

A further objection to the theory as outlined above may be raised on the ground that in computing the available elastic energy from the static solution, it is essentially assumed that the stress wave velocities are infinite. On the other hand, in the evaluation of the kinetic energy, the finiteness of the propagation velocities of the elastic disturbances is observed. In the actual problem of a large plate subjected to loads at infinity which are increased slowly up to values sufficient to initiate fracture and then held constant, the available energy to overcome the dissipation and increase the kinetic energy comes from the released elastic potential within a circular region of radius $c_1 t$, c_1, being the dilatational wave velocity in plane stress. It is obvious that outside this circle, the stress state is that of uniform tension and the velocities are zero. A similar and much simpler situation is observed in a long slender bar of unit cross-section under tension σ, in which the load or the grip in one

---

*A clear experimental verification of this argument will be found in Beebe's recent work [84] where the isochromatics obtained experimentally are compared with those obtained from the static solution and the dynamic solution given by Broberg [61].

end is suddenly released. At the instant of release, $t = 0$, the stress waves start to travel toward the loaded end, leaving behind an unloaded portion of the bar of length $c_\ell t$ moving with a (particle) velocity $\sigma c_\ell / E$. For this "disturbed" part of the bar, the released strain energy $V = \frac{1}{2E} \sigma^2 c_\ell t$ is entirely transformed into the kinetic energy, i.e., $T = \frac{1}{2} m v^2 = \frac{1}{2} \rho c_\ell t (\sigma c_\ell / E)^2 = \frac{1}{2E} \sigma^2 c_\ell t$.

In the plate problem, actually during the fracture propagation, the work of the external loads, U, is zero and V is the change in the elastic energy in the circular region $r = c_1 t$. The error introduced through replacing this energy by its static equivalent given in (28) may be difficult to estimate, but is unlikely to be negligible.

A somewhat hypothetical but a complete mathematical equivalent of Mott's problem is that of a plate with a central propagating crack under the influence of pressure p acting on the crack surfaces. Here, U is p times the total volume of the gap formed by the fracture surfaces, V is the elastic energy stored in the circular region $r = c_1 t$, T is the kinetic energy of this region and D again is $4\gamma_f a$. Initial values of all these energies are zero, hence, $E_0 = 0$, and at time t (27) becomes

$$U = T + V + D \tag{39}$$

Since the quantities U, V and T are proportional to a^2 and D is proportional to a, it is obvious that for large

34

values of the crack length 2a, the dissipation may be neglected. Thus, the propagation of crack becomes the motion of a surface disturbance in a nondissipative medium. Such a motion is known to have the velocity of the Rayleigh surface waves [69], which is the same as the velocity of the edge dislocations in the medium [70,71]. For $\nu = 0.25$, the Rayleigh velocity is $c_r = 0.9194\ c_2 = 0.581\ c_\ell$ as compared to $V_T = 0.38\ c_\ell$ obtained in [64]. It should be pointed out that the conclusion $V_T = c_r$ is based on the following assumptions: a) the crack is maintained to run along a straight path, b) γ_f is independent of crack velocity, c) the plate is infinitely large and loading conditions at infinity remain unchanged during propagation. In a real problem, none of these assumptions seems to be satisfied. It will be seen later that because of the stress state around a propagating crack, above a certain velocity ($\simeq 0.61\ c_2$), the original crack plane is no longer the weak cleavage plane and, as is amply substantiated by the experiments on glass [72], the crack tends to bifurcate. As pointed out earlier, the fracture energy is not constant and for high crack velocities, it seems to be an increasing function of the velocity. Also, for the plates of finite size, the reflected waves from free and loaded boundaries would complicate the analytical picture, however, it is not difficult to qualitatively show that in the case of fixed grips or loading attachments with high inertia, the reflected waves have the effect of superimposed compression and hence, tend to slow down the propagation velocity.

The theory described above has also been applied to the cleavage of rectangular strips by Gilman [73] and Berry [65] where simple beam equations with quasi-static assumptions have been used to evaluate kinetic and potential energies. In connection with this problem, it should be pointed out that even at very slow velocities, the growth direction of the cleavage crack for an isotropic homogeneous strip is not stable, a small deviation from the growth direction would make the crack run perpendicular to the nearest free boundary [74]. This instability may be removed by applying a longitudinal compression to the strip [75]. However, most cleavage experiments are performed by either weakening the strip along the cleavage plane by making grooves along the sides [76] or using anisotropic materials with weak cleavage planes.

1.4.2 Energy Balance Around The Crack Periphery

In considering Griffith theory for equilibrium cracks, Sanders [77] pointed out that the region for which the energy balance holds can be any portion of the body enclosed within a simple closed curve L surrounding the crack tip where the energy is being dissipated. In three dimensional cases, this curve may be the profile of a toroidal region surrounding the crack periphery. Thus, the Griffith criterion may be stated as [77], "the rate at which work is being done by forces acting across L equals the rate of increases of strain energy stored in the material inside L plus the rate at which

energy is dissipated by the growing crack", the rate being
with respect to some parameter which increases with the ex-
panding crack periphery. For dynamic problems of propagating
cracks, the implication of this approach is that the energy
balance equation (18) may also be written for such a region
by simply adding the kinetic energy component. R and S in
(19 to 20) then become the volume and the surface of this
toroidal or cylindrical region generated by L (Figure 5).

In a somewhat incomplete manner, this approach
was considered for dynamic problems by Craggs [68], McClintock
and Sukhatme [78] and Kostrov [79,80]. In these papers, the
energy balance equation is used in the form

$$U^\cdot = D^\cdot \tag{40}$$

ignoring the kinetic and potential energies[*]. It has already
been pointed out that for a nondissipative system, $U^\cdot = T^\cdot + V^\cdot$.
For small crack velocities, $T^\cdot + V^\cdot$ may indeed be negligible
(see the example discussed below). As the volume R or the
curve L surrounding the crack tip shrinks to zero, the quanti-
ties T and V as well as U approach zero, however, their time
rates do not. Obviously, for the energy balance, the particular

---

[*]In Craggs' paper, the criterion, equation (2.5), appears to
be the comparison of the strain energy in the small region
enclosing the crack and the average fracture energy for time
increment Δt. Later, however, the rate at which the work is
done by the tractions acting across a small circle surrounding
the crack tip is evaluated and compared with the dissipation
rate.

shape chosen for the region R is not important, and it is generally assumed that the curve L enclosing R has a fixed size as well as a definite shape and moves with the propagating crack. As indicated by Kostrov [79], the energy rates related to the motion of the region R are of a smaller order of magnitude and vanish in the limit as R goes to zero.

In [78], a semi-infinite crack growing in an infinite medium under longitudinal shear (applied on the crack surface travelling with the crack or at infinity) is considered. The region R is taken to be a square with the crack tip at the center. The trend of the dependence of $U^{\cdot}$ to the crack velocity seems to agree with the result of the example given below.

In [68], the energy rate equation is used to obtain the terminal crack propagation velocity for the plane problem with the central crack. The plane strain or generalized plane stress problem for the case of an internal crack growing at both ends with a constant velocity and uniform tension at infinity is solved by a much simpler method than that of Broberg by taking advantage of the self-similar character of the dynamic problem and using the method due to Goldstein and Ward [81]. It is found that, after going through a maximum at a velocity ratio $v = (V_0/c_2) = 0.3728$, $U^{\cdot}$ decreases with increasing v, becomes zero for $v = 0.721$ and, apparently, is negative thereafter. Hence, it is concluded that the terminal velocity for rectilinear cracks would be $V_T = 0.721\ c_2$ rather than the Rayleigh wave velocity as predicted by Baren-

blatt, Broberg, Stroh and others. However, the result in [68] may be incorrect. It appears that in equation (3.13) (of [68]) giving U˙ a Jacobian is missing, as the arc length used is that of transformed plane and not the real plane.

Using the solution given in [68] with a small square region of size δ^2 around the crack tip, in limit for $\delta \to 0$ for one fourth of energy rate, we find

$$U^{\cdot} = \frac{p^2 t c_2^2 v^4}{2\mu H^2} \left[\frac{2}{\sqrt{1-v^2}} \tan^{-1} \sqrt{1-v^2} \right.$$

$$- \frac{(2-v^2)^2}{2(1-k^2v^2)^{3/2}} \tan^{-1} \sqrt{1-k^2v^2} + 2\sqrt{1-v^2} \tan^{-1} \frac{1}{\sqrt{1-v^2}}$$

$$\left. - \frac{(2-v^2)^2}{2\sqrt{1-k^2v^2}} \tan^{-1} \frac{1}{\sqrt{1-k^2v^2}} \right] \tag{41}$$

$$H = \left(4 + \frac{(2-v^2)^2}{1-k^2v^2} \right) E(\sqrt{1-k^2v^2}) - \left(v^4 + \frac{k^2v^2(2-v^2)^2}{1-k^2v^2} \right) K(\sqrt{1-k^2v^2})$$

$$- 8 E(\sqrt{1-v^2}) + 4 v^2 K(\sqrt{1-v^2})$$

$$v = V_0/c_2 \ , \ k = c_2/c_1$$

where p is the stress at infinity, V_0 is the crack velocity and K and E are the complete elliptic integrals of first and second kind, respectively. U˙/4 as obtained from (41) is shown in

39

Figure 6 as a function of velocity ratio and does seem to increase with increasing v. In the limiting case when $v \to 0$, H goes to $-2v^2(1-k^2)$ and the quantity in the bracket in (41) goes to $\pi v^2(1-k^2)$; thus dividing $U^\cdot$ by $V_0 = da/dt$ and substituting $V_0 t = a$, (41) reduces to

$$\frac{dU}{da} = \frac{\pi p^2 a(1-v^2)}{2E} \qquad (42)$$

which becomes the Griffith criterion when put equal to γ_f.

The axially symmetric propagation of a penny-shaped crack with constant stresses acting at infinity perpendicular to the plane of the crack is considered by Kostrov [79]. The solution is given for constant crack velocity arguing that initially there may be such a phase if it is assumed that the main dissipation comes from the plastic work and, initially, the dimensions of the plastic zone increases linearly with the increasing crack radius. Thus, assuming that the dissipation is proportional to the volume of plastic region, D becomes proportional to $(V_0 t)^3$ and $D^\cdot$ to t^2. If such a phase exists, then $U^\cdot$ should also be proportional to t^2. Using now this as a condition for constant velocity fracture growth, it is shown that the correct dynamic solution should have a singularity at the crack tip for stresses and velocity of order $\sqrt{t/\delta}$, δ being a small distance from the crack tip. Presumably, after a while, the plastic zone size attains a stationary value and $D^\cdot$ increases only linearly with t and since $U^\cdot$ is still proportional to t^2 crack starts accelerating.

In the uniform crack propagation phase, the energy rate equation $U^{\cdot} = D^{\cdot}$ does not contain t and provides an equation for the constant crack velocity V_0. In [79], it is also shown that at $V_0 = c_r$, $U^{\cdot}$ becomes zero from which it is concluded that V_0 obtained from $U^{\cdot} = D^{\cdot}$ cannot be greater than or equal to the Rayleigh wave velocity. To compute $U^{\cdot}$, Kostrov assumed the region R to be a rectangle with sides $2\delta_1$ and $2\delta_2$ in the r and z directions, respectively, and let $\delta_2 \rightarrow 0$ for fixed δ_1. Thus, integrals along δ_2 vanish. However, in principle, $U^{\cdot}$ should be independent of the shape of the region R and since a strip of zero thickness with different orientations would give different values for $U^{\cdot}$, there is some doubt as to the validity of the method used by Kostrov to evaluate $U^{\cdot}$. This point will be discussed further in the next section. In [80], Kostrov considers the plane shear problem which is the skew-symmetric counterpart of the plane problem solved by Broberg [61] and Craggs [68]. The assumptions, the treatment and the conclusions of [80] are the same as those for the penny-shaped crack considered in [79][*].

---

[*]Recently, the penny-shaped crack problem has also been considered by Craggs [82], where with a Barenblatt-type fracture criterion in mind, the stress intensity factor in σ_z is plotted against the velocity ratio.

1.4.3 Further Discussion Of Energy Balance And Crack Closure Energy

Consider a solid fracturing along a plane. Let a(t) represent the periphery or the front of the propagating crack, R be a small region surrounding the crack periphery and the smooth curve L be the boundary of the profile of this region (Figure 5). Considering the phenomenon as a point function in time, we state that the rate of external work done on the region R by the tractions acting on its surface will be equal to the sum of the rates of potential energy (i.e., strain energy), kinetic energy and the dissipative energy in the region R:

$$U^{\cdot} = V^{\cdot} + T^{\cdot} + D^{\cdot} \tag{43}$$

In order to avoid the complications which may arise from the fact that the relative position of the curve L with respect to the crack front is independent of time, that is, region R moves with the advancing crack front, we will assume that the material is basically elastic, the zone of energy dissipation is restricted to the immediate vicinity of the crack front and R is large compared to this dissipation zone. For example, if an appreciable portion of L goes through a part of the medium which has experienced plastic deformations prior to the time under consideration, the prediction of $U^{\cdot}$ by the elastic solution may be in error. Obviously, if the dissipation zone (e.g., plastic zone) is not small compared to R, the predictions in $V^{\cdot}$ and $T^{\cdot}$ would also be in error. The term $D^{\cdot}$ in (43) in-

cludes the rate of change of surface tension energy and increase in thermal energy due to the plastic work or viscous friction in the dissipation zone.

Now, for simplicity, consider a symmetric case in which in the plane of the crack, the surface tractions vanish on the crack surface and the shear stresses and the displacement perpendicular to the plane of the crack vanish outside the crack surface. Let the solid be separated into two halves by the crack plane and be held in equilibrium by applying proper normal tractions on the cut plane. Furthermore, assume that these tractions are the same as the normal stress on the cut plane outside the crack surface obtained from the dynamic solution of the problem. The problem for the half solid then would be identically equivalent to the original crack propagation problem. On the other hand, the problem of the half solid is conceptually a simple problem in elastodynamics with time-dependent boundary conditions. If we now consider one half of the region R, the kinetic and potential energy rate densities in this region will be the same as those in the original problem, the part of the work done by the surface tractions across L will be $U^{\cdot}/2$, i.e., same as in (43), and the remainder of the external work will be done by the fictitious tractions applied along the cut plane. Since there is no rupture, $D^{\cdot}$ will be zero. As the crack front a(t) advances the surface tractions at its periphery are released. Since the displacement perpendicular to the cut plane and the shear stresses remain to be zero ahead of the crack

43

front, it is obvious that the work of the released tractions will be the only contribution to the external work from the plane boundary of the region R. It is also obvious that the time rate of this work will be a negative quantity, as the direction of the tractions are opposite to that of the displacement through the release period. Calling this energy rate $-\dot{E}_c/2$, it is seen that $\dot{E}_c$ is nothing but the time rate of the crack closure energy. If σ_y and u_y are the traction on the cut plane and the displacement on the crack surface perpendicular to the plane, referring to Figure 7, we can write

$$dE_c = \dot{E}_c \, dt = 2 \int_a^{a + \dot{a} \, dt} \frac{1}{2} \sigma_y(\alpha) \, u_y(\alpha - \dot{a} \, dt) \, d\alpha \qquad (44)$$

The energy rate balance for the half of the region R may then be expressed as

$$\frac{\dot{U}}{2} - \frac{\dot{E}_c}{2} = \frac{\dot{T}}{2} + \frac{\dot{V}}{2} \qquad (45)$$

Comparing (43) and (45), it is now seen that

$$\dot{D} = \dot{E}_c \qquad (46)$$

that is, the time rate of change of the crack closure energy is equal to the dissipation rate.

Strictly speaking (46) is correct only for ideally brittle materials in which there is no dissipation other than the surface-free energy. However, using the same argu-

ments as those employed by Irwin and Orowan in extending the Griffith theory to the quasi-brittle fracture and within the same degree of accuracy, (46) may also be used in the fracture dynamics of quasi-brittle materials. It should be noted that as the crack velocity goes to zero, $\dot{V} \to 0$, $\dot{T} \to 0$ and $\dot{U}$ approaches the rate of crack closure energy or more precisely,

$$\lim_{\dot{a} \to 0} \frac{1}{\dot{a}} \dot{E}_c = \frac{dE_c}{da} = \lim_{\dot{a} \to 0} \frac{\dot{U}}{\dot{a}} = \frac{dU}{da}$$

It should also be noted that in dynamical problems, $\dot{E}_c$ is not equal to the strain energy release rate. In fact, considering now the whole solid with an internal plane propagating crack, for the spherical (disturbed) region with radius $c_1 t$, $\dot{U} = 0$ and the energy rate equation becomes

$$\dot{V} + \dot{T} + \dot{D} = 0 \tag{47}$$

which, by using (46), may be written as

$$- \dot{V} = \dot{T} + \dot{E}_c \tag{48}$$

In (48), $-\dot{V}$ is the total strain energy release rate and $\dot{T}$ is the rate of kinetic energy for the sphere $c_1 t$. Thus, if $\dot{T}$ is not zero, the rates of strain energy release and crack closure energy will not be equal. The importance of (46) becomes more obvious if one considers the fact that $\dot{E}_c$ is the easiest energy rate to compute once the solution around the crack periphery is obtained.

45

As an example, consider the plane with a propagating central crack, the solution of which is available [61,68]. In this case, the stress on the crack plane near the tip at $x = \alpha$ is given by (8) where r corresponds to $\alpha - a$ in Figure 7 and equation (44). From [61], the displacement may be obtained as

$$u_y \simeq \frac{pv^2\sqrt{2a}}{H\mu}\sqrt{a - x}$$

$$H = 8\ E(\sqrt{1-v^2}) - (4 + \frac{(2-v^2)^2}{1-k^2v^2})\ E(\sqrt{1-k^2v^2})$$

$$- 4v^2 K(\sqrt{1-v^2}) + (v^4 + \frac{k^2v^2(2-v^2)^2}{1-k^2v^2})\ K(\sqrt{1-k^2v^2})$$

$$k = c_2/c_1\ ,\ v = V_0/c_2 \tag{49}$$

Substituting from (8) and (49) into (44) with $x = \alpha - a\cdot dt = a + r - a\cdot dt$, and observing that $a\cdot = V_0 = vc_2$, we obtain

$$\frac{1}{4}\ \dot{E}_c = \frac{\pi}{4}\ \frac{p^2c_2^2tv^4}{\mu H^2}\ [4\sqrt{1-v^2} - \frac{(2-v^2)^2}{\sqrt{1-k^2v^2}}] \tag{50}$$

In limit, as $v\to 0$, $H\to -2v^2(1-k^2)$ and from (50), we obtain

$$\frac{1}{vc_2}\ \dot{E}_c = \frac{dE_c}{da} = \frac{\pi}{2}\ \frac{p^2c_2vt}{\mu(1-k^2)} = \frac{2\pi}{E}\ p^2a(1-\nu^2) \tag{51}$$

which is nothing but the strain energy release (or closure energy) rate per unit crack extension in the static case.

In light of the above discussion, it now appears that the results found by Kostrov [79,80], are basically correct. However, the quantity he computed is not the rate of the external work, $U^{\cdot}$, done on a small region R around the crack periphery but the crack closure energy $E_c^{\cdot}$. The energy balance equation (43) is invariant with respect to the choice of the region R and the finite terms in the quantities $U^{\cdot}$, $V^{\cdot}$ and $T^{\cdot}$ are independent of the size parameter δ, if there is only one such parameter which goes to zero in limit. If there are more than one independent size parameter involved, the result will not be unique and will depend on the details of the limiting process. Thus, for example in Kostrov's method, if one lets δ_1, the size of rectangular region R in r direction, go to zero for a fixed δ_2, the size in z direction, again the volume of R is reduced to zero beforehand and hence, $T^{\cdot}$ and $V^{\cdot}$ would vanish but the value of $U^{\cdot}$ would not be equal to that computed by Kostrov.

For $\nu = 0.25$, Figure 6 shows the variation of $\frac{E_c^{\cdot}}{4}$ as obtained from (50) and that of $U^{\cdot}/4$ as given by (41) with the velocity ratio v. For small values of v, (e.g., v<.3), $T^{\cdot}$ and $V^{\cdot}$ in R are negligible and both $U^{\cdot}$ and $E_c^{\cdot}$ are approximately equal to the corresponding static value. For relatively large values of v, $U^{\cdot}>E_c^{\cdot}$, and the difference is equal to $T^{\cdot} + V^{\cdot}$ in the region R. Here, $E_c^{\cdot}$ then may be considered as the available energy to be used to overcome the dissipation or the fracture energy. From Figure 6, it is seen that $E_c^{\cdot}$ will be zero at the Rayleigh wave velocity.

This result is independent of ν and is quite general. For example, the same conclusion was arrived at by Kostrov in the two problems he considered[*]. The clear implication of this result is that, provided the crack can be maintained to run straight, the Rayleigh wave velocity, c_R, is an upper limit for the velocity of a propagating crack, may be attained as a limit only in ideally nondissipative medium (i.e., $\gamma_F = 0$) and propagation velocities above c_R require energy generation at the crack periphery, hence, practically impossible. This is perhaps, a restatement of the well-known result found by Eshelby [71] in connection with the moving edge dislocations.

We may also observe from Figure 6 that $E_c^{\cdot}$, the rate of available energy, has a maximum around $v = 0.6$ (for $\nu = 0.25$, $v = 0.62$). Even though the value of $E_c^{\cdot}$ increases with time, t linearly, the location of its maximum is independent of t. It is clear that if γ_F is constant or does not increase with increasing crack length (i.e., with time and/or crack velocity) sufficiently fast, there will be a constantly increasing excess energy rate $E_c^{\cdot} - D^{\cdot}$ which will accelerate the crack making its velocity to approach asymptotically the Rayleigh wave velocity. For example, if p_c is the value of the external load at crack initiation for a small (existing) crack $2a_o$, and γ_{Fo} is the corresponding

---

[*] For a similar result in shear cracks, see the following section.

fracture energy, from Griffith theory, we have

$$p_c^2 = \frac{2E\gamma_{F0}}{\pi a_0 (1-\nu^2)} \tag{52}$$

Letting $p = n p_c$ and $v c_2 t = a$, from (50) and (52), we obtain

$$d(n, \frac{a}{a_0}, v.) = \frac{n^2}{1-\nu} \frac{a}{a_0} \frac{v^2}{H^2} [4\sqrt{1-v^2} - \frac{(2-v^2)^2}{\sqrt{1-k^2 v^2}}] = \frac{\gamma_F}{\gamma_{F0}} \tag{53}$$

which is shown in Figure 8 for $n = 1$, $\frac{\gamma_F}{\gamma_{F0}} = 1$ and various

values of $\frac{a}{a_0}$. Figure 8 indicates that if γ_F is constant, for

$n = 1$ at $a = a_0$, there will be equilibrium. In order to start

the propagation, n has to be - even if only slightly - greater

than unity. If $n > 1$, there is some energy available for ac-

celeration; as v goes up the available energy for acceleration,

$E_c^{\cdot} - D^{\cdot}$ will also increase. This will result in either branch-

ing of the crack or increase in the fracture propagation ve-

locity approaching asymptotically the Rayleigh wave velocity.

On the other hand, for some period of the crack

growth if, as assumed by Kostrov, the dissipation is primarily

due to the plastic work in a small dissipation zone around the

crack tip, assuming this work to be proportional to the volume

of the dissipation zone, we may write $D = A_1 a^2$ and from

$a = c_2 vt$, we obtain $D^{\cdot} = Av^2 t$, A being a constant. In this

case, the fracture criterion $E_c^{\cdot} = D^{\cdot}$ would not contain t and

would provide an equation for the determination of the corre-

sponding crack velocity, provided the constant A (which will

be dependent on the structure of the material as well as the

environmental conditions) is known. Figure 9 shows such a result for a hypothetical value of A. From the figure, it is obvious that, if the assumptions mentioned above are valid, the crack growth at the terminal velocity v_T is stable, as the available energy for acceleration is positive for $v < v_T$ and negative for $v > v_T$.

In real materials, it is very unlikely that the conditions concerning $D^{\cdot}$ and γ_F would conform to either of the ideal cases shown in Figures 8 and 9. However, based on the results found so far, some general observations may be made: The experimental evidence point to the fact that at higher fracture velocities, the roughness of fracture surfaces increases, resulting in higher fracture energies. As conjectured by Irwin, this may be due to the tendency of the crack to branch or small cracks forming but not propagating at $\theta \pm 60°$ planes ahead of the running crack. However, as seen from Figure 4, branching would not be expected to take place at velocities below[*] $0.6\ c_2$ which seems to be higher

---

[*]For $\nu = .25$, at $\theta = 0$, $\dfrac{\partial \sigma_\theta}{\partial \theta} = 0$ and $\dfrac{\partial^2 \sigma_\theta}{\partial \theta^2} = 0$, for $v = 0.629$

$\dfrac{\partial^2 \sigma_\theta}{\partial \theta^2} > 0$ for $v > 0.629$, $\dfrac{\partial^2 \sigma_\theta}{\partial \theta^2} < 0$ for $v < 0.629$, meaning that the maximum cleavage stress for $v > 0.629$ will be at some angle other than $\theta = 0$.

than experimentally measured terminal crack velocities in isotropic materials. An important property of the plane problems seems to be that the velocity at which the direction of the maximum cleavage stress at the crack front deviates from the main direction of the crack is approximately the same as the velocity at which crack closure energy, E_c^*, is maximum[*] (Figures 4 and 6). Following Irwin's conjecture, it may be assumed that at fracture velocities above 0.6 c_2, the fracture energy will increase with increasing velocity at a much higher rate. Now, since for $v < 0.6$, the rate of the energy pumped into the region around the crack tip increases with increasing time and the fracture velocity, it may be expected that the crack velocity would tend to stabilize at or below $v = 0.6$ if the increase in γ_F is sufficiently high. On the other hand, the crack would bifurcate around or above $v = 0.6$ if γ_F remains to be relatively low. For example, the behavior of most metallic compounds undergoing brittle fracture belongs to the former and that of glass and some polymers at low temperatures belongs to the latter type response.

It should be noted that the foregoing observations are based on the two-dimensional analysis of infinite isotropic, homogeneous, elastic media subjected to time-independent uniform boundary conditions at infinity. It is obvious

---

[*]This does not seem to be a general rule. See, for example, the following section.

that if the medium is finite and "the external loads" are time-dependent, the reflected waves and the waves generated at the boundary would alter the stress state around the crack front. For example, in rectangular plates with fixed grips, the effect of the waves reflected from grips is similar to that of a superimposed compressive field, thereby reducing the intensity of the stress field around the crack and causing a decrease in the crack velocity. The oscillatory behavior of some of the experimentally measured crack velocities may be attributed to this effect.

In the case of anisotropic materials, because of the changes in stress state and the behavior of fracture energy due to anisotropy, the situation concerning terminal velocity and crack branching may be somewhat different. For the most part, anisotropic materials have a weak cleavage plane along which fracture energy, γ_F is lower than that for other orientations. If the fracture is propagating along such a weak plane, tendency for crack branching would take place at velocities which are higher than the velocity obtained from theoretical considerations (i.e., $\partial^2 \sigma_\theta / \partial \theta^2 = 0$). As a result, in anisotropic materials, it is possible to observe crack velocities far in excess of those observed in isotropic materials and beyond the limit of approximately 0.6 c_2 described above. For example, in a recent paper, Hull and Beardmore [83], report fracture velocities in tungsten single crystals as high as 0.83 c_2.

1.4.4 An Example: Longitudinal Shear Cracks

In this section, we will consider the anti-plane equivalent of the plane problem of a propagating internal crack in an infinite medium treated by Broberg [61], and Craggs [68]. The problem is that of an infinite elastic medium subjected to a uniformly distributed shear load $\tau_{yz} = q$ at infinity and containing a (through) crack on $y = 0$ and $|x| < a$ which grows with a constant velocity V_0, i.e., $a = V_0 t$, t being the time (Figure 10). From a practical viewpoint, the problem is not very interesting; however, since it lends itself to a relatively simple analytical treatment, it is used here as vehicle to demonstrate the application of some of the ideas discussed in the previous sections.

Here, it is assumed that the crack forms at the time $t = 0$ and spreads at a constant velocity V_0 in $y = 0$ plane. Because of the geometry and the loading conditions, it is also assumed that the perturbations arising from the motion of the crack are independent of z and are polarized in xy plane. The only nonzero component, the z-component w, of the displacement vector will then satisfy the following wave equation:

$$\frac{\partial^2 w}{\partial x^2} + \frac{\partial^2 w}{\partial y^2} = \frac{1}{c_2^2} \frac{\partial^2 w}{\partial t^2} \tag{54}$$

where $c_2 = \sqrt{\mu/\rho}$ is the shear wave velocity in the medium, μ and ρ being the shear modulus and the mass density of the material. The nonzero components of the stress tensor are

$$\tau_{xz} = \mu \frac{\partial w}{\partial x} \; , \; \tau_{yz} = \mu \frac{\partial w}{\partial y}$$

or

$$\tau_{rz} = \mu \frac{\partial w}{\partial r} \; , \; \tau_{\theta z} = \frac{\mu}{r} \frac{\partial w}{\partial \theta} \tag{55}$$

Equation (52) must be solved under the following conditions:

$$w^{\cdot} = 0, \; \tau_{yz} = q, \; \tau_{xz} = 0 \text{ for } t \leq 0, \; r \geq 0$$

$$\tau_{yz} = 0 \text{ for } y = 0, \; |x| < a = V_o t \tag{56}$$

$$w = 0 \text{ for } y = 0, \; |x| > a$$

where dot refers to differentiation with respect to time.

By superposition, it can be shown that the dynamic problem is equivalent to that in which an initially stress-free solid develops a small crack at t = 0 which propagates at a constant velocity V_o and the surface of which is subjected to constant tractions $\tau_{yz} = -q$ for t > 0. This latter problem refers to the perturbations caused by the propagating crack in the original problem and satisfies the following conditions:

$$w = 0, \; w^{\cdot} = 0 \text{ for } t = 0$$

$$\tau_{yz} = -q \text{ for } y = 0, \; |x| < V_o t \tag{57}$$

$$w = 0 \text{ for } y = 0, \; |x| > V_o t$$

To obtain a solution for the problem which is valid around the crack tips, one may use the technique developed by Goldstein and Ward [81], for the supersonic conical fields and applied by Craggs to the plane problem [68], by observing that the problem has no fundamental length. Letting

$$\tau = c_2 t, \quad v = V_0/c_2, \quad \alpha = r/\tau = \text{sech} \ (-\beta)$$

$$\zeta = \xi + i\eta = \text{sech} \ (\beta+i\theta)$$

$$w = \text{Re} \ \phi(\zeta), \quad \Phi(\zeta) = \phi'(\zeta) \ \text{for} \ \eta > 0,$$

$$\Phi(\zeta) = - \overline{\phi}'(\zeta) \ \text{for} \ \eta < 0 \tag{58}$$

We find that the crack tips $x = \mp V_0 t = \pm v\tau$ in (r,θ) plane correspond to the branch points $\xi = \pm v$ in ζ plane and the solution valid for small values of $|\zeta-v|$ can be written as

$$\Phi(\zeta) \simeq \frac{2q\tau}{\mu\pi i} \sqrt{\frac{v}{2}} \ \frac{K(v)}{\sqrt{\zeta-v}} \tag{59}$$

where $K(v)$ is the complete elliptic integral of first kind. Equation (59) with the transformations given in (58) determines w and the stress components may be obtained from

$$\tau_{rz} = \frac{\mu}{\tau} \frac{\partial w}{\partial\alpha}, \quad \tau_{\theta z} = \frac{\mu}{\alpha\tau} \frac{\partial w}{\partial\theta} \tag{60}$$

First, we obtain the shear stress $\tau_{\theta z}$ at $\theta = 0$ which, from (58), (59) and (60), may be written as

$$\tau_{\theta z}\bigg|_{\theta=0} = \frac{2q}{\pi} \sqrt{\frac{v}{2}} K(v) \frac{\sqrt{1-v^2}}{\sqrt{\alpha-v}} = \frac{2q}{\pi} \sqrt{\frac{a}{2\rho}} K(v) \sqrt{1-v^2} \qquad (61)$$

where $\rho = (\alpha-v)$ $\tau = r - a$ is a small distance from the crack tip $a = v\tau$. For small values of v, $K(v) \to \frac{\pi}{2}$ and (61) reduces to $\tau_{\theta z} = q \sqrt{\frac{a}{2\rho}}$, which is the static solution. The stress intensity factor obtained from (61) and the corresponding static value evaluated by using the same crack length are shown in Figure 11. The variation of the stress intensity factor is similar to that obtained for the plane problem which is shown in Figure 3. However, the velocity ratio at which it becomes maximum is considerably higher than the corresponding value for the plane problem (0.694 as compared to 0.39)[*]. More importantly, in the shear problem, the stress intensity factor becomes zero at the shear wave velocity c_2 rather than the Rayleigh wave velocity as observed in the plane problem.

Next, we consider the variation of the shear stress $\tau_{\phi z}$ in the neighborhood of the crack tip as a function

---

[*]The values for plane problem is for $\nu = 0.25$. In the shear problem $\frac{\partial}{\partial v} \tau_{\theta z} = 0$ leads to $2E(v) = (1+v^2)K(v)$, which gives $v = 0.694$ and is independent of the elastic constants.

of ϕ and v (Figure 12). Noting that

$$\tau_{\phi z} = \tau_{\theta z} \cos \phi - \tau_{rz} \sin \phi$$

we obtain

$$\tau_{\phi z} = \frac{2q}{\pi} \sqrt{\frac{a}{2\rho}} K(v) \sqrt{1-v^2} (\cos \frac{\psi}{2} \cos \phi$$

$$+ \frac{\sin \frac{\psi}{2} \sin \phi}{\sqrt{1-v^2}}) (1-v^2 \sin^2\phi)^{-\frac{1}{4}}$$

$$\tan \psi = \sqrt{1-v^2} \tan \phi \tag{62}$$

For $v \to 0$, (62) reduces to the static value $\tau_{\phi z} = q\sqrt{\frac{a}{2\rho}} \cos \frac{\phi}{2}$.

It is easily verified that $\phi = 0$ is a root of $\frac{\partial}{\partial \phi} \tau_{\phi z} = 0$. If the second derivative is taken, it is found that at $\phi = 0$

$$\frac{\partial^2}{\partial \phi^2} \tau_{\phi z} \begin{cases} = 0 \text{ for } v^2 = 1/3 \\ < 0 \text{ for } v^2 < 1/3 \\ > 0 \text{ for } v^2 > 1/3 \end{cases}$$

meaning that for $v > 1/\sqrt{3} \cong 0.578$, the maximum of $\tau_{\phi z}$ will occur in a plane other than $\phi = 0$. The variation of $\tau_{\phi z}$ in v and ϕ is shown in Figures 13 and 14. Figure 13 shows only the ϕ-dependent part of $\tau_{\phi z}$. However, to have an idea about the relative magnitudes of the stress intensity factors at various

57

angles - which may be important in considering branching - the complete v-dependence as well as the dependence on ϕ has to be considered. This is shown in Figure 14. It is seen that velocities up to v = 0.7, the curves are rather flat and branching may depend largely on the distribution and the orientation of the imperfections on the path of the running crack. As the velocity approaches c_2, the stress intensity factor decreases in the region $0 < \phi < \pi/2$ and continuously increases in $\frac{\pi}{2} < \phi < \pi$.

We now choose a small region R surrounding the crack tip formed by $y = \mp\delta$, $x = a \pm \delta$ and evaluate the energy rates for one half of R (i.e., $0 \leq y < \delta$, $a -\delta < x < a + \delta$). From (58) to (60), we may write

$$\tau_{rz} = \frac{2q}{\pi} \sqrt{\frac{v}{2}} \, K(v) \, \text{Im} \, \frac{1}{\left[\sqrt{(\alpha-v)} + i \sqrt{1-v^2} \, v\theta\right]^{1/2}}$$

$$\tau_{\theta z} = \frac{2q}{\pi} \sqrt{\frac{v}{2}} \, K(v) \, \text{Re} \, \frac{v}{\left[\sqrt{(\alpha-v)} + i \sqrt{1-v^2} \, v\theta\right]^{1/2}} \qquad (63)$$

$$w^{\cdot} = - \frac{2q}{\pi} \sqrt{\frac{v}{2}} \, K(v) \, \frac{c_2 v}{\mu} \, \text{Im} \, \frac{1}{\left[\sqrt{(\alpha-v)} + i \sqrt{1-v^2} \, v\theta\right]^{1/2}}$$

Substituting from (63) into (19) and (21), we obtain[*]

---

[*] Note that the quantities given in (64) and (65) and plotted in the figures are 1/4 of the total values.

$$U^{\bullet} = \frac{2q^2}{\pi^2\mu} c_2{}^2 v^2 t K^2(v) \left(\frac{\tan^{-1}v'}{v'} + v' \tan^{-1} \frac{1}{v'}\right) \Bigg\} \quad (64)$$

$$T^{\bullet} = V^{\bullet} = \frac{q^2}{\pi^2\mu} c_2{}^2 v^4 t K^2(v) \frac{\tan^{-1}v'}{v'}$$

$$U^{\bullet} - T^{\bullet} - V^{\bullet} = \frac{q^2 c_2{}^2 t}{\pi\mu} K^2(v) v^2 \sqrt{1-v^2}$$

$$\hspace{9cm} (65)$$

$$v' = \sqrt{1-v^2}$$

From the displacement of the crack surface around the crack tip

$$w = \frac{4q}{\pi\mu} K(v) \sqrt{\frac{a}{2}} \sqrt{a-r} \qquad (66)$$

and $\tau_{\theta z}$ at $\theta = 0$ as given by (61), the rate of crack closure energy may also be evaluated as follows

$$dE_c^{\bullet} = E_c^{\bullet} dt = \int_a^{a + a^{\bullet} dt} \frac{1}{2} \tau_{\theta z}(x) w(x-a^{\bullet}dt) dx$$

or

$$E_c^{\bullet} = \frac{q^2 c_2{}^2 t}{\pi\mu} K^2(v) v^2 \sqrt{1-v^2} \qquad (67)$$

As shown for the more general problem in the previous section, $E_c^{\bullet}$ is the same as $U^{\bullet} - V^{\bullet} - T^{\bullet}$. From (64) and (67), one may easily observe that as $v \to 0$, $T^{\bullet} \to 0$, $V^{\bullet} \to 0$ and substituting

59

$vc_2t = a$, we have

$$\frac{U^{\cdot}}{vc_2} = \frac{E^{\cdot}_c}{vc_2} = \frac{\pi}{4\mu} q^2 a \qquad (68)$$

which is the static value (of one fourth of the strain energy release rate per crack extension).

The energy balance criterion $E^{\cdot}_c = D^{\cdot}$ may now be written as

$$\frac{q^2 c_2^2 t}{\pi\mu} K^2(v) \ v^2 \ \sqrt{1-v^2} = \gamma_F \ c_2 \ v \qquad (69)$$

For example, if γ_F is constant, the initial flaw size is $2a_0$ and the corresponding critical load is q_c, from the condition of equilibrium crack we may write

$$\gamma_F = \frac{\pi a_0 q_c^2}{4\mu} \qquad (70)$$

Letting $c_2 vt = a$ and $q = n q_c$, from (69) and (70), we obtain

$$\frac{4n^2}{\pi^2} \frac{a}{a_0} K^2(v) \ v\sqrt{1-v^2} = v \qquad (71)$$

For $n = 1$ and various values of a/a_0, this is shown in Figure 15. From (64), it can be seen that as $v \to 1$, the quantities $U^{\cdot}$, $V^{\cdot}$ and $T^{\cdot}$ approach infinity[*]. However, it can also be

---

[*]This could perhaps be predicted from the fact that as $v \to 1$, the stress intensity factor at $\phi = \frac{\pi}{2}$ approaches infinity (see Figure 14).

shown that the rate of available energy $U^{\cdot} - T^{\cdot} - V^{\cdot}$ vanishes (see Figure 15). This means that in the longitudinal shear case the shear wave velocity is an upper limit for fracture propagation and a propagation with a velocity higher than c_2 requires energy generation rather than dissipation at the crack tip. This result agrees with the Cottrell's finding that c_2 is an upper limit for the velocity of moving screw dislocations in a crystal [70]. The simple conclusion one may draw from Figure 15 is that if the fracture energy, γ_F, is constant and the crack can be maintained to grow straight, then the propagation velocity will asymptotically approach the shear wave velocity.

A significant difference between longitudinal shear and plane problems is that in the former, the energy rates $U^{\cdot}$, $V^{\cdot}$, $T^{\cdot}$ and the stress intensity factor at $\phi = \frac{\pi}{2}$ go to infinity as the fracture velocity approaches the characteristic elastic wave velocity (which, in this case, is c_2) whereas in the latter, all of these quantities remain finite as the characteristic wave velocity c_R is approached. Another significant difference is that in the shear problem $E_c^{\cdot}$ goes through a maximum at a much higher velocity (approximately 0.91 c_2 vs. 0.62 c_2) and the possible branching velocity is somewhat lower (0.578 c_2 vs. 0.629 c_2). Hence, based on the arguments of the previous section, one possible conclusion which may be drawn here is the following: in materials with high fracture energy, the likelihood of crack bifurcation is

higher in the longitudinal shear case than in plane problems.

As another ideal case, in this problem too we may assume the dissipation primarily due to plastic work which is proportional to the volume of the plastic zone. Assuming again that the characteristic plastic zone size is approximately linear in crack length, we may write[*]

$$D_p = Aa^2 \tag{72}$$

To determine the constant A, the Griffith condition can be used if we assume that (72) is valid for all velocities and crack lengths. Thus, if a_o is the initial flaw size, we have

$$\left.\frac{dD_p}{da}\right|_{a = a_o} = 2Aa_o = \left.\gamma_F\right|_{a = a_o} = \frac{\pi q_c^2 a_o}{4\mu} \tag{73}$$

With $a = vc_2 t$, from (72) and (73) we obtain

$$D_p = \frac{\pi q_c^2}{4\mu} c_2^2 v^2 t \tag{74}$$

Again letting $q/q_c = n$, the energy balance criterion $E_c = D_p$ becomes

$$\frac{E_c}{D_p} = \frac{4}{\pi^2} n^2 K^2(v) \sqrt{1-v^2} = 1 \tag{75}$$

---

[*]For, again, one fourth of total dissipation and per unit thickness.

For n = 1 and 1.05, this is shown in Figure 16 according to which, in this ideal case, there is a stable propagation velocity for each given load ratio and it is rather high even if n is very close to unity.

Perhaps the most unrealistic aspect of the foregoing ideal model is the assumption that the dissipation rate or the fracture energy is an increasing function in v for all velocities. However, in real materials, for small values of v, γ_F is known to decrease with increasing velocity. Hence, it is more likely that the actual dissipation rate would have a v-dependence more like the dashed-line shown in Figure 16, and as a result, the terminal velocity may be considerably lower.

In this simple example, one may also give an estimate of the plastic zone size and, particularly, examine its variation with the fracture velocity. Using the Dugdale approximation [85], the plastic zone size, p, is estimated to be (see: Appendix A)

$$p = \frac{q^2}{2q_y^2} c_2 v t \, f(\frac{q}{q_y}, v)$$

(76)

$$f(\frac{q}{q_y}, v) = \frac{(1-v^2)K^2(v)}{1 - (\frac{q}{q_y})^2 K(v)[E(v)-(1-v^2)K(v)]}$$

where q_y is yield stress in shear at the corresponding velocity, vc_2 and K and E are the complete elliptic integrals. The vari-

63

ation of the function f and, for a given value of $\lambda = (q/q_y) = 0.2$, the variation of $\Delta v = v_1 - v = p/c_2 t$ with the fracture velocity v are shown in Figure 17.

The estimate given by (76) is based on the assumption that the plastic zone size p is small compared to the half-crack length a or the external load q is small compared to the yield stress q_y. For the static case, the Dugdale approximation is known to give fairly good results [86]. In the dynamic case, if one assumes that for the constant velocity fracture all the factors, (such as plastic waves, unloading, etc.), involved in the formation of the plastic zone as well as the shape of the plastic region remain autonomous during the fracture propagation, the model may still be used to obtain an estimate of a characteristic plastic zone size. However, the estimate in this case is rather qualitative and its value lies largely in the fact that it also gives some idea about the dependence of the plastic zone size on the fracture velocity. As the angular dependence of the stress intensity factor indicates (Figure 14), the shape of the plastic zone would be, particularly at high fracture velocities, quite different than the static shape. The circular shape of the plastic region corresponding to static loading would become elongated perpendicular to the direction of crack propagation and, as the Figures 14 and 17 indicate, compared to a static plastic zone size for the same crack length, the size of the plastic region decreases in the direction of the crack growth and increases in the direction perpendicular to it with the increasing crack velocity.

Figure 18 shows such a variation where p is taken from Figure 17 for q/q_y = 0.2 and the remainder is qualitative. We hasten to add that, due to the unloading and the resulting residual stresses as the crack goes through the plastic region and, at high velocities due to the change in the wave velocity in the plastic region, the size and shape of the plastic zone would be modified.

Based on the preceding discussion and the approximate calculation leading to (76), we may draw the following conclusions: a) the hypothesis made by Kostrov to the effect that the plastic zone size is linearly dependent on the crack length is not correct, particularly at fracture velocities at which dynamic effects are significant (Figure 17). However, since the plastic zone becomes elongated as the crack velocity increases, at least for longitudinal shear problems, the volume of the plastic region may remain approximately proportional to a^2, a being the half-crack length; b) the estimate of the plastic work based on the Dugdale model (e.g., [87]) would be erroneous not only because of the variation in the shape of the plastic region with the fracture velocity, but also because of the complicated nature of the plastic energy

dissipation in the plastic region, particularly around its trailing boundary*.

To have some idea about the nature of the
energy balance around a propagating crack during the initial
stage of the crack growth in the presence of plastic deforma-
tions, in connection with the longitudinal shear, one more
simple problem may be considered. Let the plastic region
around the propagating crack be P and the elastic-plastic
boundary be L. During the fracture propagation, the rate of
the external work done by the tractions acting on L is bal-
anced by the sum of the rates of kinetic energy, stored elastic
energy and the plastic work in the region P and the surface-
free energy due to the creation of new crack surface. Some
rough approximations to these energy rates are obtained in the
Appendix B by using the static solution [88,89] and a quasi-
static assumption similar to Mott's [27]. The notation for
the analysis is shown in Figure 19 and the additional approxi-
mating assumptions are stated in Appendix B. For one half of
the plastic region P around the crack tip and unit thickness,
we have

$$U^{\cdot} = \frac{\pi q^4 a a^{\cdot}}{4\mu q_y^2}$$

$$T^{\cdot} = \frac{\pi \rho q^8}{32\mu^2 q_y^6} \, a a^{\cdot}(a^{\cdot 2} + a a^{\cdot\cdot}) \tag{77}$$

$$V^{\cdot} = \frac{3\pi q^4 a a^{\cdot}}{8\mu q_y^2} = V_E^{\cdot} + V_p^{\cdot}$$

$$D^{\cdot} = \gamma a^{\cdot} + V_p^{\cdot}$$

In (77), $V_E^{\cdot}$ is the rate of elastic energy, $V_p^{\cdot}$ is the rate of

plastic work and γ is the surface-free energy, where $V_E^{\cdot} = \pi q^4 aa^{\cdot}/(8\mu q_y^2)$. $U^{\cdot}$ is the rate of energy input and $T^{\cdot} + V_E^{\cdot} + D^{\cdot} = T^{\cdot} + V^{\cdot} + \gamma a^{\cdot}$ is the rate of stored and dissipated energies. It is clear from (77) that

$$U^{\cdot} < T^{\cdot} + V^{\cdot} + \gamma a^{\cdot}$$

meaning that the initial stage of the crack propagation for which the assumptions stated in the Appendix B are valid, is stable. That is, unlike an ideally brittle material, during this period, for a continuous crack growth, the external load has to be increased continuously. It was observed by Felbeck and Orowan [90] and noted by McClintock [91] that the instability starts after the crack goes through a distance approximately equal to the plastic zone size. It is obvious that, in the presence of plastic deformations, at the initial stage of the crack propagation, the energy balance theory is not sufficient to explain the fracture and some consideration of a critical strain is necessary. Further remarks on this aspect of the problem will be found in the article by McClintock and Irwin [1].

1.5 Energy Dissipation And The Experimental Studies

A quick glance at the continuum theories on fracture
propagation outlined in the previous sections reveals that,
from a practical viewpoint there are two important aspects
of the phenomenon which should firmly influence the nature of
the theory and the assumptions involved in its formulation.
These are the actual kinematics of the crack growth and the
energy dissipation during the propagation of fracture. By
the first, we simply mean the following: In a brittle or
quasi-brittle material, starting with the time of onset of
rapid fracture, what is the behavior of the crack size vs. time
relationship? Is there really a terminal velocity and, if
there is, what is its value? What is the relative duration
of the acceleration or development period of the crack growth?
And, most importantly, is the crack growth itself a continuous
or an intermittent phenomenon, that is, is the fracture veloc-
ity a monotonously increasing continuous function of time or
is it a discontinuous and/or oscillating function with time-
dependent mean and amplitudes?

In formulating a fracture propagation theory, in a
general way, the nature of the energy dissipation as well as
its existence should be considered. The important questions
arising in this connection would be the dependence of the
fracture energy on the propagation velocity, the approximate
size and the shape of the dissipative zone and the mechanism
and thermodynamics of the energy dissipation. The last two

69

points are raised partly to investigate the applicability of the linear elastic theories as working tools and the effect of heat generation in the dissipation zone.

From the outset, two things are quite clear, namely that the answers to the two groups of questions posed above will have to come from very careful, thorough and, in certain cases, rather ingenious experimental studies, and that these answers may very heavily depend on the type of material and, to some extent, on the environmental conditions under consideration. Putting aside the high-energy type slow fracture of elastomeric solids and plane stress rupture of highly ductile metal compounds, with respect to the kinematics of the crack growth, one could perhaps classify the brittle and quasi-brittle solids in the following manner: a) brittle single crystals, b) highly brittle amorphous materials, c) polymers below glass transition temperature, and d) the polycrystalline metal compounds. There is apparently sufficient experimental evidence to substantiate the conjecture that the fracture propagation is basically an intermittent process and the period of the velocity oscillations decreases as the "brittleness" of the material and the crack velocity increases. In brittle crystals and certain glasses at low temperatures, the period may be below the detection range of measuring instruments and hence the propagation may, for all intents and purposes, be considered to be continuous. On the other hand, in polymers and polycrystalline materials, particularly at low velocities

the period of velocity oscillations may be high enough to be
detected even by the crude measuring techniques and hence may
raise serious questions as to the applicability of the theories
based on a continuous growth assumption.

In this section, we will briefly review the experi-
mental techniques and the results of notable experimental
studies and try to take a broad look at the dissipation phenom-
enon.

1.5.1   Techniques For Measuring The Crack Velocity

There are four major experimental techniques
used to measure the velocity of a propagating crack. In the
following these techniques are very briefly discussed and
proper references are given:

A) Velocity gages. These consist of a series
of conducting "wires" placed with certain intervals on the
projected path of the crack and perpendicular to the direction
of propagation. They form one leg of a bridge which is,
usually, connected to an oscilloscope. The times at which the
wires break due to the propagating crack is obtained from the
trace on the oscilloscope. Among many other investigators,
the technique has been used by Hudson and Greenfield [93],
Robertson [94], Hall and others in the University of Illinois
tests [95, 96, see also 97 for summary] and Akita and Ikeda
[98]. It is obvious that with this technique, one can only
measure average velocities over relatively large gage lengths

71

and very little, if any, information can be gained on the initial acceleration range of the crack growth. Aside from this, depending on the wire material and the method of bonding of these "wires" to the specimen, there may be serious questions raised as to the simultaneity of the passing of the crack through and the breaking of the wire at a certain point. For example Robertson in his experiments found the metal wires quite unsatisfactory and had to use graphite-coated paper. The difficulty in this case arises from the uncertainty in the delay time of the breaking of the wire caused by the shear deformation in the bonding agent and the extension in the metal wire itself.

b) <u>Impedance method</u>. The method which was developed and used by Carlsson [99] consists of measuring the impedance between two points in a plate which are symmetrically located on each side of the crack and connected to a high frequency current source. Because of the skin effect in the case of high frequency current, the current density near the crack surfaces will be very high and independent of the crack length, with the exception of locations around the crack tips and the region near the two terminal points. Carlsson studied the problem theoretically and also gave experimental calibration curves. The calibration results were obtained by placing two half plates at a certain distance apart and simulating a crack by covering a certain portion of the slit with a conducting foil or placing conducting spacers in the slit. Since the impedance can be recorded continuously using a high response

instrument, the method provides a continuous measurement of the crack length as a function of time. In using this method, one should be aware of the fact that the impedance is very sensitive to the width of the slit which undoubtedly has a shape similar to an ellipse rather than a rectangle and may not be so easy to duplicate in calibration or to use in analysis, and one may have to take into consideration the possible effect of surface irregularities of the actual fracture surfaces on the impedance.

c) High speed photography. This has been one of the more widely used techniques in recording the fracture propagation. The multiple-spark camera used by Schardin and Struth [100,101] was capable of frame rates up to 10^6 per second. The camera used by Wells and Post was also a multiple spark camera [67]. The high speed framing camera used by Beebe [84] could go up to 10^5 frames per second. Even though the best results with the high speed photography are obtained with the transparent specimens, it can also be used for non-transparent materials by properly polishing the surface of the specimen. For example, the Barr and Stroud rotating-mirror framing camera was very successfully used by van Elst [102] in studying the brittle fracture of steel plates in the so-called Robertson test plate [94]. Van Elst also used a rotating mirror streak camera in which the image is smeared over the film thus providing a continuous record of the fracture phenomenon where the crack velocity could be obtained from the slope of the contour of the picture.

d) <u>Ultrasonic method</u>. The ultrasonic method
which was developed by Kerkhof [103,104], finds its basis in
the well-known Wallner lines [105] formed by the interference
of the crack front with the (transverse) waves generated
largely at the imperfections located on the surface of the
specimen and the path of the crack. In the Kerkhof method,
the surface of the specimen is modulated by continuous ultra-
sonic waves of known frequency. In spite of the very low
magnitude of the stresses caused by these waves, when superim-
posed on the stresses at the crack tip, the periodic disturbance
they create is apparently high enough to leave time marks on
the fracture surface which are some form of ripples and may
be made visible by proper illumination. The velocity of frac-
ture propagation is evaluated from the spacing of these time
marks or ripples and the frequency of the waves. The technique
is applicable to materials which have very smooth fracture sur-
faces such as amorphous materials and single crystals. A dis-
cussion on the variations and various applications of the
technique and further references on the subject will be found
in Schardin's article [72]. Some recent applications are also
discussed by Clark and Irwin [105].

Crack velocity can also be determined from the
Wallner lines appearing on the fracture surface without the aid
of external wave generators. Using two sets of intersecting
Wallner lines, Smekal [107] was able to determine the crack
velocity in glass. Shand [108] showed that from the geometry
of the Wallner lines, a single line is sufficient to compute

the crack velocity. In both of these cases, it is assumed that the transverse wave velocity of the solid is known and Shand's technique requires that the source of the transverse elastic wave be identifiable. Recently, Hull and Beardmore [83] used these techniques to measure the crack velocity in tungsten single crystals. In this connection, one should note that the distribution of surface imperfections or flaws causing the Wallner lines is random, hence using this technique, unlike the Kerkhof method, one may not be able to obtain a systematic record of fracture velocity.

1.5.2 Techniques For Measuirng The Fracture Energy

Experimental studies aimed at measuring the fracture energy for a given solid are largely confined to static problems in which interest is on the fracture initiation and slow fracture of elastomeric solids [11,20,21] which are left outside the scope of this article. To this author's knowledge, the only place where a conscious effort is being made to experimentally study the fracture energy as a function of velocity and temperature and to measure its value is Irwin's laboratory at NRL. The results of these studies are not yet available, and the velocities which are being dealt with are still too low. This is one aspect of studying fracture which requires a great deal of ingenuity in the design and execution of the experiments and a thorough understanding of the theoretical problem.

A related problem has been studied by Krafft

and Sullivan [109]; they found that fracture toughness (which is a measure of fracture energy as used in this article) decreases as temperature decreases and as strain rate increases. They also report a relationship between plane strain critical stress intensity factor K_{Ic} and the crack velocity (see also [110]). It is shown that K_{Ic} first decreases with increasing crack velocity (apparently due to the reduction of plastic work caused by the rate effect) and then increases with increasing velocity. The later conclusion is based on the evaluation of data given in [97]. It should be noted that in such calculations, one may have to study the error involved in the evaluation of crack closure energy from the strain measurements and the static theory and separate the dynamic effects from the actual dissipation.

1.5.3 A Brief Discussion Of Typical Experimental Studies

We will use the rough classification given above for brittle and quasi-brittle materials as a guide to discuss some of the typical and significant experimental results. Even though the aims in these studies have been varied, within each group the problems studied have been more or less the same. Here we make no attempt for an exhaustive survey of the current literature.

a) Single crystals. Fracture propagation in Tungsten single crystals has recently been studied by Hull and Beardmore [83]. The rectangular specimen had a cross-section

of 0.11 x 0.05 cm and it was cleaved along the 010 plane. An

atomically sharp crack was introduced by a localized spark

discharge. The temperature was varied between 20° and 300°K.

It was observed that at low stress levels and low velocities,

fracture surface was very smooth and Wallner lines starting

at the edge flaws or cleavage steps could easily be detected.

This range corresponds to a low fracture energy which is

largely the surface-free energy of the solid. A measured value

of 6300 ergs/cm^2 for the fracture energy compares well with the

theoretical value of 4850 ergs/cm^2 of the surface-free energy.

As the stress and/or temperature increased, the smooth portion

of the fracture surface diminished and the density of the

river lines increased implying a higher fracture energy. The

significant result of this study is that the fracture energy

and the average terminal fracture velocity, V_T, are very highly

dependent on the temperature. It was found that at 77°K,

$V_T = 0.6 c_2$, at 20°K, $V_T = 0.82 c_2$ and at higher temperatures

where the river lines were more pronounced, V_T varied between

$0.2 c_2$ and $0.55 c_2$. In an earlier study, the authors found

that [111] at temperatures between 290°K and 330°K, the frac-

ture occured by slow cleavage propagation and above 330°K

fracture started as ductile tear and eventually became brittle.

The only other experimental study of the frac-

ture propagation in a single crystal was made by Gilman, Knudsen

and Walsh on the lithium floride [112] in which the terminal

crack velocity is found to be approximately one third of the

longitudinal wave velocity.

b) <u>Highly brittle amorphous solids</u>. In this category, we include mostly various kinds of glasses. The topic is neatly summarized and referenced in Schardin's article [72]. Here, we only mention some of the important results. The experiments indicate that in a plate under tension, with the exception of ballistic loading, fracture starts with a low velocity and, in this early stage of the fracture propagation, the velocity vs. time relationship is basically different than that predicted by theories based on Mott hypothesis (see also [84]). For a given glass, the terminal velocity V_T seems to be independent of the temperature and the external load. However, V_T turns out to be very highly dependent on the chemical composition of the material. Also a correlation between V_T and the microhardness is found which leads to the following empirical relation:

$$V_T = - 560 + 2.48 \sqrt{\sigma_H/\rho}$$

where σ_H is the microhardness and ρ is the mass density. There is rather a wide scatter in V_T when correlated against c_2; thus it is concluded that the generally quoted relation $V_T = 0.5 \, c_2$ is at best a rough approximation.

c) <u>Polymers below glass transition temperature</u>.

Experimental studies on the brittle fracture of polymers are confined to mostly velocity and stress measurements. A photoelastic analysis of a CR-39 plate with

an edge crack under tension was made by Wells and Post [67].
Using a fringe multiplication technique and a multiple spark
camera, they took successive pictures of the isochromatic
pattern in the plate with a running crack which also provided
a means of evaluating the crack velocity. The main findings
of this study is that: a) the difference between the fringe
orders in static and dynamic loading is quite considerable
in regions away from the crack and is small close to the
crack tip, b) the stress field is amplified as the crack grows,
c) the terminal velocity is close to the prediction of Roberts
and Wells [64], i.e., 0.38 $\sqrt{E/\rho}$. The experiments seems to
have been performed at room temperature. The last and highest
recorded velocity in this experiment was at 7/10 of the plate
width from the fracture initiation edge. Because of the close-
ness of the free boundaries, the dynamics of the problem is
rather complicated and the deviations from the infinite plate
with a central crack, on which all the existing theories are
based, are as yet unknown.

Beebe in his experiments used a plate with
a central crack of "Homalite 100", a photoviscoelastic polyester
resin polymer, and arrived at somewhat similar conclusions. How-
ever, even though there is always a possibility of 15% error in
the analysis of isochromatics, his results for the stress field
around the crack tip are quite conclusive in agreeing with the
dynamic solution given by Broberg [61] rather than the static
solution. The terminal velocity found by Beebe was 0.315 c_2
at 24°F and 0.342 c_2 at -40°F. Similar to Schardin's results

79

for glass, Beebe observed that the branching took place in all specimens tested at high (initial) loading rate and the crack length at which the branching started was dependent on the level of the external load, decreasing with the increasing load. Contrary to Carlsson's findings [113], his results indicate that the branching is not related to the elastic waves reflected from the unloaded sides of the plate. He also concludes that a model based on the Mott type analysis is inadequate to represent the early stages of the crack growth phenomenon.

Cotterell [114] used polymethyl methacrylate (plexiglas) plates with central or edge cracks in his fracture propagation studies. The crack velocity was measured by a velocity gage (formed by lines of silver paint) which is stated to give the average velocity within 5% accuracy. The maximum velocity prior to branching observed in these experiments is about 0.26 c_1, which increases to 0.36 c_1 if the fracture is guided along a pre-cut groove. These experiments too do not reveal any conclusive effect of reflected waves. Cotterell also gives values for fracture toughness of the material as a function of the crack velocity. However, these results should at best be considered as qualitative. As seen from Figure 3, the stress intensity factor will be dependent on time (or crack length) and Broberg's solution is for constant velocity crack starting with zero length. From the velocity profiles reported by Cotterell, it is rather difficult to justify the use of Broberg's solution to obtain reliable quantitative results.

Besides, in dynamic problems, except for very low velocities, the stress intensity factor squared is not proportional to the crack closure energy as may be seen from Section 1.4 of this article. In these experiments too, it was found that the roughness of the fracture surface increases with increasing crack velocity.

d) <u>Polycrystalline materials</u>. For an understandable reason, a great deal of experimental work has been done on the fracture of structural steel and aluminum-copper alloys. Felbeck and Orowan [90] studied the fracture propagation in 3/4 inch thick ship structure steel plates with an edge crack. A hydraulic machine used for testing, hence, there was considerable load relaxation during crack propagation which caused occasional crack arrest. One of the important results found in these experiments was that, to reinitiate the crack propagation after the arrest, the external load had to be raised over the arrest value, and, at the tip of the arrested crack, there was extensive plastic deformations leading to the formation of a narrow zone of fibrous fracture, which was again followed by rapid brittle fracture.

An extensive series of tests were carried out on structural steel by Hall and his associates [95 - 97] at the University of Illinois. In these tests, the interest was centered on the brittle fracture behavior of ship-structure-steels below the transition temperature. The specimens were 3/4 to 1 1/8 inch thick, 2 ft. or 6 ft. wide and 18 ft. long.

They were cooled by dry ice to 0°F or -10°F and subjected to 19,000 psi tension. A notch-wedge impact technique was used to initiate the fracture. The crack velocities were obtained by placing SR-4 type A-9 resistance gages on the path of the propagating crack. Some tests were performed on plates with residual stresses to study the slow-down and arrest of the propagating crack. The residual stresses were put into the plate by cutting two tapered slots on each side and filling them with welds which results in a tensile field near the sides between the welded slots and a compressive field in the central region of the plate. In the regular plates, the measured crack velocities varied between 1500 and 5900 fps.[*] while in plates with residual stresses, in the compressive region, crack velocities as low as 50 fps. were observed. The strain measurements in the prestressed plates clearly showed that as the crack velocity decreased, the intensity of the stress field around the tip of the running crack also decreased. In the conclusion of these studies, a critical stress criterion is proposed for the cleavage propagation which states that at the boundary of the plastic zone, the stress has to be higher than a critical value for the propagation of fracture. As shown in [97], this is basically a critical stress intensity criterion.

[*] In these tests, crack velocity as high as 7550 fps. has been observed [115]; with c_2 = 10,400 fps., it corresponds to a velocity ratio V_0/c_2 = 0.725. Even though high, this however can be explained (see Section 1.4 above)

The main difficulty with these tests is
that, the grip conditions, the geometry of the specimen and
the notch-wedge impact make the theoretical analysis quite
complicated and none of the existing dynamic solutions can
be applied with any kind of confidence. A very promising
start towards obtaining an analytical solution to the problem
was made by Gaus [116]. He used a lattice model to numerically
analyse the transient strain distribution associated with
cracks propagating in small finite jumps. Mainly due to the
inadequacy of the computer used at the time, the results had
to be considered qualitative, which were in agreement with the
main trends of the experimental findings. However, this line
of approach, which seems to be a good possibility to deal with
the effect of free boundaries, irregular geometry and nonsym-
metric external loads (such as the lateral impact), has not
been pursued further.

Similar tests on structural steel were
performed by Akita and Ikeda [98] which gave quite similar
results. It was found that the average crack velocities in-
creased with increasing initial tension prior to initiation
of fracture and decreased with increasing test temperature.
The tensile stress was varied between 50 and 20 kg/mm^2 and
the test temperature between -70°C and -10°C[*].

---

[*]The approximate dynamic solution used in [98] has an incorrect
singularity, hence the correlations and comparisons given are
of doubtful value.

Perhaps not as extensive but more significant tests on structural steel were performed by Carlsson [113] and van Elst [102]. Carlsson used an impedance method for velocity measurements and showed that the fracture propagation in structural steel (under given test conditions) is intermittent (see also Tipper [117]); the microcracks form and grow ahead of the main crack and then join it. Carlsson also studied and pointed out the effect of the non-symmetric (i.e., shear) components of the stresses around the crack tip on the crack branching. The shear stresses simply tilts the direction of the cleavage plane [17] and hence may be considered one of the causes of crack branching. One of the conclusions arrived at by Carlsson, which does not seem to be widely accepted [84, 114], is that branching is nucleated at locations where the reflected waves from the free boundary interfere with the stresses at the crack tip. The reflected dilatational waves reduces the dependence of the cleavage stress σ_θ on the angle θ and the shear waves tend to tilt the cleavage plane.

Van Elst [102] used a Robertson apparatus in his experiments, thus crack arrest took place at higher temperatures. By means of a streak camera, a continuous record of crack length vs. time was obtained. Crack velocities were measured also by using high speed framing camera. The test temperatures were varied from -35°C (with solid carbon dioxide coolant) to room termperature (arrest temperature: 27°C). Van Elst also found that the fracture propagates in discrete steps ranging from as high as 30 mm. near the arrest temperature to

2 mm. at lower temperatures and the halting times varied between 20 microseconds for high and 1 microsecond for low temperatures. However, it should be recognized that in the tests on structural steel, the fracture is basically plane strain, but the pictures and the crack velocity measurements refer to the crack as observed on the surface. Even though there is no evidence of large scale plastic deformations on the surface of the specimen ahead of a running crack, it is difficult to interpret the less-discernible contrast ahead of the main crack seen on the pictures taken by the framing camera in van Elst's tests in terms of the actual crack front. Hence, categorical statements about the details and the nature of stepwise fracture propagation and particularly about their sizes will have to wait for the conduct of further studies. In principle, however, van Elst's results, particularly the stress distribution ahead of the running crack obtained by using the photo-stress coating, seem to provide conclusive evidence about the intermittent character of the fracture propagation in structural steel.

1.5.4 Some Remarks On The Energy Dissipation

In the ideally brittle materials surface-free energy is the only mode of energy dissipation during fracture propagation. Crystalline brittle solids exhibiting no rheological or plastic behavior, rate-independent glasses and some polymers at very low temperatures may be included in this group. In such materials, the energy dissipation or the fracture energy per unit crack extension, γ_f, is directly related to the

geometry of the fracture surface, that is, γ_f increases with

the increasing surface roughness. The irregularity of the

fracture surface may present itself in various forms. In

single crystals, one may observe cleavage steps which develop

when the crack front intersects lines of screw dislocations

[62]. Or, crack may wander from one crystallographic plane

to another if the crystal does not have a cleavage plane which

is substantially weaker than the others. In the polycrystalline

materials, due to the random orientation of the grains, generally

the crack entering a grain is not parallel to the weak cleavage

plane, as a result it becomes segmented in order to maximize

its surface lying parallel to the preferred cleavage plane [62].

In the case of amorphous solids such as glass and polymers,

the surface roughness takes the form of commonly observed rib

structure and hackles. The rib structure or the river line

pattern is generally observed during the initiation period of

the crack propagation (or, the reinitiation period of the ar-

rested crack) and is considered to be the cause for the rela-

tively high value of fracture energy at the initiation of crack

growth. The development of hackles may be attributed to the

formation of microcracks ahead of the main crack and in planes

which are not co-planar with the main crack. Whatever the

cause of these surface irregularities, it is generally agreed

that they absorb energy (which may be, in some cases, inpro-

portionately high compared to the relative increase in the area

of fracture surface because of the particular mechanism creating

the irregularity) and the intensity of roughness increases with

the increasing fracture velocity (above a certain velocity) and, in most cases, with the increasing temperature.

In brittle fracture of most polymers and quasi-brittle fracture of metal compounds and some single crystals, which constitute by far the largest group of materials of technological interest, the dissipation phenomenon taking place during fracture propagation is much more complicated. In such materials, the main component of energy dissipation is due to the viscous effects or the plastic deformations and the contribution of surface-free energy is rather insignificant. The main reason for the complexity of the problem in this case lies in the fact that the irreversible effects such as viscous and plastic deformations are very highly dependent on the geometry of the solid, details of the stress state around the propagating crack, the microstructure and the constitutive properties of the material and the environmental conditions, and most of these factors do not lend themselves to manageable analytical treatment. Furthermore, some of these factors may vary from material to material quite drastically, hence preventing simple generalizations.

On the other hand, concerning the propagation of brittle fracture, there are some simple commonly observed facts which are enumerated below for the sake of subsequent discussion:

a) For materials with preferred (weak) cleavage planes, the fracture velocity may reach very high values ($0.8\ c_2$ and over) and yet no branching would take place.

b) For materials with isotropic or near-isotropic fracture properties, there seems to be a maximum fracture velocity depending on the particular environmental conditions, which may not be exceeded and at which the crack branching takes place. Usually this limiting velocity is independent of the level of the external loads which simply control the duration of the time in which this velocity is attained in a given situation. In most cases, this velocity is much lower than that corresponding to $\frac{\partial^2 \sigma_\phi}{\partial \phi^2} = 0$, σ_ϕ being the cleavage stress at the crack tip and ϕ being the angle measured from the crack direction; the former generally varies between $0.3\ c_2$ and $0.6\ c_2$ and the latter is around $0.6\ c_2$.

c) The limiting crack velocity, among other factors, seems to depend on the chemical composition and the microstructure of the material.

In addition to these, based on the theoretical studies, we make the following observations:

a) In fracture propagation problems, the inertia effects are not negligible, the dynamic solution rather than static should be used and the kinetic energy should be included in any kind of energy balance.

b) If the dissipation zone around the crack tip is small, the available energy to be used to overcome the dissipation around the crack tip can be obtained from

$$U^\cdot - V^\cdot - T^\cdot = E_c^\cdot$$

where $U^{\bullet}$, $V^{\bullet}$, $T^{\bullet}$ are, respectively, the time rates of external work, elastic energy and kinetic energy for a small region surrounding the crack tip and $E_c^{\bullet}$ is the rate of crack closure energy. If $D^{\bullet}$ is the rate of dissipative energy, then at constant velocity crack growth $E_c^{\bullet} = D^{\bullet}$. For a given velocity, if the calculated $E_c^{\bullet}$ is greater than $D^{\bullet}$ corresponding to the same velocity, the excess energy will be used to accelerate the crack.

c) Provided the crack can be maintained to run straight, the theoretical limits for the velocity of fracture propagation are the shear wave velocity in longitudinal shear problems and the Rayleigh wave velocity in plane and three-dimensional problems, meaning that fracture propagation at velocities exceeding these limits require energy generation (rather than dissipation) around the crack periphery.

Similar to Griffith criterion, we first state that the crack will propagate in the direction of maximum $E_c^{\bullet}/D^{\bullet}$ ratio. This presumably is the reason for curved cracks and cracks with irregular shapes.

Next, we consider the case in which $D^{\bullet}$, the dissipation rate around the propagating crack is an increasing function of velocity. $D^{\bullet}$ may also depend on the crack length as mentioned in Section 1.4. From Figure 6, we observe that, up to a certain velocity (~ 0.6 c_2), $E_c^{\bullet}$ is a linear function in time and also an increasing function of velocity. In the neighborhood of a given fracture velocity, it may be possible that a further increase in the crack velocity would cause a

89

steep increase in $D^{\cdot}$; furthermore, it may also turn out that combined with the other effects at the crack tip (such as non-symmetric stress components and small imperfections), the total dissipation $D^{\cdot}$ in a forked crack may give a more $E_c^{\cdot}/D^{\cdot}$ ratio. In this case, the crack would branch. The propagation of each branch would in turn be governed by the respective $E_c^{\cdot}/D^{\cdot}$ ratios in the resulting dynamic problem with the new geometry. This may be a possible explanation of crack branching at relatively low velocities (0.3 c_2 to 0.5 c_2).

As for the two most important questions concerning the fracture propagation, namely the actual kinematics of the crack growth and the nature of energy dissipation, it is tempting to conjecture that the crack propagation is inherently an intermittent process, that in the limiting case of an ideal crystal, the atomic spacings may constitute a propagation step and that in the other extreme of quasi-brittle polycrystalline metal compounds and polymers at below and near the brittle-ductile transition temperature, the series of microcracks forming, growing and joining ahead of the main crack may cause the discontinuous growth with relatively large steps. In between, one may argue that the size of these steps becomes smaller as the "brittleness" and the degree of homogeneity of the material increases. Even though this is clearly an over-simplified picture and the question cannot be isolated from the microstructure of the material, it may be important in raising the question concerning the possible differences between the dynamic responses obtained by treating the problem as a con-

tinuous or intermittent phenomenon. This is one of the areas which requires careful experimental as well as analytical attention.

At this point, the greatest hope in throwing some light on the fracture energy lies in performing some meaningful experimental work in which all the relevant factors can be controlled and their effects can be separated. There is not much sense in trying to estimate γ_f from the strain measurements around the propagating crack if the fracture velocity is not constant for a substantial period of time, the region is not free from the influence of the reflected waves, the relative locations and timings of the points where the strains are measured with respect to the propagating crack cannot with a reasonable degree of accuracy, be determined[*] and the initial and the boundary conditions as well as the geometric configuration assumed for the theoretical analysis cannot experimentally be duplicated within again a reasonable degree of approximation. In this connection, two analytical problems which emerge as being important are the elastic (dynamic) analysis of the accelerating crack and the dynamic elastic-plastic problem of the constant velocity propagation of fracture. Since the intensity of the stress state around the crack tip grows with the growing crack length, it is reasonable to expect that, to a certain degree, the dissipation zone as well as the dissipated energy

---

[*]In this sense, the photoelastic specimen or the photostress coating offers an advantage.

91

will also grow with the growing crack. It is then important to have a simplified dynamic model for the plastic region in order to have some idea about the plastic work. As seen from the Appendix B and the related discussion in Section 1.4, a quasi-static model is completely insufficient for this purpose. For small crack velocities, the inertia effects are, of course, negligible and a quasi-static model taking into consideration the rate dependence of the phenomenon may be adequate. In this range, for example, the strain rate effects explain the decrease in γ_f following the onset of rapid fracture.

1.6 Summary

In the first part of this article, the crack propagation theories in brittle and quasi-brittle solids fracturing under a single application of the external loads have been discussed. In particular, the dynamic aspects of the phenomenon have been emphasized and the discussion has been restricted to the theories based on the approach of continuum mechanics and classical thermodynamics.

First, the dynamic crack propagation theory based on the concept of the modulus of cohesion proposed by Barenblatt and his co-workers has been presented, a critical discussion has been given and some modifications have been offered. The main advantage of this theory lies in its simplicity and directness and its main objectionable feature is the weakness of the underlying physical argument.

Next, the theories based, in one form or another, on the energy balance at the periphery of the propagating crack have been considered. The physical basis of these theories, which simply consists of the first law of thermodynamics, is basically very sound. However, because of the complexity of the required mathematical analysis and the lack of our physical understanding of the energy dissipation phenomenon resulting from the fracture of solids, considerable difficulty has been encountered in their applications. In general terms, an energy balance theory may be stated as, "in a fracturing solid, the crack will propagate along a surface offering the least thermo-

dynamic resistance and the velocity of the propagation at the crack periphery will depend on the difference between the rate at which the work is done on the solid by the external loads and the sum of the rates of stored recoverable energy, the kinetic energy and the dissipative energy". The reason for crack branching is seen to be inherent in the statement of the theory. Also, it is obvious that in real materials, the phenomenon is basically a non-equilibrium type process.

Largely because of mathematical expediency, the existing theories deal only with the idealized cases. In this article, after formulating the general problem, the theory based on the quasi-static assumption proposed by Mott has been presented and its results have been discussed. Next, an energy balance theory for brittle and quasi-brittle materials considering the energy exchange process only in the close neighborhood of the crack periphery has been developed. It is shown that the energy available at the crack periphery to create new fracture surfaces or to overcome the dissipative energy due to fracture is equivalent to the crack closure energy which is not equal to the strain energy release if the inertia effects are not negligible. One of the main conclusions of this theory is that if the crack can be maintained to propagate along a plane, the Rayleigh wave velocity in the plane and axially symmetric problems and the shear wave velocity in the anti-plane problems form the upper limits for the respective fracture propagation velocities, meaning that for propagation beyond these velocities, energy has to be generated rather than dissipated at the crack periphery. In

practice, such high velocities can be attained as a limit provided the medium is very large, the fracture energy is either independent of the fracture velocity or does not increase with it appreciably and because of its geometry (e.g., deeply gorroved or weakly bonded specimens) or constitution (e.g., highly anisotropic specimens) the medium has a preferred weak fracture plane. The energy balance theory in the revised form is then applied to plane extensional and anti-plane shear problems with propagating central cracks.

The experimental work involving the techniques of crack velocity and fracture energy measurements have been reviewed. The important techniques for velocity measurements, namely, the velocity gages, the impedance method, high speed photography and the ultrasonic methods, have been briefly discussed. The results of some typical experimental studies dealing with the dynamic aspects of the fracture propagation phenomenon have been discussed by loosely classifying them in four groups, which are single crystals, highly brittle amorphous solids, polymers below glass transition temperature and polycrystalline materials. The published results of the experimental studies so far provide very little information about the nature of the dissipation phenomenon in general and the velocity variation of the fracture energy and the size of the dissipation zone in particular. There seems to be an agreement about the discontinuous character of the crack growth in structural steel — a behavior which has not been observed in other materials. This question apparently cannot be isolated from the microstructure and the degree of "brittleness"

95

of the material and one may cautiously conjecture that fracture phenomenon is essentially an intermittent process where the period of velocity oscillations depends on the microstructure and the "brittleness" of the solid, decreasing rapidly as the degree of brittleness and amorphousness of the material increases.

Finally, the general question of crack branching and its relation to the variation of dissipative energy and the stress state around the crack periphery has been discussed.

1.7 Suggestions For Further Research

After reviewing the present state of our knowledge on the dynamics of fracture propagation in solids, it is not difficult to conclude that, compared to other areas of research dealing with the mechanical response of deformable solids, the field is rather in its primitive stage. This has been due to the highly complex nature of the problem rather than a general lack of interest in it. The importance of the topic has long been recognized and it has been studied by a great number of investigators at the atomic, microstructural and continuum levels. Further research is needed obviously at all these levels. However, reflecting only one point of view, the following recommendations deal only with the studies based on a continuum type of approach. Again, ductile fracture propagation has been left out of the considerations.

The efforts to develop partially empirical crack propagation models will have to continue. However, the success of

these efforts will depend as much on the soundness of the underlying physical principles and the understanding of the fracture propagation mechanism in a given type of material as on the effectiveness of performing the required mathematical analysis. Perhaps the first question which requires clarification and further study is the nature of an acceptable failure criterion. The existing criteria such as the cohesion modulus of Barenblatt, critical strain of McClintock and the energy balance seem to be far from satisfactory; or at least, they are not developed to the point that they can be used as prediction tools. It is quite conceivable that a single criterion or model applicable to all materials undergoing brittle fracture may not be possible to develop or practical to consider.

There is a strong possibility that the actual kinematics of the crack growth and the mechanism of fracture may be sufficiently different in materials with basically different microstructures (e.g., amorphous vs. polycrystalline) to warrant a closer look at the fracture propagation at the microstructural level before adopting a particular continuum model. In this connection, one question concerns the continuous vs. intermittent propagation of the crack. If the discontinuous nature of the fracture growth is severe enough to alter the dynamic stress distribution around the crack, it may have to be taken into account in the formulation as well as the application of the fracture propagation theory. Photoelastic studies of van Elst indicate that this may be the case in structural steel. However, further quantitative studies are obviously needed. Another

related question is whether this discontinuity is due to the formation of the microcracks or voids ahead of the propagating crack or not. This may introduce an element of randomness into the discontinuous fracture propagation, if that is the case. These questions will have to be answered primarily through experimental studies on various types of materials.

At present, perhaps the most important area which requires close attention and systematic experimental studies is the process of energy dissipation resulting from the creation of new fracture surfaces. The question has a bearing on such important phenomena as fracture stability, crack branching, terminal velocity and crack arrest. It is easy to argue that the energy dissipation will exhibit itself in the form of surface-free energy, plastic work and/or viscous friction. The important questions are, where and how these phenomena take place, how do they depend on the fracture velocity, the microstructure and the environmental conditions, and what is the significance of the transformation of the great bulk of this energy into heat. These studies too will have to be performed on all the typical groups of materials behaving in brittle or quasi-brittle manner.

In the type of studies mentioned above, it is important to keep the available theoretical solutions in mind and design the experiments in such a way that the secondary effects such as those caused by the geometry, the reflected waves and in-plane shear, can be avoided or estimated and then studied by

introducing them in a controlled manner.

Analytical problems, the solutions of which would be desirable to obtain are, in most part, rather difficult. From the viewpoint of studying the dynamics of crack propagation, the following may be mentioned among such problems:

A solution for an accelerating crack for the simplest possible case;

Development of a theoretical method for the evaluation of the size of plastic enclave, taking into consideration the effect of the plastic waves. For plane loading, even the static problem has no closed form solution. For this as well as the accelerating crack problem, anti-plane shear case may be manageable if a numerical approach is used.

The estimate of the effect of reflected waves from the free boundaries of a rectangular plate with a propagating central crack.

The effect of unloading waves from the grips.

2. Fatigue Crack Propagation

It is generally accepted that in structures subjected to repeated external loads, the microcracks may be nucleated very early in the fatigue life. As a result, it has been common practice to consider the fatigue life of a given part in three phases, namely the nucleation and the propagation phases of the fatigue cracks and the final failure. Final failure simply is the fracture of the solid under a single application (i.e., last quarter cycle) of the load and may be treated with the techniques covered in the previous sections. However, the distinction between the first two phases does not seem to be as clear. Some investigators prefer to include the propagation of microcracks as a separate phase between the phases of nucleation and macrocrack propagation. The question as to at what size or stage a microcrack becomes a macrocrack cannot, of course, be divorced from the microstructure and overall geometry of the material — the grain size and the smallest local dimension of the solid being the two most important factors. With due consideration to the microstructure of the medium, one may, for example consider the crack as being a macrocrack if it is large enough to permit the application of the notions of a homogeneous continuum. By fatigue crack propagation, in this article, we will understand the growth of macrocracks and assume that the continuum approach is applicable.

According to the most widely accepted microstructural theories, the basic mechanism of crack nucleation as well as

100

its propagation is the cyclic slip and resulting extrusions and intrusions [28 - 33]. The percentage of fatigue life of the structure which is spent during each one of these two phases depends largely on the geometry of the particular part. If the part is rather bulky with no distinct stress raiser, the nucleation period of the fatigue crack would be very long compared to the propagation period. In such cases, the techniques used for the prediction of fatigue life are based on the studies leading to S-N type curves. On the other hand, in structures with severe stress concentrations, particularly in thin plates and shells, the formation of a dominant macrocrack takes place relatively very early in the fatigue life and hence, in terms of the number of load cycles, the propagation phase constitutes the major portion of the total life.

Up to now, the main objective of microstructural fatigue theories has been to provide a rational mechanism by which the nucleation and propagation of fatigue cracks can be explained. Due to the extreme complexity of the problem at this level, these theories are, as yet, far from providing quantitative working tools. Such tools, on the other hand, have been developed by approaching the problem from the continuum viewpoint. In what follows, we will first briefly review some of the existing continuum models for fatigue crack propagation, then discuss a simple model in some detail and present some experimental results.

2.1 A Review Of Continuum Models

Partly due to the fact that crack propagation represents a large portion of the fatigue life mostly in thin plates and shells, partly because of the importance of fatigue in such elements as they appear in the airplane design and ship-building and partly because of the analytical simplicity of the problem resulting from a two-dimensional idealization, the existing quantitative continuum models of fatigue crack propagation have almost exclusively dealt with a plate with a straight through crack subjected to uniaxial repeated extensional loads. If a is the half-length or the length of the crack and n is the number of load cycles, in all these models, it is assumed that $\frac{da}{dn}$ is a continuous function of such variables as the external load, the dimensions and the material properties. The primary objective is then to determine this function.

One of the earlier continuum models is due to Head [34]. In his analysis, Head considered an infinite plate with a central crack of length 2a and subjected to one-dimensional repeated loads with the range value σ. By using a mechanical model in which he assumed rigid-plastic work-hardening elements ahead of the crack tip and elastic elements over the remainder of the plate, he arrived at the following relationship:

$$\frac{da}{dn} = \frac{C_1 \sigma^3 a^{3/2}}{(\sigma_{ys} - \sigma)p^{1/2}} \tag{78}$$

where σ_{ys} is the yield stress, p is plastic zone size and C_1

102

is a constant which depends on the mechanical properties of the material and has to be determined experimentally.

In Head's analysis, p was assumed to be constant during the propagation of the crack. It was pointed out by Frost and Dugdale [35] that p is not independent of the crack length and is proportional to $\sigma^2 a$. On the basis of dimensional analysis, Frost and Dugdale arrived at the conclusion that the crack propagation rate, $\frac{da}{dn}$ is linearly dependent on the crack length. From the experimental data, they also observed that $\frac{da}{dn}$ is proportional to σ^3 and hence proposed the following model:

$$\frac{da}{dn} = C_2 \sigma^3 a \tag{79}$$

where C_2 is a characteristic parameter of the material.

Again, using dimensional and similarity analysis in a more elegant fashion, Liu [38] also arrived at the conclusion that

$$\frac{da}{dn} = F(\sigma, \sigma_m) a \tag{80}$$

where F is a function of the mean (σ_m) and the range (σ) components of the external loads. Liu further analyzed the problem [122] by considering a hysteresis energy dissipation model and pointed out that the effect of the mean stress in crack propagation is not significant and the function F is proportional to σ^2:

$$\frac{da}{dn} = C_3 \sigma^2 a \tag{81}$$

McEvily and Illg [36], approaching the problem from
a somewhat different point of view, argued that the local
stress immediately ahead of the crack tip is raised to the
fracture level as a result of work hardening under cyclic load
thus causing rupture. It was then stated that the crack propa-
gation rate $\frac{da}{dn}$ must be a function of the maximum stress around
the crack tip:

$$\frac{da}{dn} = f(\sigma_{max}) \tag{82}$$

Assuming the crack as being a flat elliptic hole, σ_{max} may be
expressed as

$$\sigma_{max} = K_s\sigma = (1 + 2\sqrt{\frac{a}{\rho}})\sigma \tag{83}$$

where K_s is the static stress concentration factor and ρ is
the radius of curvature at the tip region of the crack. The
specific form of the function (82) was given by McEvily and
Illg by analyzing the experimental results (on the aluminum-
copper alloys) in the following form:

$$\log_{10}(\frac{da}{dn}) = 0.00509 \, K_s\sigma - 5.472 - \frac{34}{K_s\sigma - 34} \tag{84}$$

Observing that $\sigma\sqrt{a} = k$ is the stress intensity factor
for the configuration under consideration, Hardrath and McEvily
later [118] pointed out that (82) may also be considered to be
a function k. From (83), it is indeed seen that $\sigma_{max} \simeq 2k/\sqrt{\rho}$,
as $1 << 2\sqrt{a/\rho}$. This point was independently observed by Paris,
pointed out in various publications [39,42,119,120] and elu-

cidated in his thesis [121]. The central point in this argument is that the stress intensity factor is a parameter which represents both the geometry and the external loads and is the true measure of the stress state around the crack tip. Hence, it should be the most important factor affecting the crack growth rate.

Similar continuum models have been developed by McClintock [123] and Schijve [37]. A critical analysis of various models mentioned above is given in [42], where on the basis of a broad range of data, it was tentatively concluded that

$$\frac{da}{dn} = C_4 k^4, \quad k = \sigma\sqrt{a} \tag{85}$$

the constant C_4 being a function of the material parameters (see Figures 20 and 21). In a discussion of [42], McEvily pointed out that even though the fourth power model (85) represents the data on high strength aluminum alloys quite satisfactorily, it is not so satisfactory for some other copper alloys. He further argued that crack growth rate would be proportional to the energy stored in the plastic zone. Assuming that the density of this energy around the crack tip can be represented by k^2 and the relevant volume of the plastic zone by that of a rectangular strip ep ahead of the advancing crack, one obtains

$$\frac{da}{dn} \sim k^2 ep \tag{86}$$

where e is a constant and p is the plastic zone size. For

small values of p/a ratio, it can be shown that $p \sim k^2$ and hence (86) reduces to (85). If p/a is not small, p is no longer proportional to k^2, which explains the higher powers observed in the copper alloys referred to by McEvily [124].

Recent work on the fatigue crack propagation indicates that there is a sudden surge of enthusiasm for using the stress intensity factor as a correlation parameter[*], partly no doubt due to the appealing simplicity of the approach. Even though the underlying basic idea seems to be sound, the user should be aware of its potential as well as the limitations. In the following section, this point will be elaborated somewhat further.

2.2 A Simple Model

The primary aim of all the continuum models is to provide the design engineer with a quantitative tool which can be used in predicting fatigue crack growth characteristics in a given structure under given external loads and environmental conditions. On one hand, to be useful, the model must be relatively simple and must contain only the field parameters of the system which are readily available to or can be evaluated by the design engineers. On the other hand, to have a wide range of application without significant modifications, it must have a sound physical basis, that is, it must conform as

[*]See, for example, the papers presented at the 1966 Annual Meeting in Atlantic City, New Jersey.

106

closely as possible to the basic features of the microstructural theories which are known to correctly explain the phenomenon of fatigue. Thus, one of the important functions of such a model would be that it can be used to predict the crack growth characteristics of structures with more complicated geometries and subjected to more complex loading conditions from the results of simple one-dimensional experiments, that is, it would serve as a basis of comparison in fatigue studies and predictions.

If one considers then the composition and the microstructure of the actual materials, the diversity in geometry, loading conditions and environment, and finally the nebulous state of the microstructural fatigue theories, even to talk about quantitative predictions by means of a unified model would sound rather pretentious. However, here too, once again empiricism seems to come to one's aid. In technical literature today, there is a great wealth of experimental fatigue data which has been attempted for correlation in every conceivable way. The output in these studies has been invariably the (surface) measurements of the size of fatigue cracks as a function of load cycle. The results of no two experiments may be identical, but there is an apparent similarity in the trends and separately, all seem to be surprisingly very smooth. This then indicates that no matter what the complexity of the phenomenon, a semi-empirical continuum approach to the problem is justified.

107

However, this seemingly smooth growth of macrocracks
should be understood in light of relatively low sensitivity
or detection power of the measuring instruments and as an
average of basically irregular fracture propagation in indi-
vidual grains and through the grain boundaries. Neither the
crack front is a smooth curve remaining parallel to a given
direction as it propagates nor is the fracture surface a
mirror-smooth plane. Some fractographic studies indicate that
the crack grows in every cycle [37,125,126] (e.g., in aluminum
copper alloys), and some indicate the growth as being basically
discontinuous [118,127] (e.g., in aluminum-zink alloys and
cold-rolled aluminum). Also, there is every indication that
the direction of observed striations depends on the orientation
of the particular grain and is not necessarily perpendicular
to the gross crack growth direction [125].

Against this background then, in order to derive a
quantitative model, we will now assume that at the microstruc-
tural level the crack nucleation and growth are caused by
cyclic slip which is a geometric consequence of dislocation
movements along the glide planes. In the whole, the fatigue
crack propagation is due to the formation, the growth and the
coalescence of microcracks, be it at the tip of the main crack
or ahead of it and co-planar or not. It then appears that
since at the microstructural level, dislocation motions are
the most important factor contributing to the (local) nucle-
ation, growth and propagation of the fatigue cracks, in the
final analysis, the (continuum) factors controlling the density

of these dislocations and the forces moving them have to be the primary factors which influence the fatigue crack propagation. Thus, we will start with the following simple expression for the crack growth rate [37,129]:

$$\frac{\Delta a}{\Delta n} = \phi m b \tag{87}$$

where a is the characteristic length of the fatigue crack (e.g., half-crack-length in a wide plate with a central crack), n is the number of load cycles, m represents some kind of an average (on the primary glide planes along the crack front) of the total number of moving dislocations which could possibly contribute to the crack extension, ϕ is a coefficient representing the fraction of the total number of dislocations which effectively contribute to the crack growth ($0 < \phi < 1$) and b is the magnitude of the Burgers vector. It is generally assumed that [37] at low growth rates, the dislocations move towards the crack and "flow" into the tip region (the dislocation-absorption mechanism) and at high rates, due to the presence of high shear stresses, they are "generated" at the crack tip (the dislocation-generation mechanism). It is more likely that both mechanisms may be active simultaneously, the former being more dominant in low rates and the latter in high rates.

It is obvious that the quantities ϕ and m will depend on the microstructure of the particular material as well as the field variables such as the geometry, temperature and stress (or strain) distribution around the crack front. One

of the basic deficiencies of the continuum models (including the present one) is their inability to account for the microstructural effects (even as simple and as important a factor as grain size) in a quantitative and rational manner, or, in fact, their total exclusion of such factors from the considerations. Thus, even if the whole reasoning leading to the relationship between ϕ and m on one hand and the continuum variables on the other is flawless, the model is bound to be only partially successful. This, of course, is the reason for the discrepancies observed in correlating against the same parameter (such as the stress intensity factor), the fatigue results obtained for basically the same material with different microstructures. The continuum models for a complex phenomenon such as fatigue must then be viewed in light of this somewhat serious limitation.

To relate the microstructural variables ϕ and m to continuum variables around the crack front, here we will assume that the dislocation movements are concentrated mostly in the plastic zone and those confined to a plane emanating from the crack front will primarily be responsible for the creation of a new surface in a given cycle. Quantitatively, these two groups of variables are related by

$$\epsilon_p = \rho A b \tag{88}$$

where ϵ_p is the plastic strain, ρ is the dislocation density, A is the total area swept by the dislocations and b is the magnitude of the Burgers vector. Thus, it may be assumed that

the factor m will be a function of a representative length of the plastic zone measured from the crack tip and the magnitude of the plastic strains. At present, the only reliable information on plastic strains is available for the longitudinal shear of virgin material [88,89]. Hence, on account of a lack of quantitative information about plastic strains in plane problems under repeated loads and considering the fact that the plastic zone size, p, is dependent on the distribution of these strains, with the simplifying assumption of geometric similarity, it may conversely be assumed that the magnitude of the plastic strains will be dependent on the plastic zone size. Since m refers to the total number of dislocations in a given glide plane, it may then be expressed as a function of maximum plastic zone size:

$$m = f_1(p_{max}) \tag{89}$$

It is easy to argue that the coefficient ϕ will have to be a function of the factors compelling the dislocations to move. We also recognize that the crack growth is due to the phenomena taking place within the plastic region and that the true measure of the severity of the forces moving the dislocations in the plastic region is the magnitude of the plastic strains. Thus, we may assume ϕ to be a function of the range value of the plastic strains, or following a similar argument as before, a function of a corresponding range component of the plastic zone size, p_r:

$$\phi = f_2(p_r) \tag{90}$$

111

As shown by Schijve [37] and Crews and Hardrath [130], the strains around the tip of a crack or notch stabilizes after the first few load cycles and hence it is not unreasonable to talk about the maximum or range values of plastic strains or corresponding plastic zone sizes.

The nature of the functions f_1 and f_2 is unknown except that they are monotonically increasing functions and vanish at zero. Thus, within given ranges of p_{max} and p_r, f_1 and f_2 may be approximated by appropriate power functions as follows:

$$f_1(p_{max}) \simeq A_1 p_{max}^{\alpha_1} \quad , \quad f_2(p_r) \simeq A_2 p_r^{\alpha_2} \tag{91}$$

where A_1, A_2, α_1 and α_2 are positive constants. Combining the constants and considering the crack growth as a continuous process, (87) may then be written as

$$\frac{da}{dn} \simeq A \; p_{max}^{\alpha_1} \; p_r^{\alpha_2} \tag{92}$$

From the arguments leading to (92), it is clear that the nature of the functions f_1 and f_2, and hence, the values of the constants A, α_1 and α_2 will be different for different materials as well as for the same material with different microstructures. Also, because of the limited scope of the approximations given by (91), the constants α_1 and α_2 are expected to depend on the range of the variables p_{max} and p_r, attaining greater values for greater p_{max} and p_r. Thus, the

112

possibility of a universal power law has been ruled out.

In order to apply the model given by (92), analytical estimates of p_{max} and p_r and experimental evaluation of the constants A, α_1, α_2 will be needed. Even though the exact solutions are not available, the plastic zone sizes may be closely estimated in various ways. The technique used by Dugdale [85] for this purpose and later extended to work-hardening materials by Rosenfield, Dai and Hahn [131] appears to be fairly realistic and the estimate seems to agree with the experimental results quite satisfactorily. Dugdale's technique is based on the removal of the stress singularity at the crack tip by introducing a rigid plastic strip ahead of the crack. For the plane problem with a central crack of length 2a, Dugdale model gives

$$p = a [\sec(\frac{\pi\sigma^\infty}{2\sigma_{ys}}) - 1] \tag{93}$$

where σ^∞ is the uniaxial stress at infinity and σ_{ys} is the yield stress. To find estimates for p_{max} and p_r, in (93), σ^∞ may be replaced by the maximum and the range value of the cyclic stress while using a somewhat greater value for σ_{ys} because of the work-hardening in the material. Note that if the width-to-crack length ratio-in the plane is not sufficiently large, necessary corrections for p_{max} and p_r will have to be made.

For small scale yielding, that is, if the plastic zone size is small compared to the crack length, (93) may be approx-

113

imated as

$$p \simeq \frac{a}{2} \left(\frac{\pi \sigma^\infty}{2\sigma_{ys}}\right)^2 = \frac{1}{2} \left(\frac{\pi}{2\sigma_{ys}}\right)^2 k^2 \tag{94}$$

where $k = \sigma^\infty \sqrt{a}$ is the stress intensity factor. With $k_{max} = \sigma_{max}^\infty \sqrt{a}$ and $k_r = \sigma_r^\infty \sqrt{a}$, it then follows that

$$p_{max} \simeq \frac{1}{2} k_{max}^2 \left(\frac{\pi}{2\sigma_{ys}}\right)^2 \; ; \; p_r \simeq \frac{1}{2} k_r^2 \left(\frac{\pi}{2\sigma_{ys}}\right)^2 \tag{95}$$

where $\sigma_r^\infty = (\sigma_{max}^\infty - \sigma_{min}^\infty)/2$. With (95), the crack propagation model, (92) becomes

$$\frac{da}{dn} = B \, k_{max}^{2\alpha_1} \, k_r^{2\alpha_2}$$

or letting $\beta = (\sigma_{max}^\infty + \sigma_{min}^\infty)/(\sigma_{max}^\infty - \sigma_{min}^\infty)$, we have

$$\frac{da}{dn} = B(1 + \beta)^{2\alpha_1} \, k_r^{2(\alpha_1 + \alpha_2)} \tag{96}$$

The obvious advantage of (96) is that as long as the small scale yielding approximation is valid, it is applicable to all plane problems with a propagating through crack - not just the infinite plane with a central crack loaded at infinity, for which it is derived.

To demonstrate the applicability of the model as a comparative tool, we consider the problem of cylindrical bending of a thin plate. In this case, the plastic zone size p_b is

114

estimated to be [127]

$$p_b = a[\sec(\frac{\pi \sigma_b^\infty}{4\sigma_{ys}}) - 1] \qquad (97)$$

where σ_b^∞ is the value of the surface stress at infinity. Again for small scale yielding, we may write

$$p_{b\ max} \simeq \frac{1}{2} k_{b\ max}^2 (\frac{\pi}{4\sigma_{ys}})^2 \ , \ p_{br} \simeq \frac{1}{2} k_{br}^2 (\frac{\pi}{4\sigma_{ys}})^2 \qquad (98)$$

where $k_b = \sigma_b^\infty \sqrt{a}$ is the stress intensity factor in bending. Because of the similarity of fracture modes, if one assumes that the constants A, α_1 and α_2 in (92) will be the same for extension and bending, substituting from (98) into (92), we obtain

$$(\frac{da}{dn})_b = B(1+\beta)^{2\alpha_1} (\frac{k_{br}}{2})^{2(\alpha_1+\alpha_2)} \qquad (99)$$

Comparing with (96), it is found that

$$(\frac{da}{dn})_b = \frac{1}{2^{2(\alpha_1+\alpha_2)}} (\frac{k_{br}}{k_r})^{2(\alpha_1+\alpha_2)} (\frac{1+\beta_b}{1+\beta})^{2\alpha_1} \frac{da}{dn} \qquad (100)$$

that is, if the fatigue crack growth characteristics for extension is known, for the same material crack growth rate for bending may be obtained from (100). In (100), the subscript b refers to the bending case. Finally, it should be pointed out that in the model discussed above, the effects of microstructure, the temperature and other environmental factors

115

such as the atmospheric conditions have not been taken into account. It is believed that the empirical constants A (or, B), α_1 and α_2 are sufficient to account for the variations in loading conditions and geometry, but it is doubtful that by any proper adjustments they can be made to fully account for the other factors mentioned above; in fact, it is doubtful that any continuum model can.

2.3 Some Experimental Results

As an application of the model given in the form of (96), we will consider the experimental data given by Broek and Schijve [130]*. In [130], 2024-T3 and 7075-T6 aluminum alloy plates with central cracks were used as specimens and the primary purpose was a systematic study of the effect of mean stress on the crack growth rate, where β was varied between 1.13 to 4.8. In the following analysis, the stress intensity factors were corrected for plate width by using Isida's results [131].

In analyzing the results of [130], first the crack growth rates da/dn were correlated against k_r for each value of β, noting that for a fixed β, $B(1+\beta)^{2\alpha_1}$ is constant. In a log-log plot, this gives the values for $2(\alpha_1+\alpha_2)$ which are seen on column 2 of Tables I and II. Column 3 in the tables

*In the data given in [130], for all specimens $\sigma^\infty_{max}/\sigma_{ys}$ was less than 0.5; thus the error involved in the respective plastic zone sizes because of the approximations (95) will be less than 15% (see: [127]).

116

shows the correlation coefficients, r for the least square straight-line fits of log $(\frac{da}{dn})$ vs. log k_r. The closeness of r to unity indicates that within the range under consideration, the assumption of the power relationship is justified. For all tests, $2(\alpha_1+\alpha_2)$ ranged between 3.05 and 4.34, with an average of 3.62 for 2024-T3 and 3.9 for 7075-T6. Column 4 in the tables give the values of $B(1+\beta)^{2\alpha_1}$ obtained from (96) by using the average values for $2(\alpha_1+\alpha_2)$. The values of B and α_1 were then obtained from the log-log plot of $B(1+\beta)^{2\alpha_1}$ vs. $(1+\beta)$. In this case too, least square straight line fits resulted in correlation coefficients very close to unity. Using these values, the crack growth rates for the tests reported in [130] may be expressed as

$$\frac{da}{dn} = 2.679 \cdot 10^{-19} (1+\beta)^{1.72} k_r^{3.62} \text{ for 2024-T3}$$

$$(101)$$

$$\frac{da}{dn} = 6.221 \cdot 10^{-20} (1+\beta)^{1.78} k_r^{3.9} \text{ for 7075-T6}$$

For extreme values of β, the experimental results and the solution given by (101) are shown in Figures 22 and 23. The figures indicate the shift in the theoretical curves as well as in the experimental data for varying values of β. Considering the fact that the scale is logarithmic, parallel to the da/dn axis, the shift is not insignificant.

Figures 24 and 25 show the crack propagation rates in 2024-T3 and 7075-T6 aluminum plates with central cracks and subjected to cylindrical bending [127]. Comparable extensional results for $\beta=0$ were obtained earlier by Illg and McEvily [132] and are shown in Figures 26 and 27. The summary of these results is seen in Table III. Columns 3, 4 and 5 show the exponent $2(\alpha_1+\alpha_2)$, the constant B and the correlation coefficient r for a best fit in the log-log plot of $\frac{da}{dn}$ vs. k_r. In the case of $\beta=0$, from (100) it is seen that the crack growth rate in bending may be obtained by multiplying the crack growth rate for the extension corresponding to the same stress intensity factor by $2^{-2(\alpha_1+\alpha_2)}$. From (96) and (99), we thus obtain:

$$\left(\frac{da}{dn}\right)_{ext.} = B\, k_r^{2(\alpha_1+\alpha_2)}, \quad \left(\frac{da}{dn}\right)_{bend.} = B\left(\frac{k_{rb}}{2}\right)^{2(\alpha_1+\alpha_2)} \qquad (102)$$

In (102), because of the similarity of fracture modes, as a first approximation, it was assumed that the constants B, α_1 and α_2 would have the same values in extension and bending. Table III indicates that different set of values are obtained not only for bending and extension but for each group of tests in either type of loading. Hence, to compare the crack growth rates under extension and bending, we may have to select an appropriate fixed value for $2(\alpha_1+\alpha_2)$. For convenience, here we select $2(\alpha_1+\alpha_2) = 4$ and express the experimental results in the following form

$$\left(\frac{da}{dn}\right)_{ext.} = B'\, k_r^4, \quad \left(\frac{da}{dn}\right)_{bend.} = B'\, \lambda^4\, k_{br}^4 \qquad (103)$$

From (102), it is seen that the theoretical value of λ is 0.5 whereas the experimental values are shown in Table III. Considering the possible differences in the materials used in the extension and bending tests and the approximation involved in selecting the common exponent $2(\alpha_1+\alpha_2)$, the agreement seems to be acceptable.

Figure 28 shows the crack growth rates in extension and bending, (the latter shown only by its scatter band covering 95% of the population) plotted against the plastic zone size. In a limited sense, Figure 28 may be considered as a verification of the model given by (92) as well as the fact that the constants B and $\alpha_1+\alpha_2$ are essentially the same for bending and extension. However, due to the very limited nature of the data, this conclusion should be regarded as tentative and any firm statements to this effect will have to wait for the results of further studies.

Finally, we will make the following remarks concerning the importance and necessity of the plastic zone size and the plastic strains as correlation parameters in analyzing the fatigue crack propagation phenomenon:

a) In the presence of any appreciable plastic deformations, the plastic strains and the plastic zone size are the true measure of mechanical phenomena taking place around the periphery of the propagating crack and their range of application is not restricted by the stress ratio $\sigma^{\infty}/\sigma_{ys}$. In this respect, for example, it is difficult to justify the use of

the stress intensity factor as a correlation parameter for high values of σ/σ^{∞}.

b) In certain configurations with theoretically same stress intensity factor, it is possible to have very different growth rates which cannot be predicted with the stress intensity factor as the correlation parameter but could easily be explained by using the plastic zone size. The plate bending vs. extension discussed above is one example. Perhaps as a more important example, one could mention flat vs. shear or plane strain vs. plane stress modes of crack propagation in relatively thin plates. Although this point may require a more careful and extensive study, the results given by Schijve [133] indicate a definite change in the crack growth rates at the flat-to-shear transition point, growth rates being higher in the shear mode. Since for the same intensity factor, the plastic zone size in plane stress is greater than that corresponding to plane strain, the model outlined above seems in principle to account for this variation.

c) Plastic deformations may be considered as the natural link between purely mechanical continuum variables and the microstructure of the material. As mentioned earlier, an elementary rational fatigue model should include not only the mechanical factors but also some of the important microstructural factors such as the grain size. The chances of success towards developing such an integrated model may be improved if one tries to link the important microstructural factors quantitatively to the plastic deformations.

2.4 Summary

In this part, the continuum theories of the fatigue crack propagation have been reviewed. The existing theories deal, almost exclusively, with the propagation of fatigue cracks in thin plates under symmetric plane extensional loads. and consider only the effects of mechanical continuum variables. The results are invariably expressed by a model of the form

$$\frac{da}{dn} = f(\sigma, a, C)$$

where $\frac{da}{dn}$ is the crack growth rate, σ represents the external loads, usually the range value of the cyclic stress, a is the half-crack length and C is a material constant which is to be determined experimentally. Aside from the technological importance of the problem, the investigators in this field have been encouraged by the smooth and monotonic nature of the experimental data in their search for a continuum model, particularly in the form of power functions.

In recent years, the use of the stress intensity factor as the correlation parameter in analyzing the fatigue results has acquired considerable prominence. The main reasons for this seem to be the simplicity and the universality of the concept as well as the fact that almost all the existing theories can fully or approximately be expressed in terms of the stress intensity factor. However, in using it, certain inherent limitations of the concept should be kept in mind, namely that,

a) in the presence of appreciable plastic deformations around crack tip, it no longer represents the true mechanical conditions, b) it fails to distinguish between two basically different phenomena which may have same numerical values for stress intensity factors (for example, plane strain vs. plane stress and plane extension vs. cylindrical plate bending).

The model based on the plastic deformations around the crack front has been developed partly to overcome these limitations and partly for the belief that a quantity based on the plastic deformations may prove to be a more rational correlation factor if one eventually considers incorporating some of the important microstructural effects into the crack propagation theories.

To demonstrate the application of the model, the crack propagation in plates with variable mean stress and the fully-reversed cylindrical bending problem have been considered. Analysis of bending results indicate that the model may prove to be adequate as a satisfactory comparative tool in studying fatigue crack propagation in the same material under different type of loading conditions.

2.5 Suggestions For Further Research

Perhaps one of the most important areas in the study of fatigue crack propagation which requires close attention is the quantitative analysis of microstructural and environmental effects and the inclusion of some of the more important of these

effects in an integrated theory. Particularly, among these areas which should be studied, one may include the effect of grain size ranging from the fine grained materials to the case in which the grain size is no longer small compared to the smallest geometric dimension.

The effect of orientation and distortion of the grains (e.g., due to the cold working). In some cases, this effect may be studied as an anisotropic continuum phenomenon by taking into consideration the variations in the mechanical bulk properties of the material with changing directions. However, since these variations are insignificant compared to the observed changes in the fatigue crack growth characteristics in the material*, a satisfactory explanation cannot be obtained without considering the microstructure.

Environmental effects, emphasizing the temperature and the atmospheric conditions.

Another area which needs to be studied is the plastic deformations around the front of a propagating crack with the cyclic nature of the load taken into consideration and the related problems such as ductile-to-brittle and flat-to-shear transition phenomena which are observed in thin plates. This problem requires experimental as well as extensive analytical effort.

---

*For example, Schijve [133] reports that in the 2024-T3 aluminum plates loaded perpendicular to the direction of rolling, the crack growth rate was 40% higher than that observed in the specimens loaded parallel to the rolling direction.

A group of problems which is worthwhile to investigate is related to certain macroscopic factors. Among these, we may mention a systematic study of the effect of plate thickness, frequency of loading, time-dependent nature of the magnitude (and possibly the frequency) of the external loads (random or deterministic) and the complex nature of the loading conditions giving rise to theoretically more than one mode of fracture at the crack tip. For example, Schijve [135] reports that the crack growth rate increases with increasing plate thickness and slightly decreases with increasing frequency. Qualitatively, one may explain the former by a statistical size effect and the latter by the strain rate effects. However, a quantitative analysis would be very useful.

From the practical viewpoint, the cumulative effect of the varying load amplitudes on the crack propagation rate is one of the most important factors which merits a systematic study and which may have to be thoroughly understood before any meaningful attempt can be made to study the crack growth phenomenon under random loads.

TABLE I

(2024-T3, Ref. 130)

1 β	2 $2(\alpha_1 + \alpha_2)$	3 r	4 $B(1+\beta)^{2\alpha_1} \cdot 10^{18}$ $(2(\alpha_1+\alpha_2) = 3.62)$
4.80	3.584	.988	3.715
3.60	3.814	.967	2.827
3.00	3.639	.982	2.332
2.25	3.697	.980	1.661
1.85	4.176	.982	1.544
1.80	3.378	.981	1.428
1.38	3.816	.984	0.961
1.41	3.445	.979	1.112
1.13	3.048	.976	.719

TABLE II

(7075-T6, Ref. 130)

1	2	3	4
β	$2(\alpha_1+\alpha_2)$	r	$B(1+\beta)^{2\alpha_1} \cdot 10^{19}$ $(2(\alpha_1+\alpha_2) = 3.9)$
4.80	4.199	.989	28.719
3.60	3.817	.989	18.559
3.00	4.262	.983	14.311
2.25	3.731	.977	9.594
1.85	4.343	.983	5.148
1.80	3.462	.984	7.390
1.38	4.208	.991	4.272
1.41	3.463	.984	4.704
1.13	3.644	.976	2.939

TABLE III

1	2 Thickness (in)	3 $2(\alpha_1+\alpha_2)$	4 B	5 r	6 λ $(2(\alpha_1+\alpha_2)=4)$
7075-T6	.050	3.06	$2.62 \cdot 10^{-18}$	.87	.460
Bare and Clad	.100	3.21	$8.80 \cdot 10^{-19}$	.96	.474
Bending, $\beta=0$	.120	2.83	$3.80 \cdot 10^{-17}$	.99	.479
2024-T3	.050	4.19	$5.35 \cdot 10^{-23}$	.96	.483
Bare and Clad	.080	4.43	$5.20 \cdot 10^{-24}$	.97	.493
Bending, $\beta=0$	.100	4.35	$1.08 \cdot 10^{-23}$	.97	.500
	.125	3.99	$3.99 \cdot 10^{-22}$	.99	.502
	.160	2.89	$9.20 \cdot 10^{-18}$	.98	.441
7075-T6 Extension, $\beta=0$ [132]	.081	3.68	$4.12 \cdot 10^{-20}$	.98	
2024-T3 Extension, $\beta=0$ [132]	.081	3.84	$2.09 \cdot 10^{-20}$	.99	

LIST OF SYMBOLS

a	Half-crack length
c_1	Dilatational wave velocity; $c_1^2 = (\lambda' + 2\mu)/\rho$, $\lambda' = \lambda$ for plane strain, $\lambda' = 2\lambda\mu/(\lambda+2\mu)$ for plane stress
c_2	Shear wave velocity; $c_2^2 = \mu/\rho$
c_R	Rayleigh surface wave velocity
c_ℓ	Longitudinal wave velocity; $c_\ell^2 = E/\rho$
E	Young's modulus
ν	Poisson's ratio
λ, μ	Lame's constants; $\lambda = E\nu/(1+\nu)(1-2\nu)$ $\mu = E/2(1+\nu)$
ρ	Mass density
k	$= c_2/c_1$
p, q	Stresses at infinity
V_0	Crack velocity
v	$= V_0/c_2$
r, θ	Polar coordinates
x, y, z	Rectangular coordinates
$u_i(u, v, w)$	Components of displacement vector
t	Time
τ	$= c_2 t$
γ_F	Fracture energy
U	Work of the external forces
V	Elastic potential
T	Kinetic energy

128

D	Dissipative energy
σ_{ij} $(\sigma_x,\ \tau_{xy},..)$	Components of stress tensor
ε_{ij} $(\varepsilon_x,\ \varepsilon_{xy},..)$	Components of strain tensor
$\dfrac{da}{dn}$	Fatigue crack growth rate
$k_r,\ k_{max}$	Range and maximum values of stress intensity factor for cyclic loads
$p,\ p_b$	Plastic zone size
q_y	Yield stress in shear
σ_{ys}	Yield stress in extension

<u>REFERENCES</u>

1. F. A. McClintock and G. R. Irwin, in "Fracture Toughness Testing and its Applications", ASTM Special Technical Publication No. 381, p. 84, (1965).

2. A. H. Cottrell, in "Fracture", B. L. Averbach, D. K. Felbeck, G. T. Hahn, D. A. Thomas, Editors, Technology Press, M.I.T. and John Wiley and Sons, p. 20, (1959).

3. J. R. Low, Jr., ibid, p. 68.

4. G. T. Hahn, B. L. Averbach, W. S. Owen and M. Cohen, ibid, p. 91.

5. E. Orowan, ibid, p. 147.

6. A. N. Stroh, Phil. Mag. 46, p. 968, (1955); Phil. Mag. 3, 597, (1958); Advances in Physics 6, 418, (1957).

7. J. J. Gilman, Trans. AIME, 200, p. 621, (1954).

8. F. A. McClintock and A. S. Argon, "Mechanical Behavior of Materials", Addison-Wesley Publishing Company, (1966).

9. I. Wolock, J. A. Kies and S. B. Newman, in "Fracture", Technology Press, M.I.T. and John Wiley and Sons, p. 250, (1959).

10. A. M. Bueche and J. P. Berry, ibid, p. 265.

11. H. W. Greensmith, L. Mullins and A. G. Thomas, Trans. Soc. Rheology 4, p. 179, (1960).

12. J. P. Berry, in "Fracture Process of Polymeric Solids", edited by B. Rosen, Interscience Publishers, (1964).

13. J. C. Halpin, J. Appl. Phys. 35, p. 3133, (1964).

14. F. A. McClintock, J. Appl. Mech. 25, p. 582, (1958).

15. J. M. Krafft and G. R. Irwin, in "Fracture Toughness Testing and its Applications", ASTM Special Technical Publication No. 381, p. 114, (1965).

16. G. I. Barenblatt, Advances in Applied Mechanics, Vol. VII, Academic Press, p. 55, (1962).

17. F. Erdogan and G. C. Sih, J. Basic Engin. Trans. ASME 85, p. 519, (1963).

18. A. A. Griffith, Phil. Trans. Roy. Soc. (London), A, 222 p. 180, (1921).

130

19. A. A. Griffith, Proceedings of the First International Congress for Applied Mechanics, Delft, p. 55, (1925).

20. R. S. Rivlin and A. G. Thomas, J. Polymer Science, 10, p. 291, (1952).

21. M. L. Williams, Int. J. Fracture Mechanics, 1, p. 292, (1965).

22. W. G. Knauss, Proceedings of the First International Conference on Fracture, Sendai, Japan, p. C-1, (1965).

23. T. L. Smith, J. Polymer Science, 1, A, p. 3597, (1963).

24. M. L. Williams, in "Fracture of Solids", D. C. Drucker and J. J. Gilman, editors, Interscience Publishers, p. 157, (1963).

25. E. Orowan, Welding Research Supplement, The Welding Journal 34, p. 157-s, (1955).

26. G. R. Irwin, in "Handbuch der Physik", Vol. VI, Springer, Berlin, p. 551, (1958).

27. N. F. Mott, Engineering, 165, p. 16, (1948).

28. P. J. E. Forsyth, Proc. Roy. Soc. (London), A, 242, p. 198, (1957).

29. A. H. Cottrell and D. Hull, Proc. Roy. Soc. (London), A, 242, p. 211, (1957).

30. N. J. Wadsworth and J. Hutchings, Phil. Mag., 3, p. 1154, (1958).

31. N. F. Mott, Acta Met. 6, p. 195, (1958).

32. N. Thompson, in "Fracture", Technology Press, M.I.T. and John Wiley and Sons, p. 354, (1959).

33. W. A. Wood, ibid, p. 412.

34. A. K. Head, Phil. Mag. 44, p. 925, (1953).

35. N. E. Frost and D. S. Dugdale, J. Mech. Phys. Solids, 6, p. 92, (1958).

36. A. J. McEvily and W. Illg, NACA Tech. Note 4394, (1958).

37. J. Schijve, N.L.R., TR M. 2122, Amsterdam, (1964).

38. H. W. Liu, J. Basic Engin. Trans. ASME, 83, p. 23, (1961).

39. W. E. Anderson and P. C. Paris, Metals Engineering Quarterly, 1, p. 33, (1961).

40. S. S. Manson, Int. J. Fracture Mechanics, 2, p. 327, (1966).

41. L. F. Coffin and J. Tavernelli, Trans. AIME, 215, p. 794, (1959).

42. P. C. Paris and F. Erdogan, J. Basic Engin. Trans. ASME, 85, p. 528, (1963).

43. E. F. Poncelet, Colloid Chem. 6, p. 77, (1946).

44. E. F. Poncelet, in "Fracturing of Metals", ASM, Cleveland, p. 201, (1948).

45. S. N. Zhurkov, Int. J. Fracture Mechanics, 1, p. 311, (1965).

46. J. H. Hollomon, in "Fracturing of Metals", ASM, Cleveland, p. 262, (1948).

47. E. Saibel, in "Fracturing of Metals", ASM, Cleveland, p. 275, (1948).

48. P. Gibbs and I. B. Cutler, J. Am. Ceram. Soc. 34, p. 200, (1951).

49. S. Glasstone, K. J. Laidler and H. Eyring, "Theory of Rate Processes", McGraw-Hill, (1941).

50. J. W. Fredrickson and H. Eyring, "Statistical Rate Theory of Metals: I, Mechanism of Flow and Applications to Tensile Properties", Am. Inst. Mining Met. Engin., Inst. Metals Div., Metals Technol. 15, Tech. Pub. No. 2523, (1948).

51. P. Gibbs and H. Eyring, Can. J. Research, 27 B, p. 374, (1949).

52. H. Eyring and G. Halsey, "High Polymer Physics", Remsen Press Div., Chemical Publishing Co., (1948).

53. E. O. Hall, J. Mech. Phys. Sol. 1, p. 227, (1953).

54. E. Orowan, Rept. Prog. Phys. 12, p. 185, (1949).

55. E. Orowan, Trans. Inst. Engin. Shipb., Scotl, 89, p. 165, (1945).

56. G. I. Barenblatt and G. P. Cherepanov, PMM (Transl. J. Appl. Math. Mech.) 24, p. 993, (1960).

57. G. I. Barenblatt and G. P. Cherepanov, PMM (Transl. J. Appl. Math. Mech.) 25, p. 1654, (1961).

58. G. I. Barenblatt, R. L. Salganik and G. P. Cherepanov, PMM (Transl. J. Appl. Math. Mech.) 26, p. 469, (1962).

59. G. R. Irwin, "Fracture Dynamics, Fracturing of Metals", ASM, Cleveland, p. 147, (1948).

60. G. R. Irwin, J. Appl. Mech. 24, p. 361, (1957).

61. K. B. Broberg, Arkiv fur Fysik 18, p. 159, (1960).

62. J. W. Craggs, J. Mech. Phys. Solids, 8, p. 66, (1960).

63. J. J. Gilman, J. Appl. Phys. 27, p. 1262, (1956).

64. D. K. Roberts and A. A. Wells, Engineering, 178, p. 820, (1954).

65. J. P. Berry, J. Mech. Phys. Solids, 8, p. 194, (1960).

66. E. N. Dulaney and W. F. Brace, J. Appl. Phys. 31, p. 2233, (1960).

67. A. A. Wells and D. Post, Proc. Soc. Exp. Stress Anal., 16, p. 69, (1958).

68. J. W. Craggs, in "Fracture of Solids", John Wiley and Sons, p. 51, (1963).

69. A. E. H. Love, "The Mathematical Theory of Elasticity", Cambridge Univ. Press, (1944).

70. A. H. Cottrell, "Theory of Crystal Dislocations", Gordon and Breach, (1964).

71. J. D. Eshelby, Proc. Phys. Soc. A62, No. 353A, (1949).

72. H. Schardin, in "Fracture", The Technology Press, M.I.T., and John Wiley and Sons, p. 297, (1959).

73. J. J. Gilman, ibid, p. 193.

74. R. Guernsey and J. J. Gilman, Proc. Soc. Exptl. Stress Anal. 18, p. 50, (1961).

75. J. J. Benbow and F. C. Roesler, Proc. Phys. Soc. (London), B70, p. 201, (1957).

76. J. P. Berry, J. Appl. Phys. 34, p. 62, (1963).

77. J. L. Sanders, J. Appl. Mech. 27, p. 352, (1960).

78. F. A. McClintock and S. P. Sukhatme, J. Mech. Phys. Solids, 8, p. 187, (1960).

79. B. V. Kostrov, PMM (Transl. J. Appl. Math. Mech.) 28, p. 793, (1964).

80. B. V. Kostrov, ibid, p. 1077.

81. G. N. Ward, "Linearized Theory of Steady High-Speed Flow", Cambridge Univ. Press, (1955).

82. J. W. Craggs, Int. J. Engin. Sci. 4, p. 113, (1966).

83. O. Hull and P. Beardmore, Int. J. Fracture Mechanics, p. 468, (1966).

84. W. M. Beebe, Ph.D. Dissertation, California Institute of Technology, (1966).

85. D. S. Dugdale, J. Mech. Phys. Solids, 8, p. 100, (1960).

86. F. Erdogan, Int. J. Solids Structures, 2, p. 447, (1966).

87. J. N. Goodier and F. A. Field, in "Fracture of Solids", John Wiley and Sons, p. 103, (1963).

88. J. A. H. Hult and F. A. McClintock, Proc. 9th Int. Cong. Appl. Mech. 8, p. 51, (1957).

89. J. R. Rice, Int. J. Fracture Mech., 2, p. 426, (1966).

90. D. K. Felbeck and E. Orowan, Welding Research Supplement, Weld. J., p. 570-s, (1955).

91. F. A. McClintock, in "Fracture of Solids", John Wiley and Sons, p. 65, (1963).

92. T. Yokobori, M. Ichikawa, Research Institute for Strength and Fracture of Materials, Vol. 2, No. 1, (1966).

93. G. Hudson and N. Greenfield, J. Appl. Phys. 18, p. 405, (19 7).

94. T. S. Robertson, J. Iron Steel Inst. 175, p. 361, (1953).

95. F. W. Barton and W. J. Hall, Welding Research Supplement, Weld. J., p. 379-s, (1960).

96. W. J. Hall and F. W. Barton, U.S. Navy Ship Structure Committee Report No. SSC-149, (1963).

97. R. N. Wright, W. J. Hall, S. W. Terry, W. J. Nordell and G. R. Erhard, ibid, SSC-170, (1965).

98. Y. Akita and K. Ikeda, Transportation Technical Research Institute, Report No. 40, Tokyo, Japan, (1959).

99. A. J. Carlsson, Trans. Roy. Institute of Technology, Stockholm, Sweden, No. 207, (1963).

100. H. Schardin and W. Struth, Z. tech. Physik, 18, p. 474, (1937).

101. H. Schardin and W. Struth, Glastech. Ber., 16, p. 219, (1938).

102. H. C. van Elst, Trans. AIME, 230, p. 460, (1964).

103. F. Kerkhof, Naturw. 40, p. 478, (1953).

104. F. Kerkhof, Proc. 3rd Int. Congr. High-Speed Photography, London, p. 194, (1956).

105. H. Wallner, Z. Physik, 114, p. 368, (1939).

106. A. B. J. Clark and G. R. Irwin, J. Soc. Exper. Stress Analysis, 6, p. 321, (1966).

107. A. Smekal, Glastechn. Ber., 23, p. 57, (1950).

108. E. B. Shand, J. Amer. Ceram. Soc., 37, p. 52, (1954).

109. J. M. Krafft and A. M. Sullivan, ASM Trans. 56, p. 160, (1963).

110. J. M. Krafft and G. R. Irwin, in "Fracture Toughness Testing and its Applications", ASTM Spec. Tech. Publ. No. 381, p. 114, (1965).

111. D. Hull, P. Beardmore and A. Valintine, Phil. Mag. 12, p. 1021, (1965).

112. J. J. Gilman, C. Knudsen and W. P. Walsh, J. Appl. Phys., 29, p. 601, (1958).

113. A. J. Carlsson, Trans. Roy. Institute of Technology, Stockholm, Sweden, No. 205, (1963).

114. B. Cotterell, Appl. Materials Research, p. 227, (1965).

115. R. Lazar and W. J. Hall, U.S. Navy Ship Structure Committee Report No. SSC-112, (1959).

116. M. P. Gaus, ibid, SSC-129, (1959).

117. C. F. Tipper, J. Iron Steel Inst., 185, p. 4, (1957).

118. H. F. Hardrath and A. J. McEvily, Proc. Crack Propagation Symposium, Cranfield, England, (1961).

119. P. C. Paris, M. P. Gomez and W. E. Anderson, The Trend in Engin. 13, p. 9, (1961).

120. P. C. Paris, ASME Paper No. 62 - Met. - 3.

121. P. C. Paris, Ph.D. Dissertation, Lehigh University, (1962).

122. H. W. Liu, J. Basic Engin. Trans. ASME, 85, p. 116, (1963).

123. A. J. McEvily and R. C. Boettner, Int. Conf. on Mechanism of Fatigue, Orlando, Florida, (1962).

124. R. W. Hertzberg, Ph.D. Dissertation, Lehigh University, (1965).

125. C. Laird and G. C. Smith, Phil. Mag. 7, p. 847, (1962).

126. H. A. Lipsitt, F. W. Forbes and R. B. Baird, Proc. ASTM 59, p. 734, (1959).

127. F. Erdogan and R. Roberts, Proc. 1st. Int. Conf. on Fracture, Sendai, Japan, (1965).

128. J. H. Crews, Jr. and H. F. Hardrath, J. Soc. Exper. Stress Analysis 6, p. 313, (1966).

129. A. R. Rosenfield, P. K. Dai and G. T. Hahn, Proc. 1st. Int. Conf. on Fracture, Sendai, Japan, (1965).

130. D. Broek and J. Schijve, N.L.R. Report M.2111, Amsterdam, (1963).

131. M. Isida, Proc. 4th U.S. Nat. Congr. of Appl. Mech., p. 955, (1962).

132. W. Illg and A. J. McEvily, NACA TND-52, (1959).

133. J. Schijve, N.L.R. Report MP.243, Paper presented at the Annual ASTM Meeting, (1966).

APPENDIX A

AN ESTIMATE OF THE PLASTIC ZONE IN THE SHEAR PROBLEM

In order to examine the validity of the ideal model proposed by Kostrov [79,80] and used in Sections 1.4.3 and 1.4.4 of this chapter, namely that the characteristic plastic zone size around the periphery of the propagating crack is proportional to the characteristic size of the crack itself, we will give an estimate of the plastic zone size by using a method due to Dugdale [85]. In the case of propagating longitudinal shear crack, the problem is the following: Let the velocity of an internal crack in an infinite medium under anti-plane shear be $V_0 = vc_2$; assume that the only plastic deformation in the solid takes place along very thin strips lying in the plane of the crack and ahead of the crack tips and let the propagation velocity of the (outer) ends of these strips be $V_1 = v_1 c_2$; further, assume that in the plastic strips, the stress state is uniform and equal to the value of yield stress of the material in shear, q_y; what is the velocity V_1?

The criterion to be used to determine V_1 is that the stress state at $x = \mp V_1 t$ obtained from the superposition of stresses due to the external load q at infinity and tractions $\tau_{yz} = q_y$ on the crack surface $V_0 t < |x| < V_1 t$ in a medium containing a propagating crack of length $2V_1 t$ be nonsingular. A similar problem for a plane with a semi-infinite crack and subjected to travelling pressure on the crack surface was considered by Goodier and Field [87].

For shear stress $\tau_{yz} = q$ at infinity, the solution valid for small values of $|\zeta - v_1|$ was found to be (see Section 1.4.4)

$$\Phi_1(\ ) \cong \frac{2q\tau}{\mu\pi} v_1 K(v_1) \frac{1}{\sqrt{\zeta^2 - v_1^2}} \qquad (A.1)$$

For the solution due to the tractions $\tau_{yz} = q_y$ on the crack surface, $v\tau < |x| < v_1\tau$, we obtain

$$\Phi_2(\zeta) = -\frac{q_y\tau}{\pi\mu i} \frac{1}{\sqrt{\zeta^2 - v_1^2}} \left(\int_{-v_1}^{-v} + \int_v^{v_1}\right) \frac{\sqrt{\sigma^2 - v_1^2}}{(\sigma - \zeta)\sqrt{1 - \sigma^2}} d\sigma$$

which, for small values of $|\zeta - v_1|$, may be written as

$$\Phi_2(\zeta) = -\frac{2q_y}{\mu\pi i} v_1 F(v_1, \alpha_1) \frac{1}{\sqrt{\zeta^2 - v_1^2}} \qquad (A.2)$$

$$\sin \alpha_1 = \frac{1}{v_1} \sqrt{\frac{v_1^2 - v^2}{1 - v^2}}$$

where $F(v_1, \alpha_1)$ is the elliptic integral of first kind.

From (A.1) and (A.2), the condition of finiteness of the stresses at $x = Fv_1\tau$ may be obtained as

$$q K(v_1) = q_y F(v_1, \alpha_1) \qquad (A.3)$$

Noting that $\Delta v = v_1 - v$ is small compared to v and using the asymptotic expansions for the elliptic integrals (A.3) may be reduced to the following more convenient form:

$$v_1 - v = \Delta v = \frac{q^2 v}{2q_y^2} f\left(\frac{q}{q_y}, v\right) ,$$

$$\text{(A.4)}$$

$$f\left(\frac{q}{q_y}, v\right) = \frac{(1-v^2)K^2(v)}{1-\left(\frac{q}{q_y}\right)^2 K(v)[E(v)-(1-v^2)K(v)]}$$

It is easily verified that as $v \to 0$ (A.4) reduces to the expression giving the plastic zone size, p, in the static case. In fact, multiplying (A.4) by τ, letting $\Delta v\tau = p$ and $v\tau = a$, we find

$$p = \frac{\pi^2 q^2 a}{8q_y^2} \qquad\qquad \text{(A.5)}$$

which is the result obtained in static problem for small scale yielding [86]. After determining v_1 from (A.4), the plastic zone size is obtained from $p = (v_1-v)c_2 t$.

APPENDIX B

EVALUATION OF VARIOUS ENERGIES IN THE PLASTIC REGION

To have some idea about the nature of energy balance around a running crack in the presence of plastic deformations, in a very simple manner, we compute below various components of energies for the longitudinal shear problem. For simplicity, we do this under rather restrictive assumptions, namely, that the crack velocity is small, hence the quasi-static assumption similar to that made by Mott [27] is valid, there is no strain hardening, the plastic region is small compared to the crack length, is circular and remain so while the crack is growing and, more importantly, that the time rates of the external work done by the tractions on the plastic zone boundary, the plastic work, the stored elastic energy and the kinetic energy in the plastic region may be approximately evaluated by neglecting the effects of unloading, residual stresses and plastic waves arising from the motion of the plastic region with the moving crack. This last assumption is rather severe and may diminish the reliability of the results; however, it may be justified only by considering the fact that all these effects remain somewhat autonomous during the crack propagation and the error involved may not be great enough to change the nature of the qualitative conclusions.

For the longitudinal shear problem, in the circular plastic region ahead of the crack tip, the displacement and the strains may be written as follows [88,89]:

$$w(r,\theta,a) = \frac{q^2 a}{\mu q_y} \sin \theta$$

$$\text{(B.1)}$$

$$\gamma_{rz} = 0, \quad \gamma_{\theta z} = \frac{q^2 a}{\mu q_y} \frac{\cos \theta}{r}$$

where the notation is shown in Figure 19. From the quasi-static assumption, we have $w^\cdot = \frac{\partial w}{\partial a} a^\cdot$. For one-half of the plastic region and the unit thickness, we then obtain

$$T = \frac{1}{2} \int_0^{\frac{\pi}{2}} \int_0^{p \cos \theta} \rho w^{\cdot 2} \, r \, dr \, d\theta = \frac{\pi \rho q^8 a^2 a^{\cdot 2}}{64 \mu^2 q_y^6}$$

$$\text{(B.2)}$$

$$T^\cdot = \frac{\pi \rho q^8}{32 \mu^2 q_y^6} \, a a^\cdot (a^{\cdot 2} + a a^{\cdot \cdot})$$

$$V = \int_0^{\frac{\pi}{2}} \int_0^{p \cos \theta} [q_y(\gamma_{\theta z} - \frac{1}{\mu} q_y) + \frac{1}{2\mu} q_y^2] \, r \, dr \, d\theta$$

$$= \frac{3\pi q^4 a^2}{16 \mu q_y^2} \qquad \text{(B.3)}$$

$$V^\cdot = \frac{3\pi q^4 a a^\cdot}{8 \mu q_y^2}$$

$$U^\cdot = \int \tau_{nz} w^\cdot \, ds = \int (\tau_{\theta z} \, dr + \tau_{rz} \, r \, d\theta) w^\cdot$$

$$\text{(B.4)}$$

$$U^\cdot = \frac{\pi q^4 a a^\cdot}{4 \mu q_y^2}$$

In (B.3), V is the sum of elastic energy $V_E = \frac{\pi q^4 a^2}{16 \mu q_y^2}$ and the plastic work V_p.
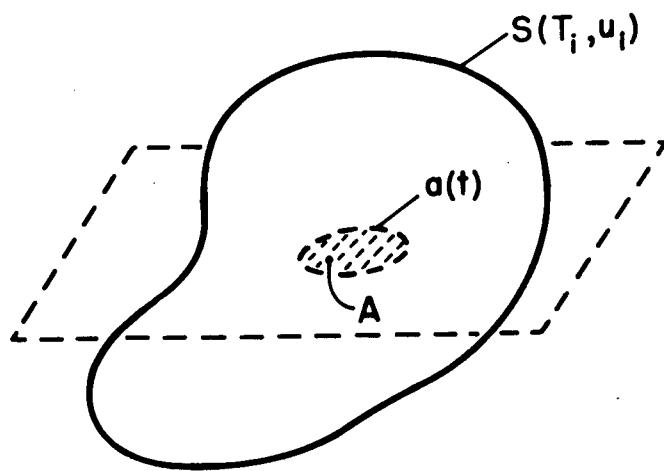
FIGURE 1 - SOLID WITH AN INTERNAL CRACK
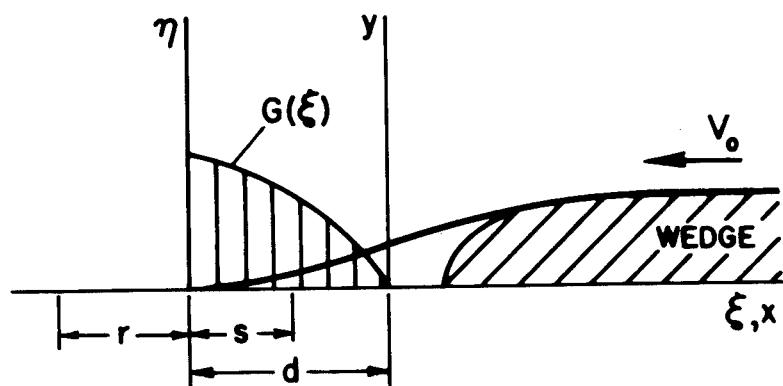
FIGURE 2 - COHESIVE STRESSES AT THE CRACK TIP
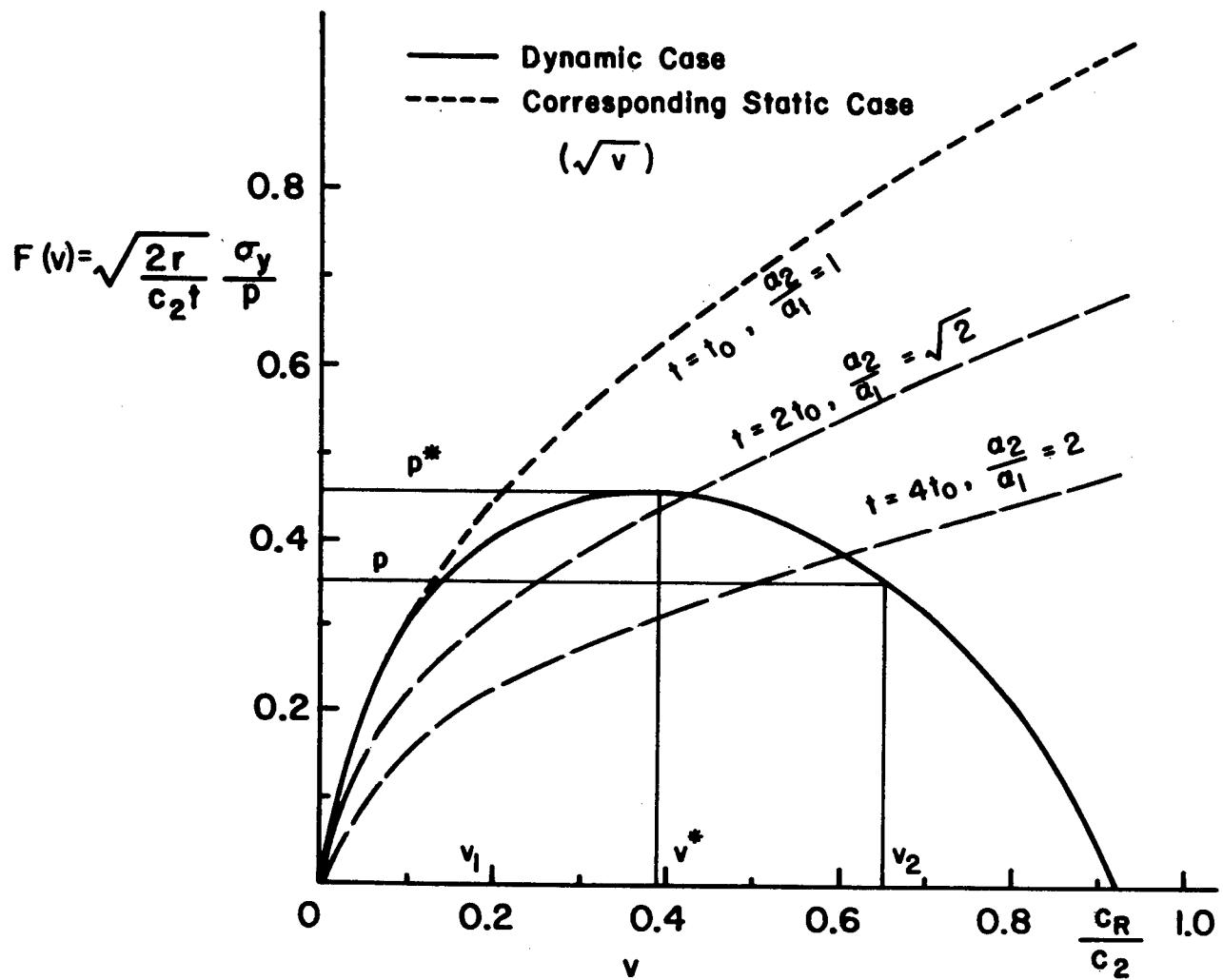
FIGURE   3 - STRESS INTENSITY FACTOR VS. VELOCITY RATIO
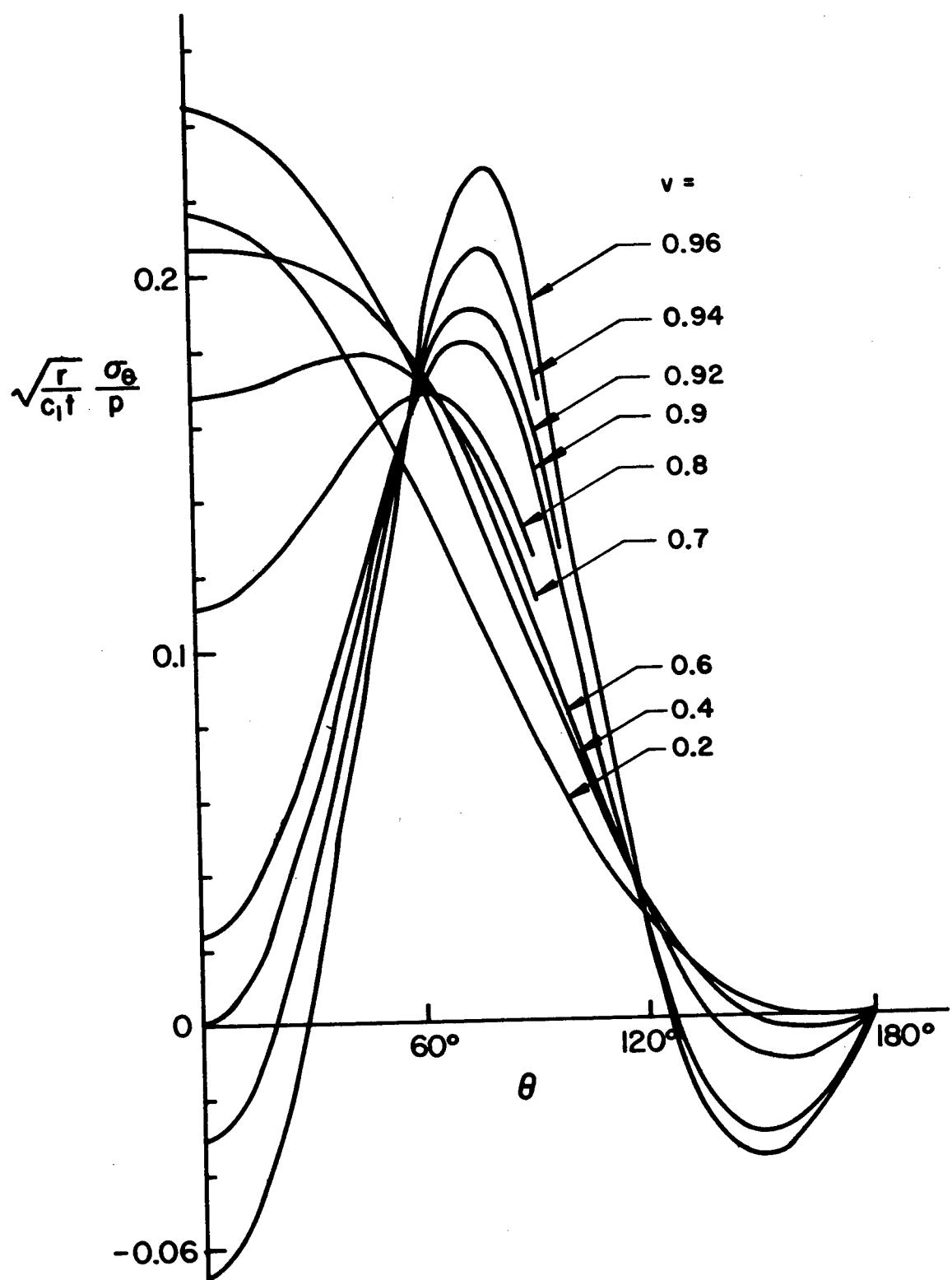
FIGURE 4 - ANGULAR VARIATION OF THE CLEAVAGE STRESS

145
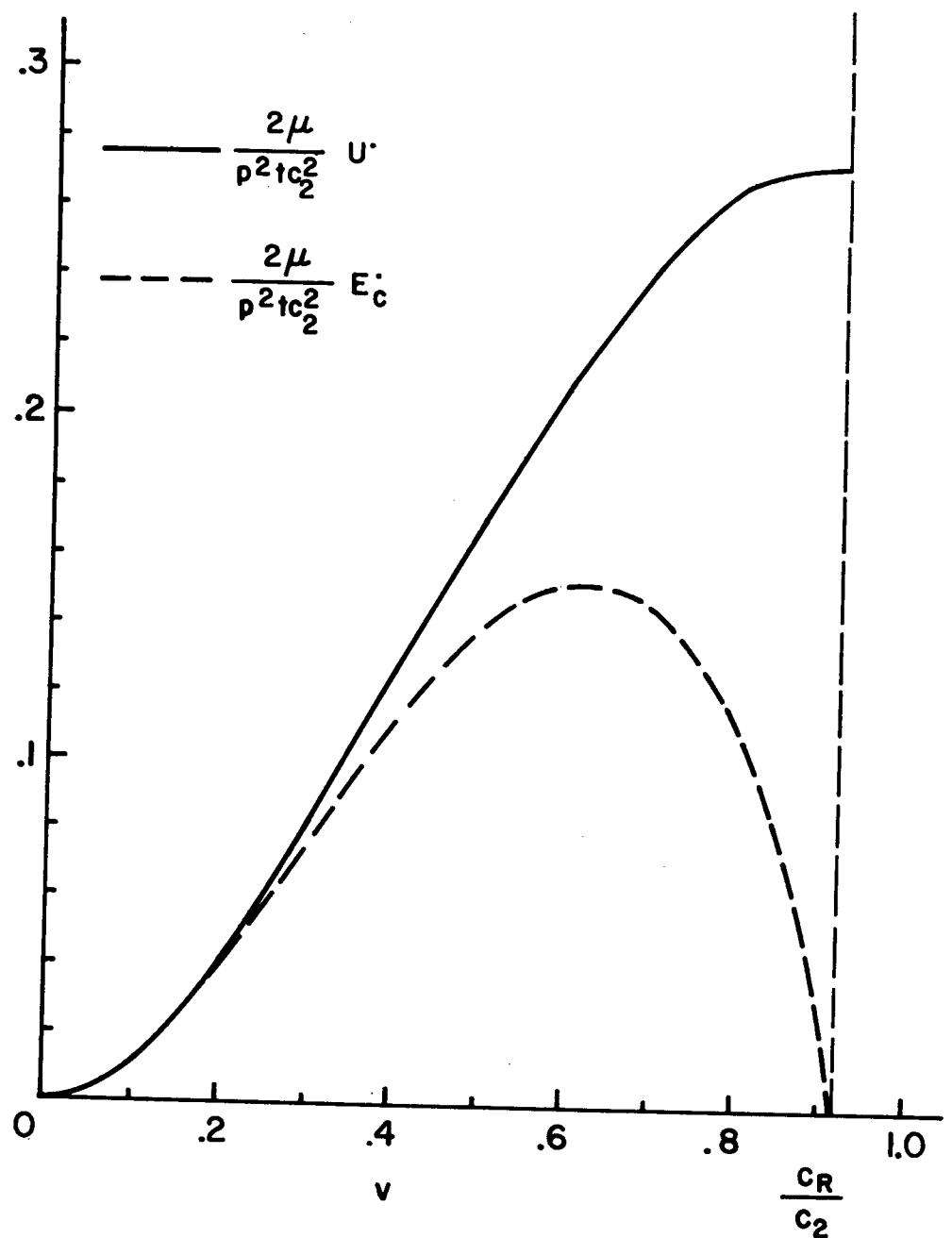
FIGURE 6 - RATES OF EXTERNAL WORK AND CRACK CLOSURE ENERGY

146
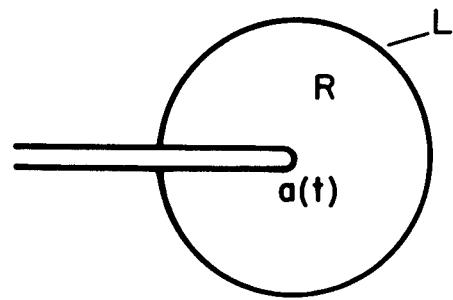
FIGURE 5 - SMALL REGION AROUND THE CRACK PERIPHERY
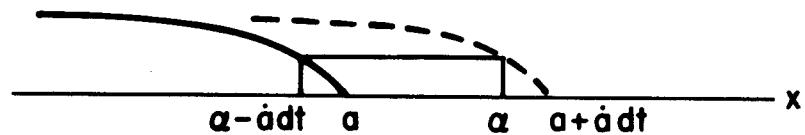
FIGURE 7 - NOTATION FOR THE CALCULATION OF $E_c^{\cdot}$
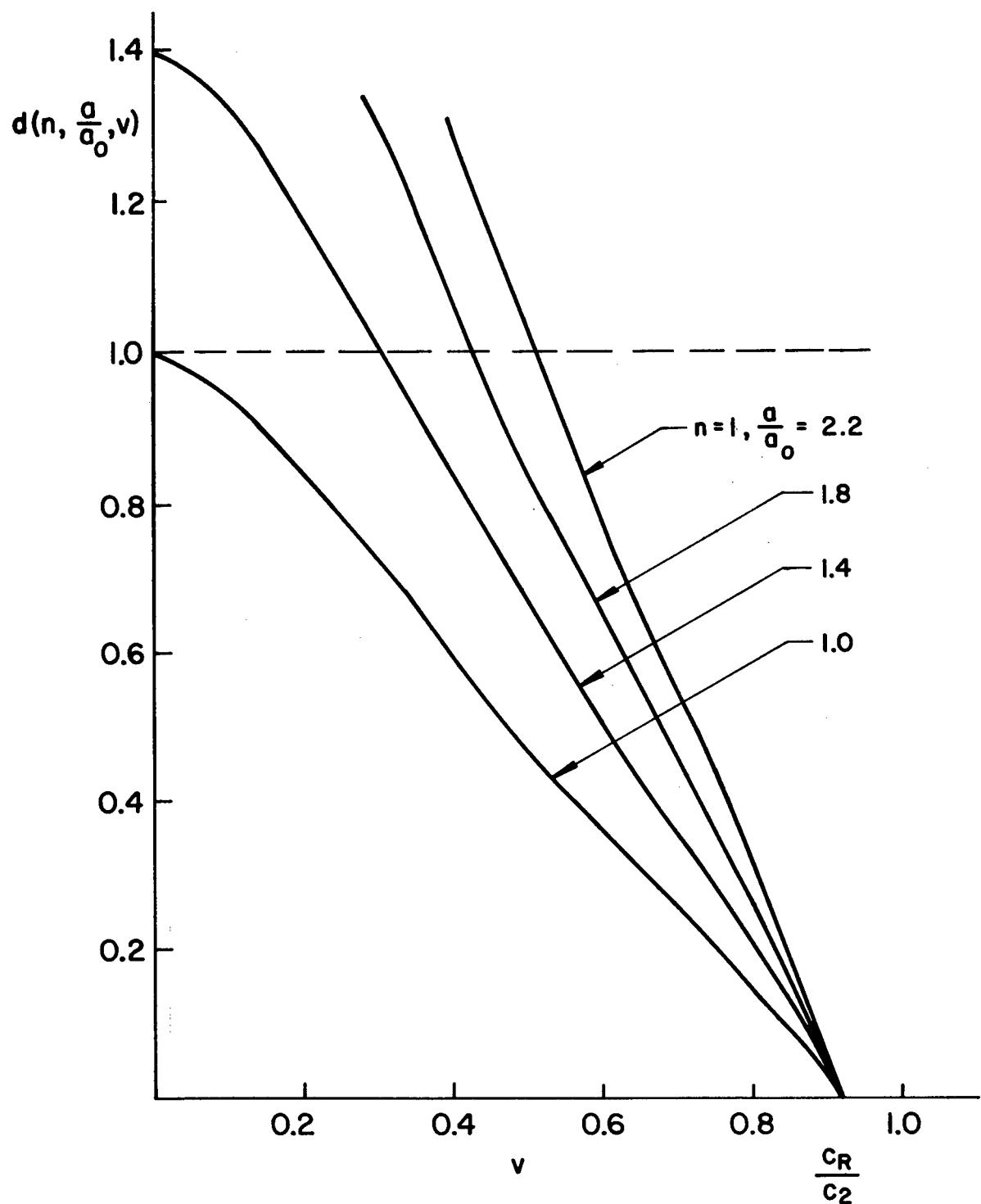
FIGURE 8 - ENERGY AVAILABLE FOR FRACTURE ACCELERATION
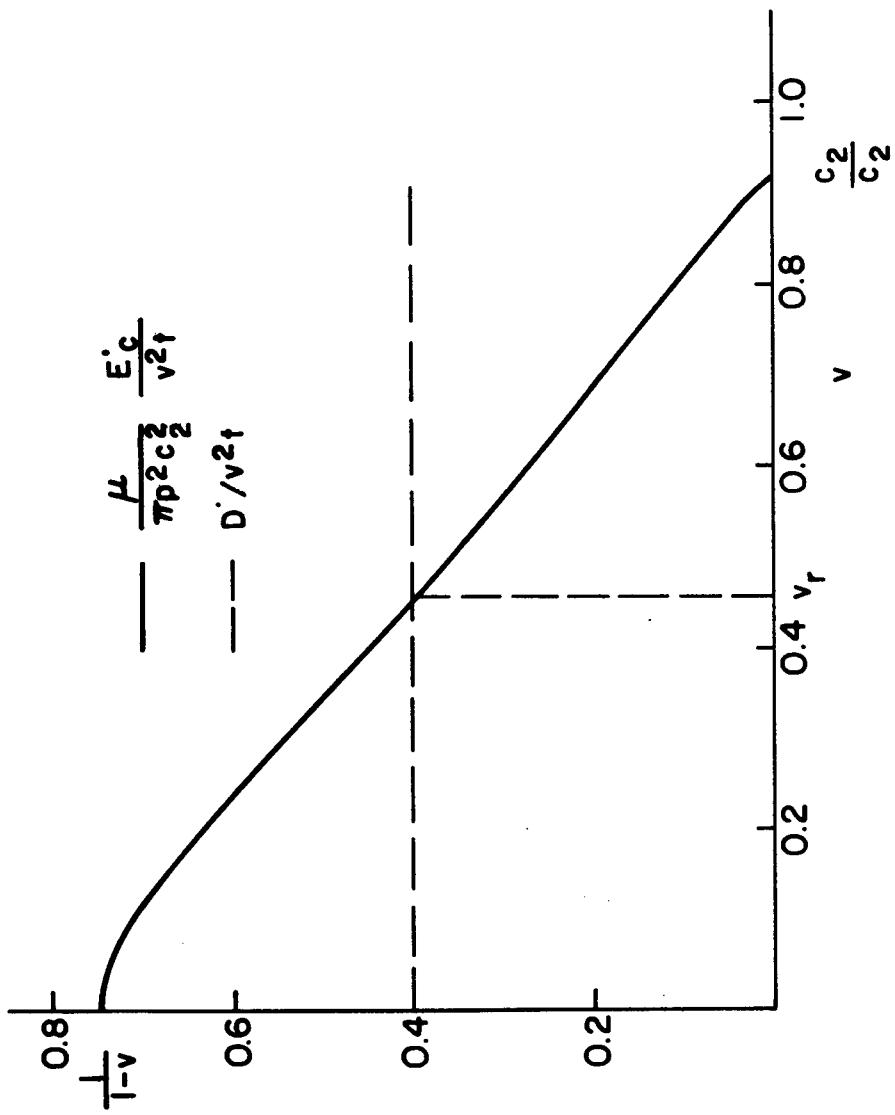
FIGURE 9 - ENERGY BALANCE FOR $\gamma_F \sim v^2 t$
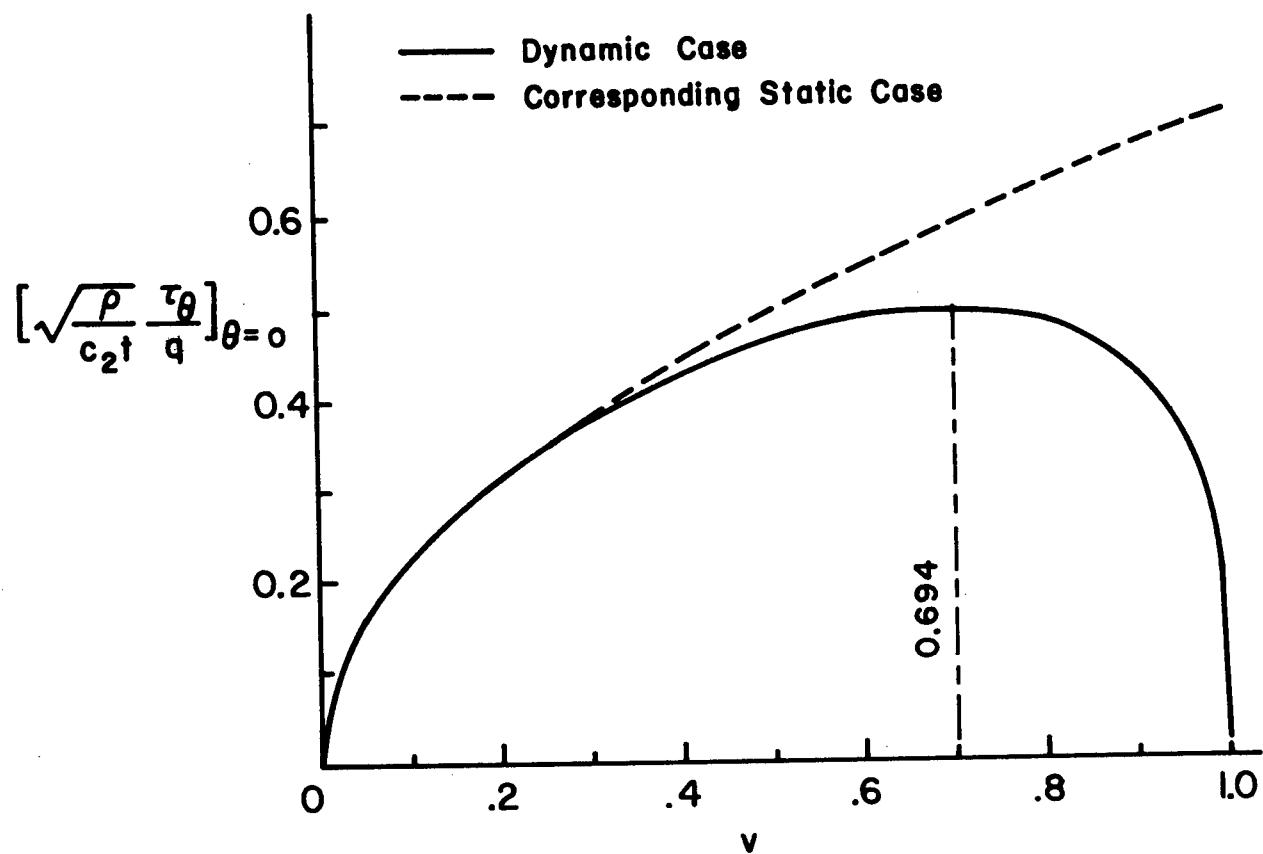
FIGURE 11 – STRESS INTENSITY FACTOR VS. VELOCITY RATIO IN
ANTI-PLANE SHEAR
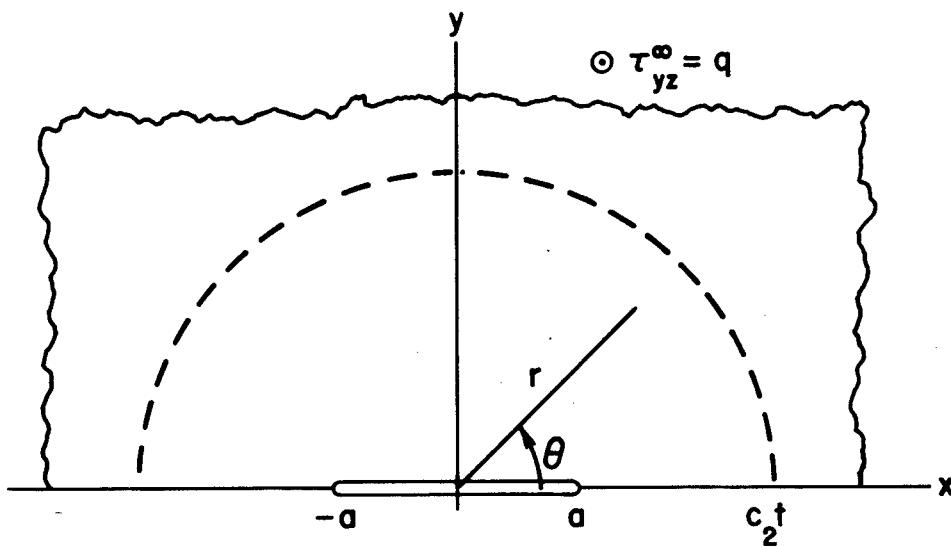
FIGURE 10 - PLANE UNDER LONGITUDINAL SHEAR
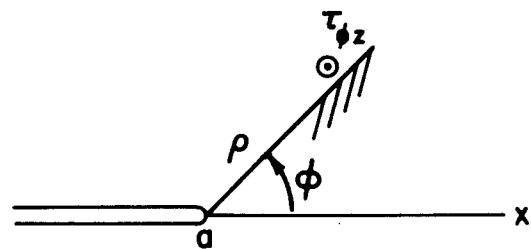
FIGURE 12 - NOTATION FOR SHEAR CLEAVAGE

151

$$\left(\frac{\pi}{K(M)\sqrt{2v(1-v^2)}} \right) \sqrt{\frac{\rho}{c_2 t}} \ \frac{\tau_\phi}{q}$$
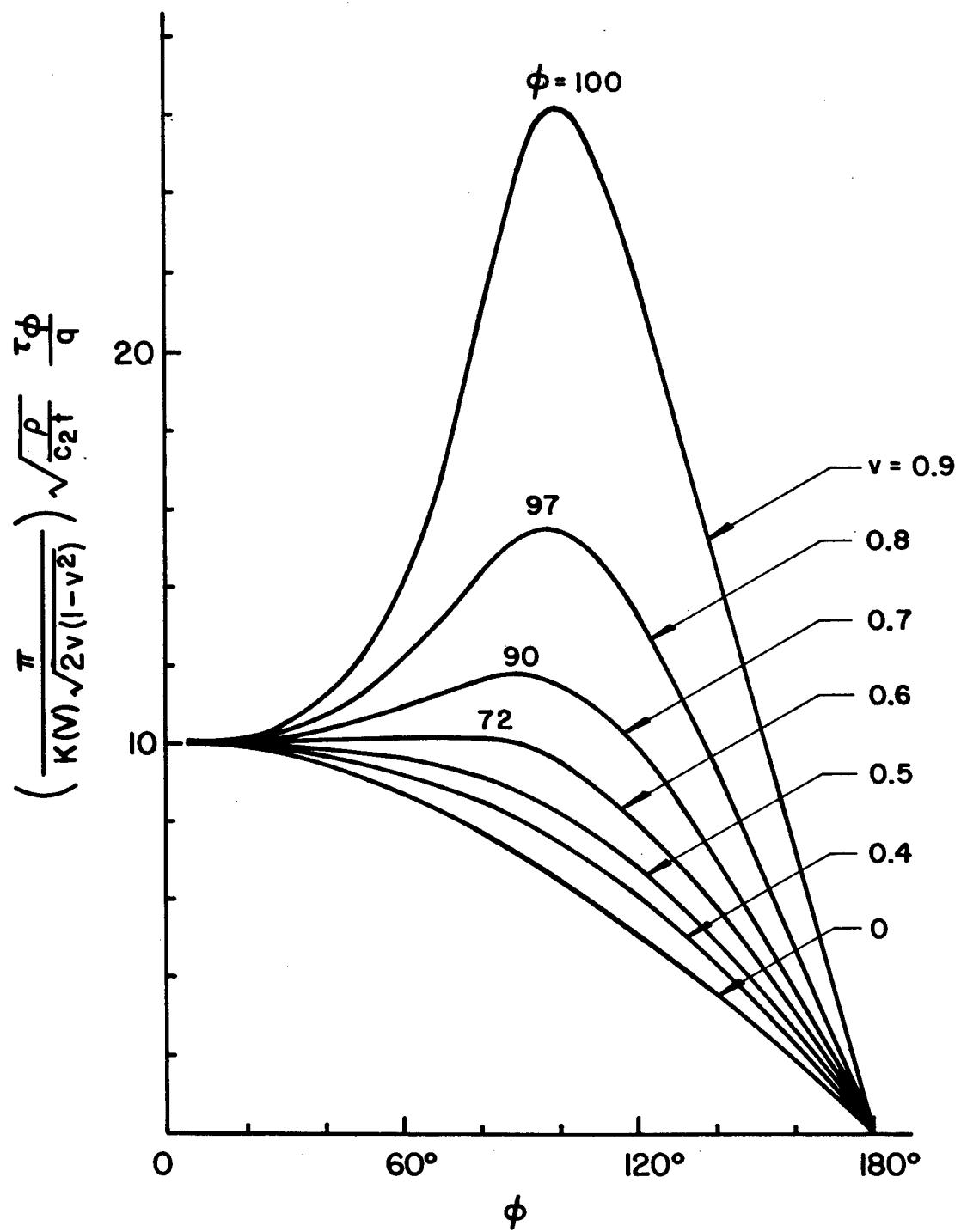
FIGURE 13 - ANGULAR VARIATION OF SHEAR CLEAVAGE STRESS
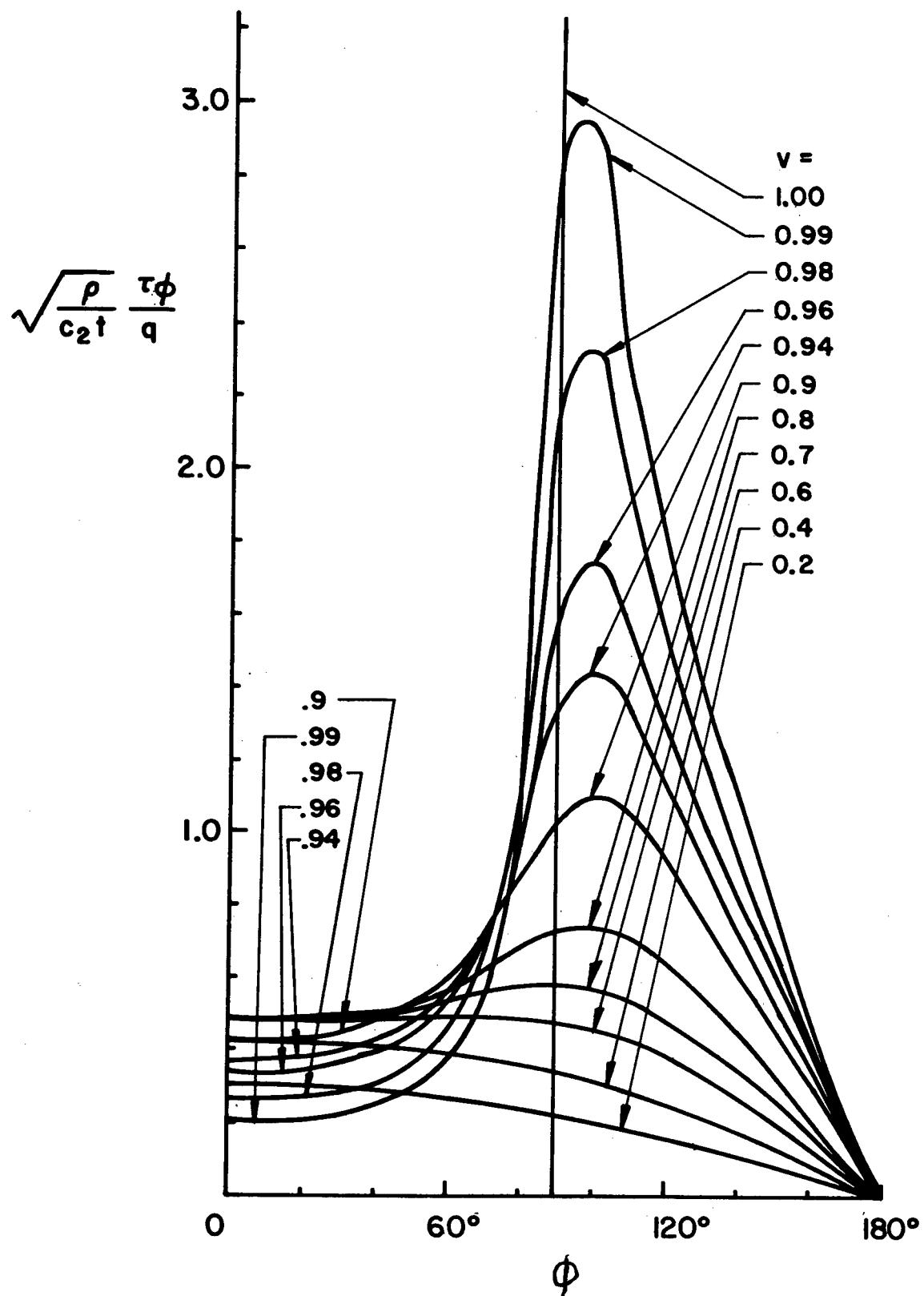
FIGURE 14 - ANGULAR VARIATION OF SHEAR CLEAVAGE STRESS

153
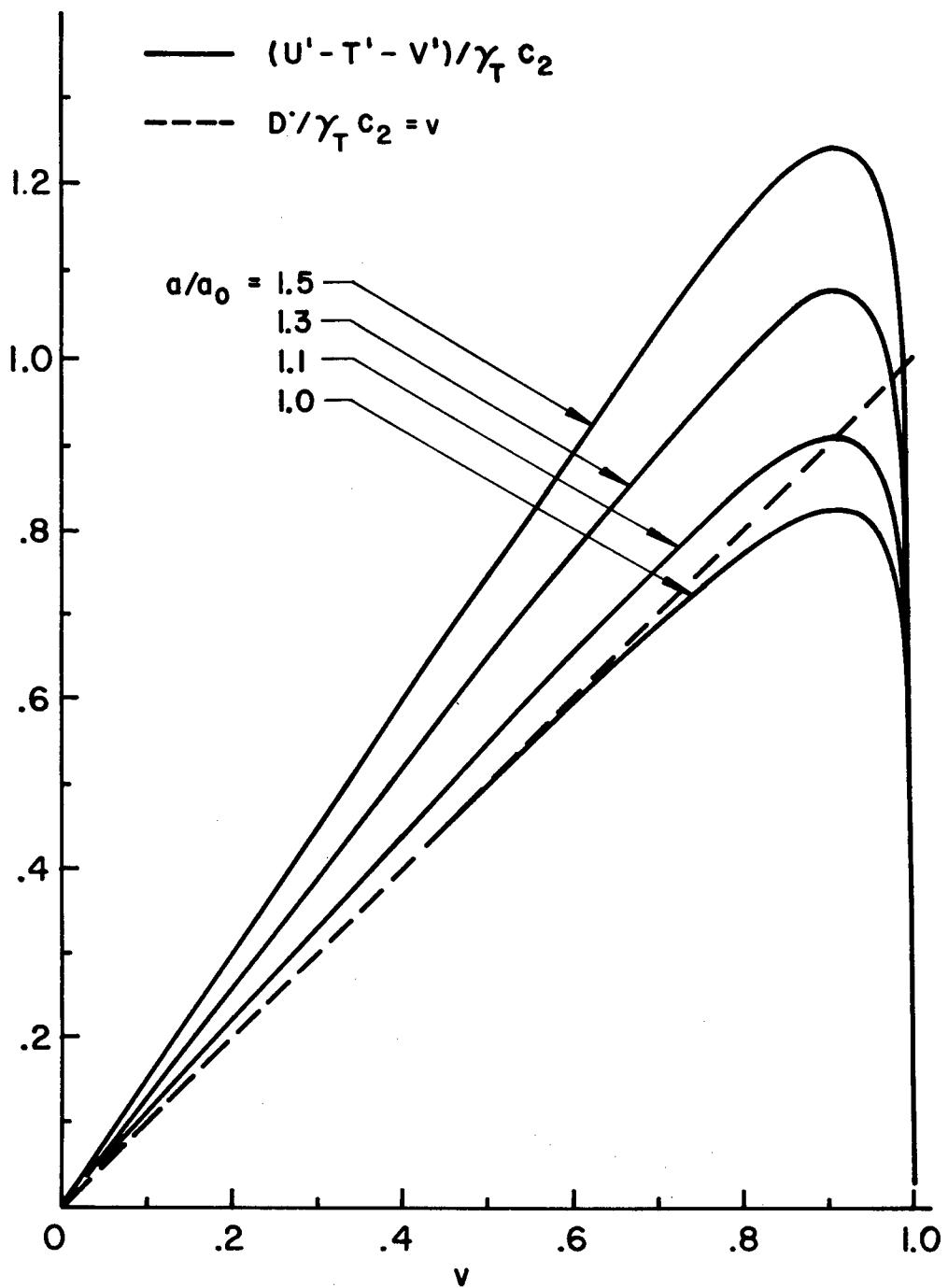
FIGURE 15 - ENERGY RATES VS. VELOCITY RATIO
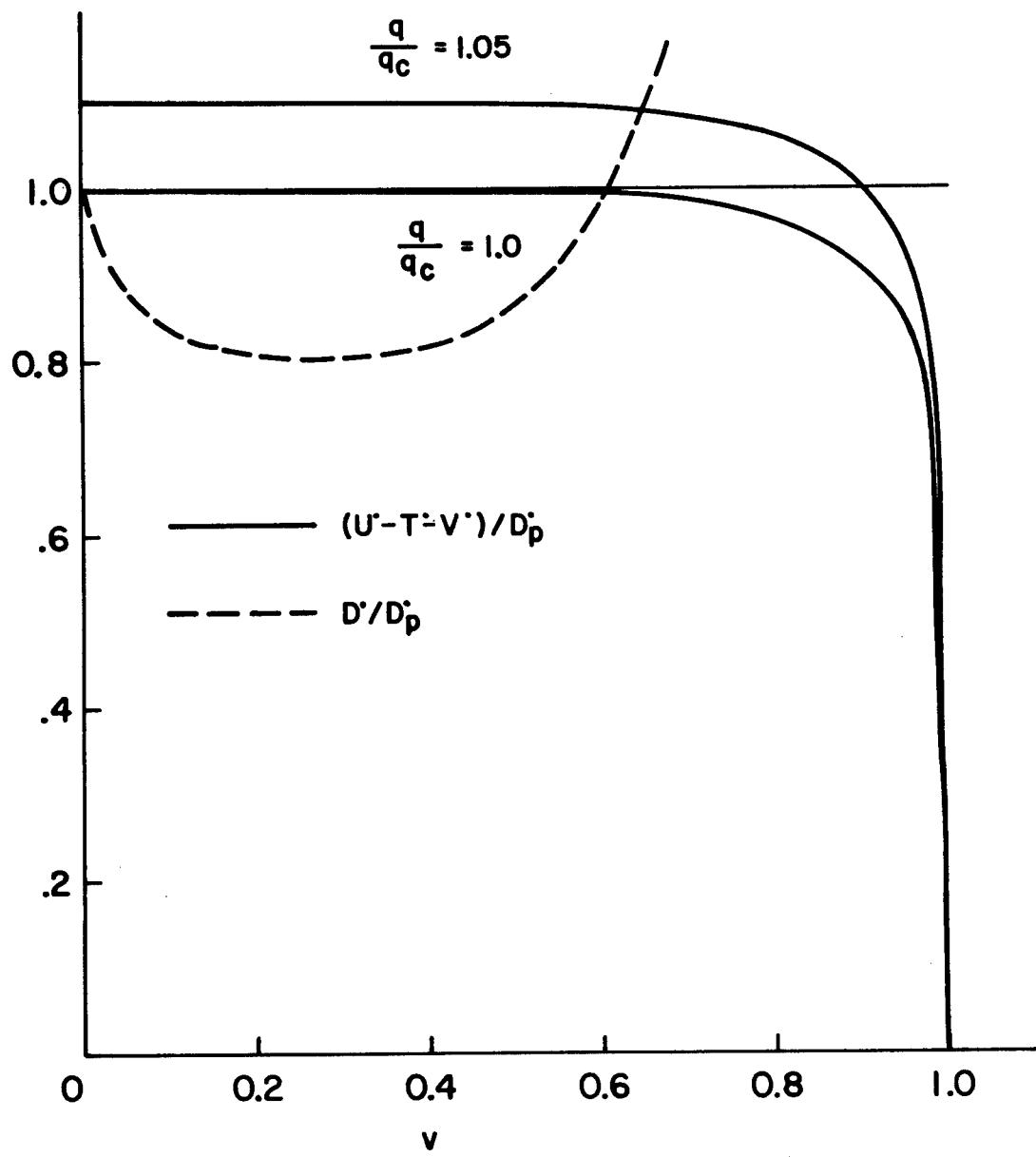
FIGURE 16 - ENERGY RATES VS. VELOCITY RATIO
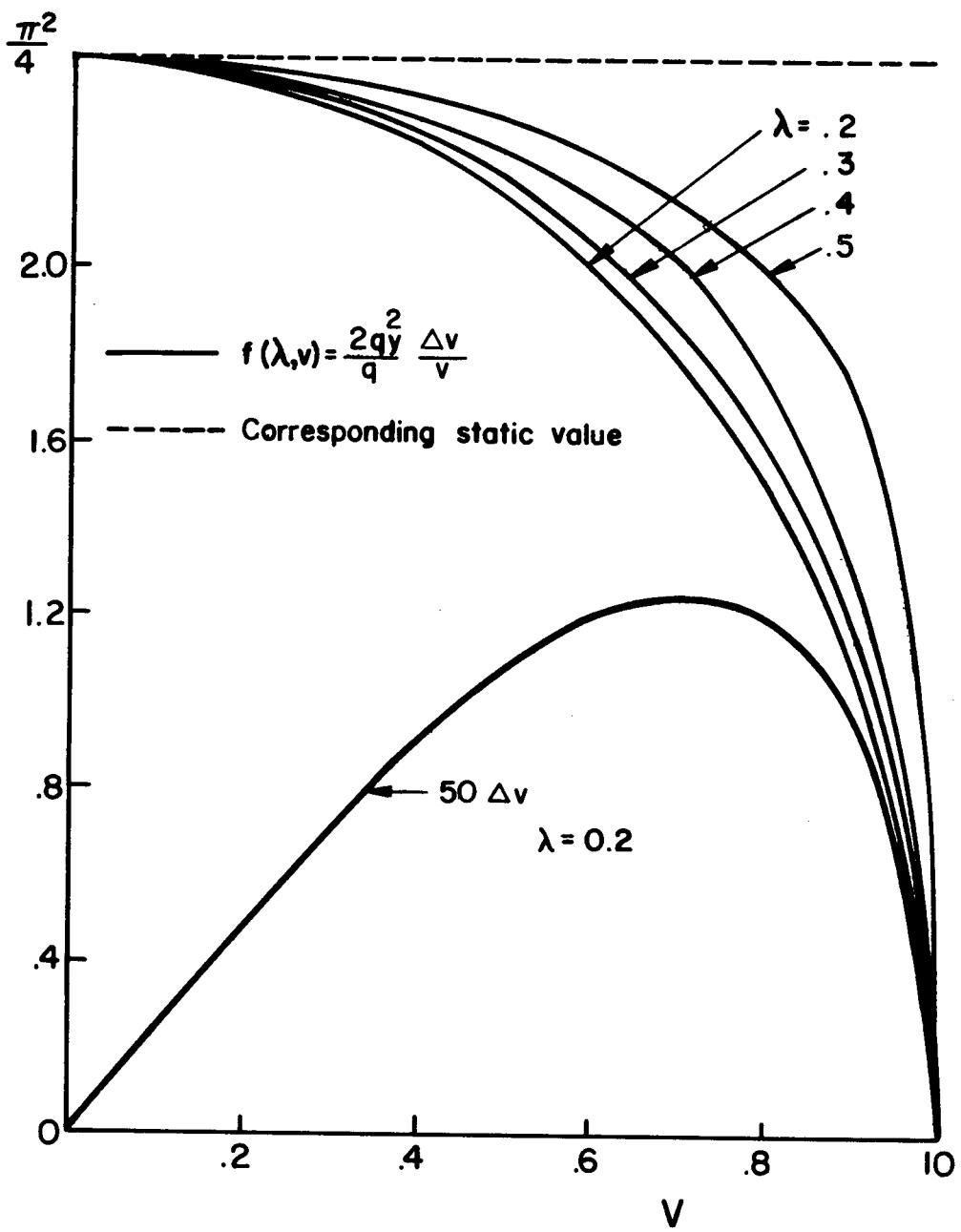
FIGURE 17 - RELATIVE SIZE OF PLASTIC ZONE
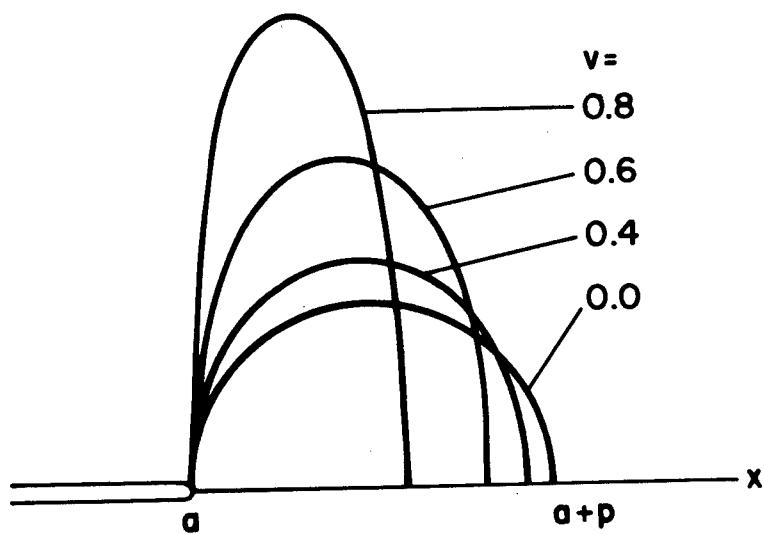
FIGURE 18 - POSSIBLE SHAPE OF THE PLASTIC ZONE
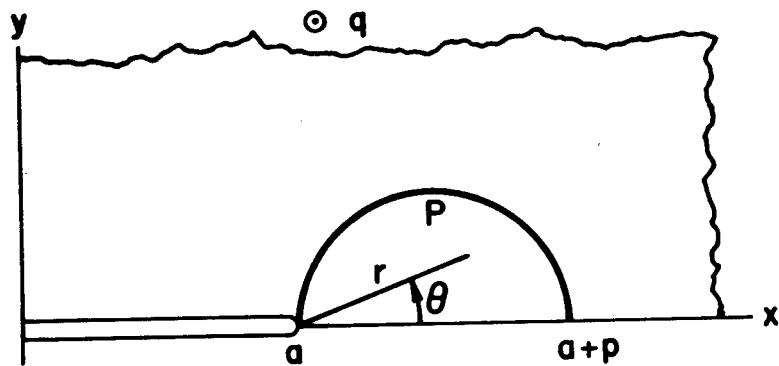
FIGURE 19 - PLASTIC ZONE AROUND THE CRACK TIP

157
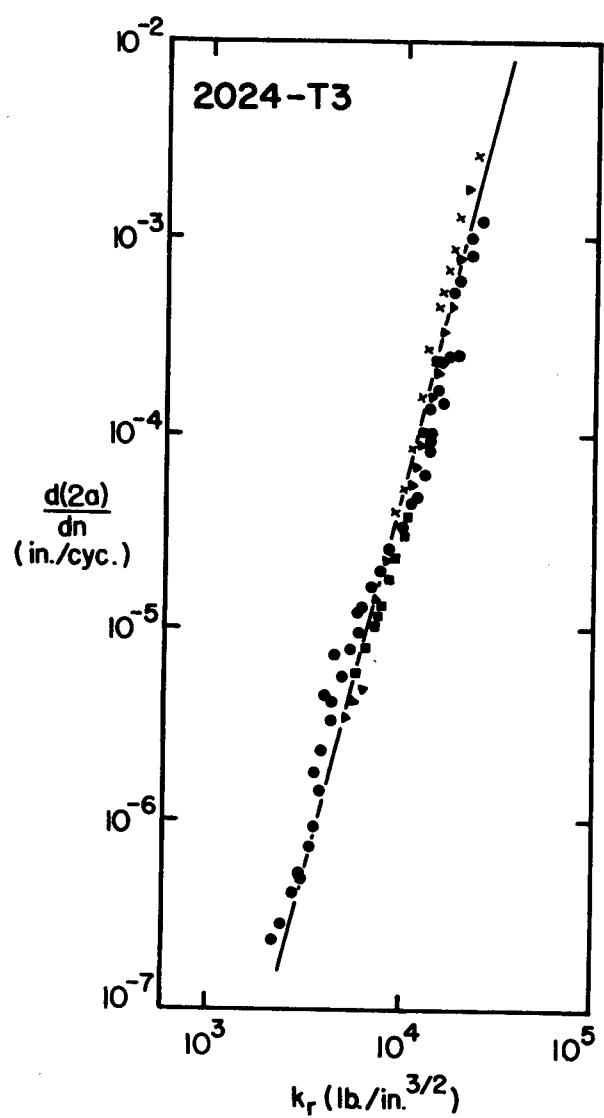
FIGURE 20 - CRACK GROWTH RATE IN 2024-T3 ALUMINUM PLATES IN
TENSION
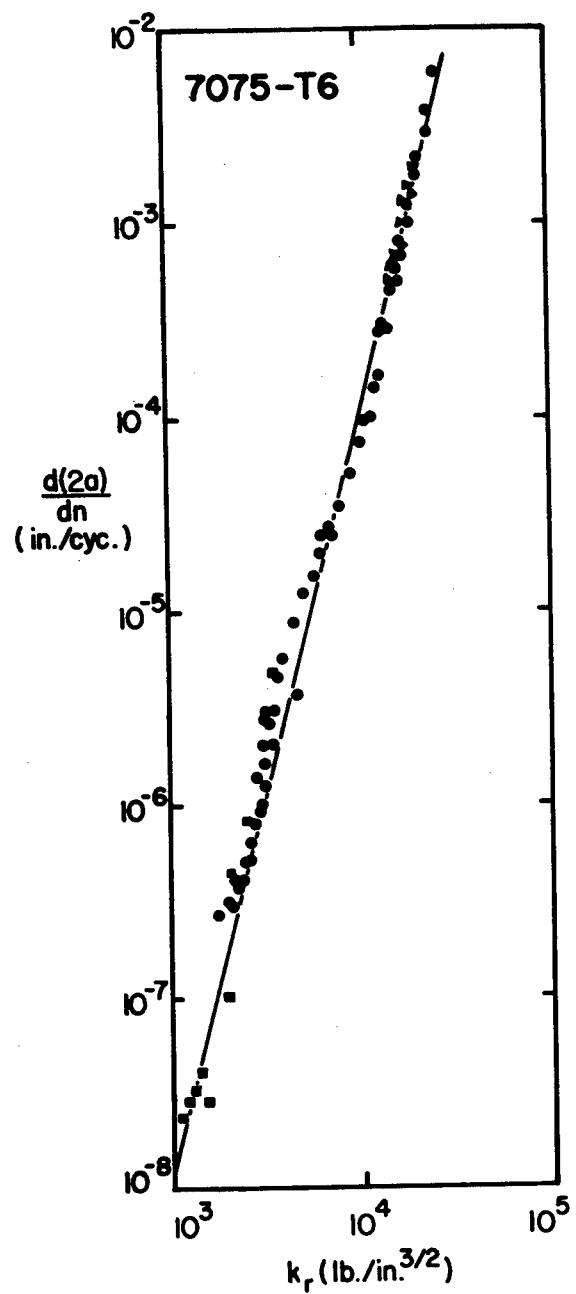
FIGURE 21 - CRACK GROWTH RATE IN 7075-T6 ALUMINUM PLATES IN
TENSION
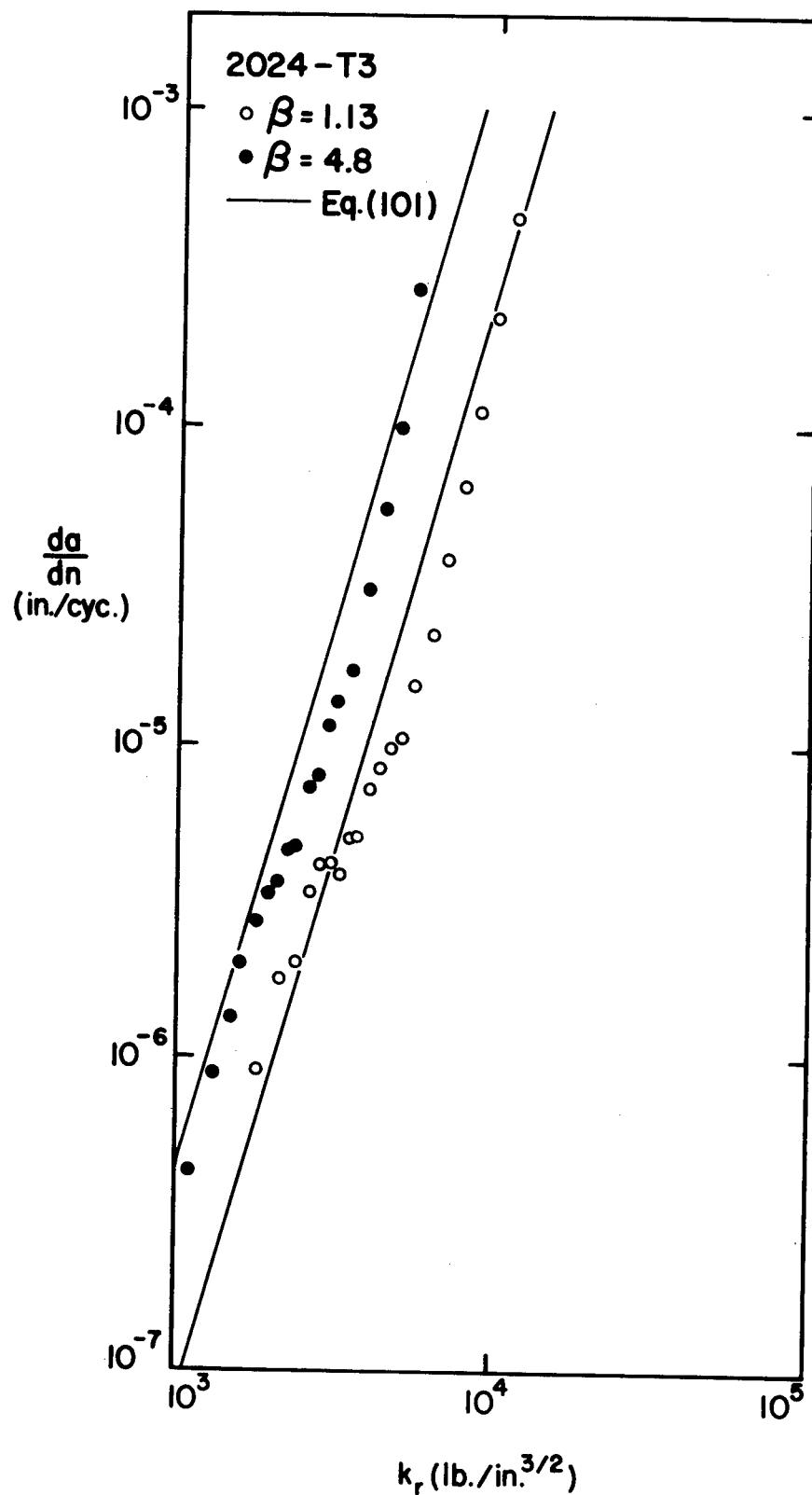
FIGURE 22 - CRACK GROWTH RATE IN 2024-T3 ALUMINUM PLATES WITH
VARIABLE MEAN LOAD
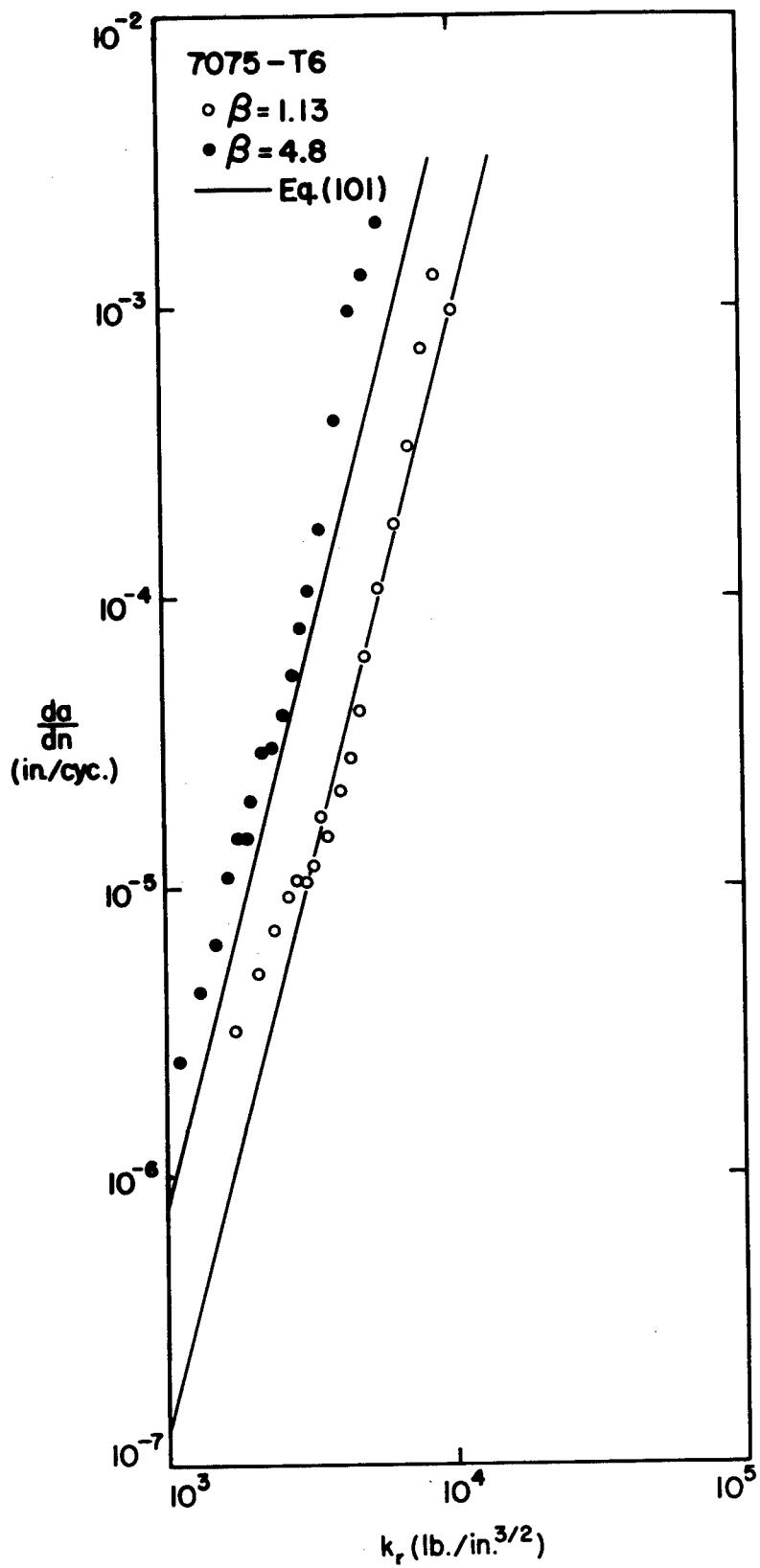
FIGURE 23 - CRACK GROWTH RATE IN 7075-T6 ALUMINUM PLATES WITH
VARIABLE MEAN LOAD

161
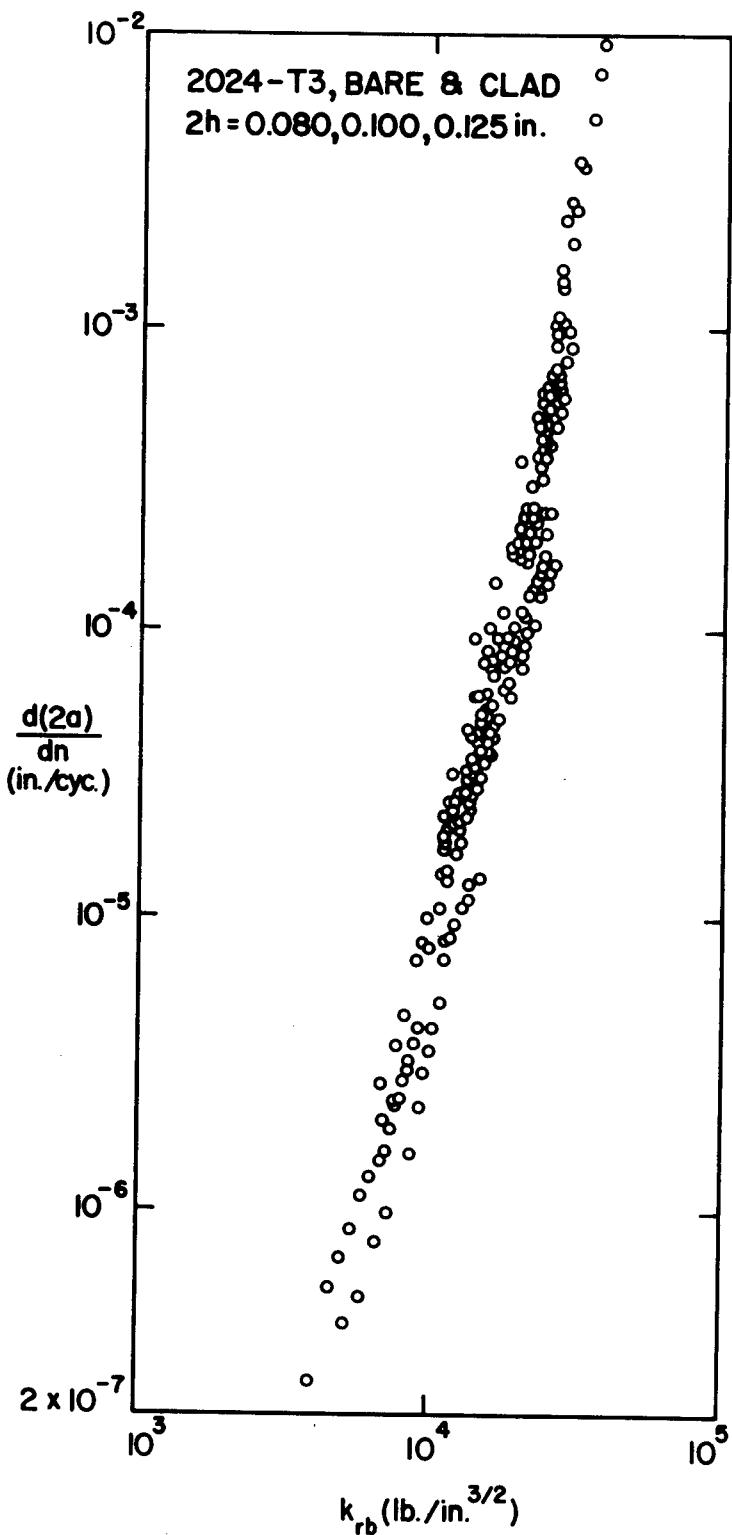
FIGURE 24 - CRACK GROWTH RATE IN 2024-T3 ALUMINUM PLATES UNDER BENDING
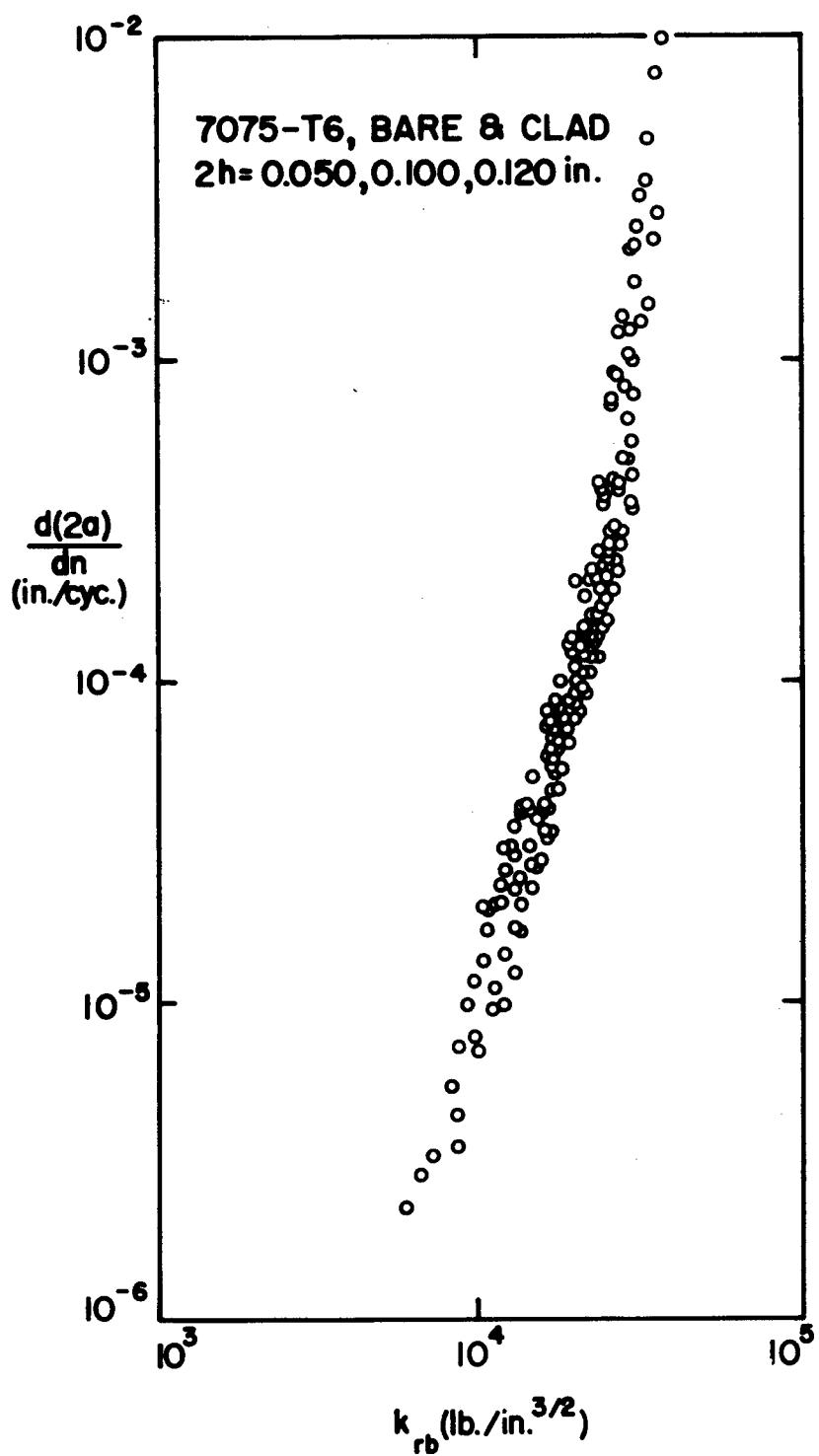
FIGURE 25 - CRACK GROWTH RATE IN 7075-T6 ALUMINUM PLATES UNDER
BENDING
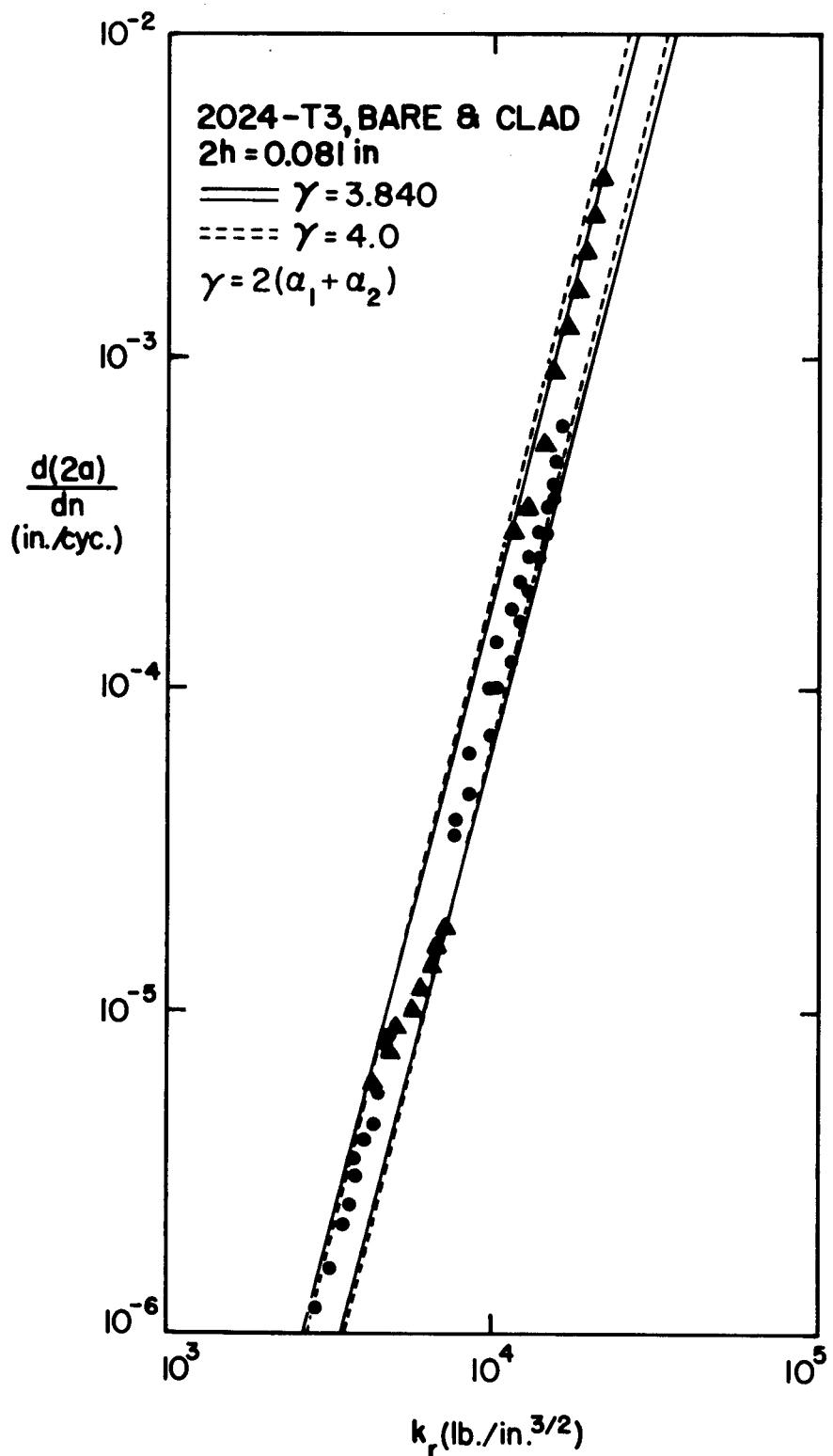
FIGURE 26 - CRACK GROWTH RATE IN 2024-T3 ALUMINUM PLATES UNDER
FULLY-REVERSED EXTENSION

164
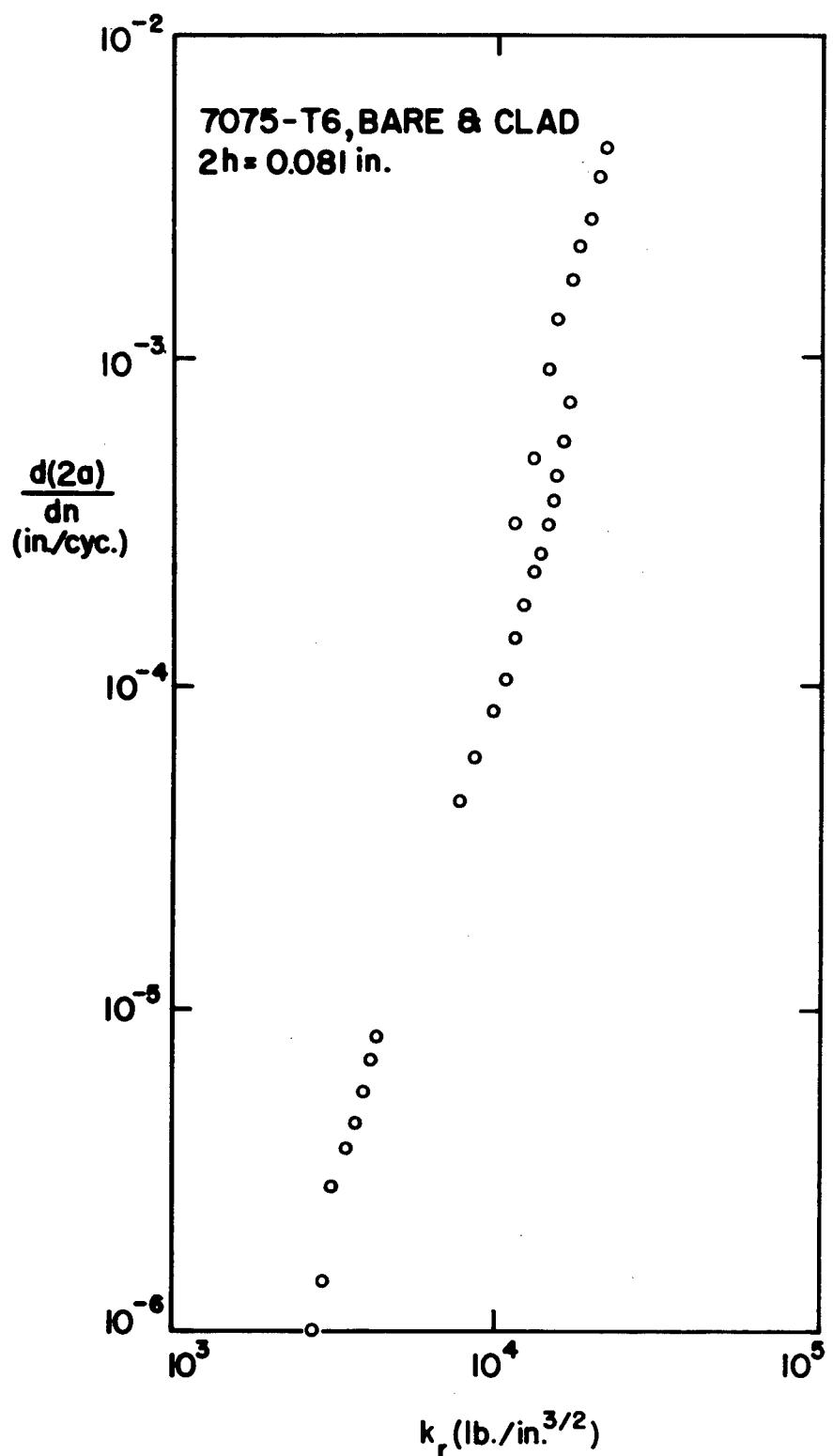
FIGURE 27 - CRACK GROWTH RATE IN 7075-T6 ALUMINUM PLATES UNDER
FULLY-REVERSED EXTENSION

165
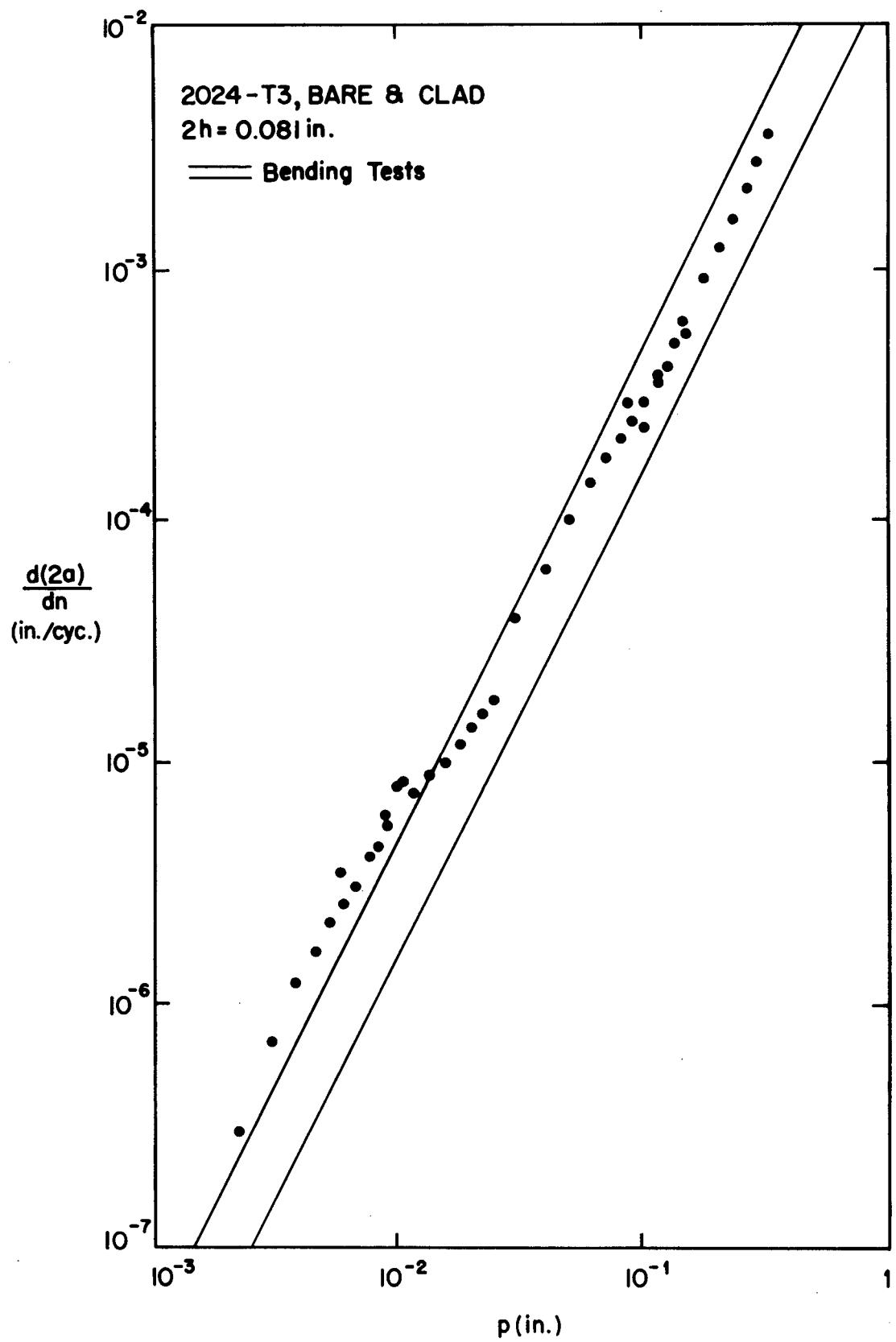
FIGURE 28 - CRACK GROWTH RATE VS. PLASTIC ZONE SIZE